



A PROPOSED MATHEMATICAL MODEL FOR PREDICTING MILITARY
ELECTRONIC EQUIPMENT COMPONENT FAILURE RATES
AND ISOLATING UNDERLYING FAILURE CAUSES

AD733389

A thesis presented to the faculty of the U.S. Army
Command and General Staff College in partial
fulfillment of the requirements of the
degree

MASTER OF MILITARY ART AND SCIENCE

Reproduced by
NATIONAL TECHNICAL
INFORMATION SERVICE
Springfield, Va. 22151

DDC
RECEIVED
DEC 3 1971
REGULATED
A

by

RAYMOND E. STARS MAN, MAJ, USA
B.S., United States Military Academy, 1961
M.S., University of Arizona, 1970

Fort Leavenworth, Kansas
1970

DISTRIBUTION STATEMENT A
Approved for public release;
Distribution unlimited

157

AD733389

A PROPOSED MATHEMATICAL MODEL FOR PREDICTING MILITARY
ELECTRONIC EQUIPMENT COMPONENT FAILURE RATES
AND ISOLATING UNDERLYING FAILURE CAUSES

A thesis presented to the faculty of the U.S. Army
Command and General Staff College in partial
fulfillment of the requirements of the
degree

MASTER OF MILITARY ART AND SCIENCE

Reproduced by
NATIONAL TECHNICAL
INFORMATION SERVICE
Springfield, Va. 22151

D D C
RECEIVED
DEC 3 1971
A

by

RAYMOND E. STARS MAN, MAJ, USA
B.S., United States Military Academy, 1961
M.S., University of Arizona, 1970

Fort Leavenworth, Kansas
1970

DISTRIBUTION STATEMENT A
Approved for public release:
Distribution unlimited

157

**Best
Available
Copy**

THESIS APPROVAL PAGE

Name of Candidate MAJOR RAYMOND E. STARSMAN

Title of Thesis A PROPOSED MATHEMATICAL MODEL FOR PREDICTING

MILITARY ELECTRONIC EQUIPMENT COMPONENT FAILURE RATES AND

ISOLATING UNDERLYING FAILURE CAUSES

Approved by:

Robert Rene, Research and Thesis Advisor

Thomas J. III, Member, Graduate Research Faculty

Fredrick E. Bitt, Member, Graduate Research Faculty

John D. Proctor, Member, Consulting Faculty

Date: 9 JUNE 1971

The opinions and conclusions expressed herein are those of the individual student author and do not necessarily represent the views of either the U. S. Army Command and General Staff College or any other governmental agency. (References to this study should include the foregoing statement.)

ABSTRACT

A mathematical expression for combining the entire failure rate curve is derived based on the assumption that the failure population is composed of three subpopulations, early, chance, and wearout. A graphical method is provided for separating the subpopulations and determining the parameters of the model. The expression is then applied to observed failure data in three detailed examples and in each case the model is shown to represent the observed data at the .05 significance level using the Kolmogorov-Smirnov Test. Two BASIC language computer programs are provided to simplify the use of the proposed model. The proposed expression is compared with techniques presently used to model failure data and is shown to be superior in three ways:

1. It is more accurate than methods presently in use.
2. It's greater flexibility permits the modeling of data which is beyond the capabilities of present failure modeling techniques.
3. The proposed model yields essential information for managers as well as theoreticians concerning failure periods and underlying failure causes, information which is obscured by present modeling methods.

TABLE OF CONTENTS

	Page
LIST OF TABLES.....	vii
LIST OF FIGURES.....	ix
 Chapter	
1. INTRODUCTION	1
2. FUNCTIONS USED IN LIFE TESTING	7
2.1 Introduction	7
2.2 Probability Density Function	8
2.3 Instantaneous Failure Rate Function.	10
2.4 Reliability Function	11
2.5 Mission Reliability Function	12
2.6 Summary	12
2.7 Symbols Introduced in Chapter 2.	14
3. DISTRIBUTIONS USED IN LIFE TESTING	15
3.1 The Exponential Distribution	15
3.2 The Normal Distribution	17
3.3 The Weibull Distribution	21
3.4 Test for Goodness-of-Fit	27
3.5 Symbols Introduced in Chapter 3.	30
4. THE FAILURE RATE CURVE	31
4.1 Introduction	31
4.2 Early Failures	32
4.3 Chance Failures.	34
4.4 Wearout Failures	36
4.5 Summary	36
5. THE BASIS FOR A UNIFIED EXPRESSION	37
5.1 Criteria for a Good Model.	37
5.2 The Product Rule	38
5.3 The Summation Rule	43
5.4 Combined Product and Summation Rules	48
5.5 Comparison of Different Models	51
5.6 Symbols Introduced in Chapter 5	56

TABLE OF CONTENTS - Continued

	Page
6. TECHNIQUE FOR APPLYING THE RELIABILITY SUMMATION MODEL	58
6.1 Introduction	58
6.2 Parameter Determination	60
7. APPLICATION OF THE RELIABILITY SUMMATION MODEL TO HUMAN MORTALITY	63
7.1 The Data to be Analysed	63
7.2 Parameter Determination	67
7.3 Goodness-of-Fit	76
7.4 Analysis of Underlying Failure Causes	78
8. APPLICATION OF THE RELIABILITY SUMMATION MODEL TO KLYSTRON FAILURES	83
8.1 The Data to be Analysed	83
8.2 Parameter Determination	83
8.3 Goodness-of-Fit	93
8.4 Analysis of Underlying Failure Causes	95
9. APPLICATION OF THE RELIABILITY SUMMATION MODEL TO MAGNETRON FAILURES	100
9.1 The Data to be Analysed	100
9.2 Parameter Determination	100
9.3 Goodness-of-Fit	109
9.4 Analysis of Underlying Failure Causes	110
10. COMPARISON OF PRESENT AND PROPOSED MODELS	119
10.1 Weibull Model of Magnetron Failures	119
10.2 Comparison of Goodness-of-Fit	122
10.3 Comparison of Failure Rate.	124
10.4 Comparison of Analytical Power.	124
11. SUMMARY AND RECOMMENDATIONS	128
11.1 Summary.	128
11.2 Recommendations.	130

TABLE OF CONTENTS - Continued

	Page
APPENDIXES	
A. ATTEMPTED EXTENSION OF KAO'S METHOD FOR GRAPHICAL ESTIMATION OF MIXED WEIBULL PARAMETERS.	132
B. BASIC LANGUAGE COMPUTER PROGRAMS FOR APPLY- ING THE PROPOSED RELIABILITY SUMMATION MODEL WITH KNOWN, THEORIZED, OR GRAPHICALLY ESTIMATED PARAMETERS.	142
REFERENCES	145

LIST OF TABLES

Table	Page
3.1 D Values for the Kolmogorov-Smirnov Goodness-of-Fit Test at Various Significance Levels and Sample Sizes.	29
7.1 Mortality Table for 1000 Americans	64
7.2 Mortality Data Prepared for Plotting	68
7.3 Mortality Data Prepared for Subpopulation Replot	71
7.4 Absolute Difference Between Expected and Observed Cumulative Mortality Data (Summation Model).	77
8.1 Raw Failure Data for 92 Klystrons.	84
8.2 Klystron Failure Data Prepared for Plotting. .	85
8.3 Klystron Failure Data Prepared for Subpopulation Replot.	89
8.4 Absolute Difference Between Expected and Observed Cumulative Klystron Failures (Summation Model).	94
9.1 Raw Failure Data for 38 Magnetrons	101
9.2 Magnetron Failure Data Prepared for Plotting .	102
9.3 Magnetron Failure Data Prepared for Subpopulation Replot	105
9.4 Absolute Difference Between Expected and Observed Cumulative Magnetron Failures (Summation Model)	111

LIST OF TABLES - Continued

Table		Page
10.1	Absolute Difference Between Expected and Observed Cumulative Magnetron Failures (Weibull Distribution)	121
A.1	Mortality Data Prepared for Subpopulation Replot (Extended Method)	136
A.2	Absolute Difference Between Expected and Observed Cumulative Mortality Data (Expected Data Determined by the Extended Method)	139
A.3	Comparison of Weibull Parameters Determined by Two Different Methods	140

LIST OF FIGURES

Figure		Page
1.1	Failure Rate Versus Component Age for a Component Population Exhibiting Infantile, Chance, and Wearout Failures.	3
3.1	Failure Rate, Reliability, and Probability Density Versus Time for Exponentially Distributed Populations	16
3.2	Failure Rate, Reliability, and Probability Density Versus Time for Normally Distributed Populations	20
3.3	Failure Rate, Reliability, and Probability Density Versus Time for Weibull Distributed Populations	22
3.4	Determination of the γ Parameter for the Weibull Distribution	26
4.1	Failure Rate, Reliability, and Probability Density Versus Time for a Mixed Failure Population Exhibiting Early, Chance, and Wearout Failures.	33
4.2	Early, Chance, and Wearout Failure Mechanisms.	35
5.1	Venn Diagram for Early, Chance, and Wearout Failures Considered as Independent Events . .	39
7.1	Mortality Histogram for 1000 Americans. . . .	65
7.2	Force of Mortality Histogram for 1000 Americans	66
7.3	Weibull Plot of Human Mortality Mixed Population.	69

LIST OF FIGURES - Continued

Figure	Page
7.4 Mortality Early Subpopulation Replot	72
7.5 Mortality Chance Subpopulation Replot.	73
7.6 Mortality wearout Subpopulation Replot	74
7.7 Plot of Expected and Observed Cumulative Mortality Versus Time (Summation Model).	79
8.1 Weibull Plot of Klystron Mixed Failure Population	86
8.2 Klystron Failure Early Subpopulation Replot.	90
8.3 Klystron Failure Chance Subpopulation Replot	91
8.4 Klystron Failure Wearout Subpopulation Replot.	92
8.5 Plot of Expected and Observed Cumulative Klystron Failures Versus Time (Summation Model)	96
8.6 Plot of Expected Klystron Failure Rate Versus Time.	98
9.1 Weibull Plot of Magnetron Mixed Failure Population	103
9.2 Magnetron Failure Early Subpopulation Replot	106
9.3 Magnetron Failure Chance Subpopulation Replot.	107
9.4 Magnetron Failure Wearout Subpopulation Replot	108
9.5 Plot of Expected and Observed Cumulative Magnetron Failures Versus Time in Hours (Summation Model).	113
9.6 Plot of Expected Magnetron Subpopulation Failure Rates Versus Time in Hours	114
9.7 Plot of Magnetron Failure Rate Versus Time in Hours	116

LIST OF FIGURES - Continued

Figure		Page
10.1	Weibull Plot of Magnetron Failures from Assumed Homogeneous Population.	120
10.2	Comparison of Weibull and Summation Model Cumulative Failures Versus Time in Hours. . .	123
10.3	Comparison of Weibull and Summation Model Failure Rates Versus Time in Hours.	125
A.1	Weibull Plot of Human Mortality Mixed Population (Extended Method).	133
A.2	Mortality Early, Chance, and Wearout Subpopulation Replots (Extended Method).	137

CHAPTER I

INTRODUCTION

This study has two purposes. The primary purpose is to propose a general mathematical model, derived from reliability theory, which will predict military electronic equipment component failure rates more precisely than current models. A subsidiary purpose is to test the hypothesis that the proposed model will, as a result of the nature of its derivation, provide a mathematical means of isolating the underlying causes of component failure as a possible alternative to the costly and time consuming technique of physically examining each failed item.

Reliability may be defined as, "The probability of a device performing its mission adequately for the period of time intended under the operating conditions expected to be encountered" (1). Equipment reliability is one of the bases for procurement of military hardware and is a central consideration for the allocation of maintenance resources. The reliability of a new item of military electronic equipment is a function of the individual failure rates of its component parts. Hence, a more precise component failure rate

model would produce a resultant increase in the accuracy of end item reliability predictions.

The theoretical basis for current failure rate models must be considered before fully understanding why there is still room for improving model accuracy. Fundamental reliability theory indicates that three distinct failure phenomena occur during the operational life of components of military electronic equipment. These phenomena are infantile, deterioration, and chance failures. Infantile failures occur early in component life and normally components failing in this mode are considered to have been substandard prior to operation. Deterioration failures occur late in component life, during the wearout period, and are the result of physical or chemical aging. Chance failures are caused by randomly occurring stresses that exceed component strength. These failures are not a function of component age, but are as likely to occur in early life as in the wearout period. Chance failures are the only failure phenomena to occur during the period of component age between the end of early life and the beginning of wearout. It is during this period that it is most economical to operate components and therefore the period has been named component useful life. Figure 1.1 is a graphical representation of failure rate versus component age. It is

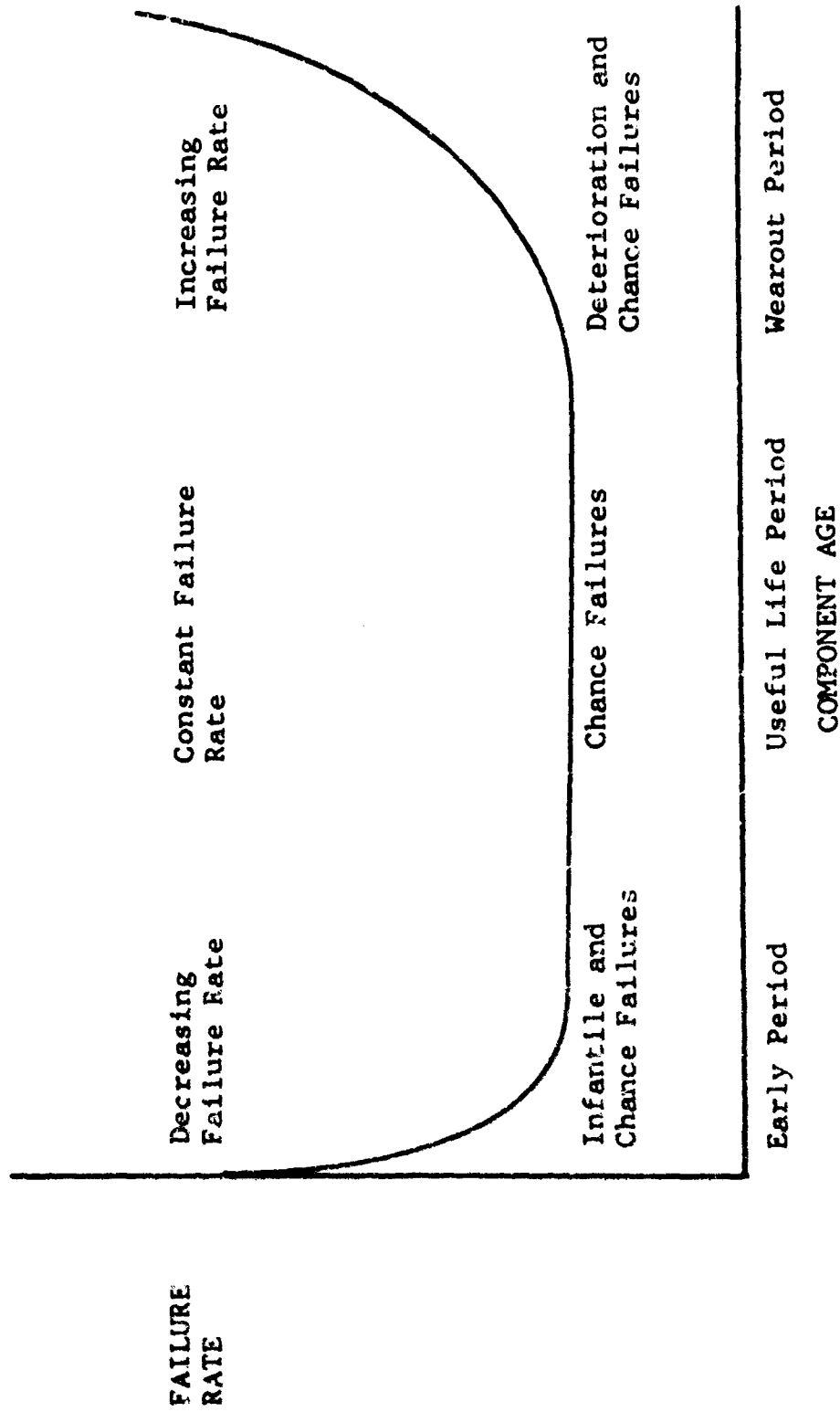


Figure 1.1. Failure Rate Versus Component Age for a Component Population Exhibiting Infantile, Chance, and Wearout Failures

noteworthy that each of the three failure periods exhibits an individual failure rate characteristic which is decreasing during early life, constant during useful life, and increasing during wearout. The result of the combination of these three failure rate periods is the nonmonotonic failure rate curve or more commonly, the bathtub curve shown in Figure 1.1.

Although the failure behavior described above is widely accepted in Reliability Engineering literature and provides the basis for much of classic Reliability Theory, very little has been done to combine the entire failure rate curve mathematically by the use of a unified expression. Instead the failure population is usually assumed to exhibit only one or possibly two of the three failure rate periods. There are three methods by which this assumption is applied:

1. The early failure period may be neglected by assuming that the population is fully burned-in or debugged prior to the analysis of failure data. The failure data may then be modeled by a statistical distribution which exhibits a monotonically increasing failure rate.

2. The wearout failure period may be neglected by truncating the analysis of failure data prior to the onset of wearout. The failure data may then be modeled by a statistical distribution which exhibits a monotonically decreasing

failure rate.

3. Both early and wearout periods may be neglected by combining procedures 1 and 2 above. In this case the failure rate is assumed to be constant and may be associated with either increasing or decreasing monotonic failure rate distributions.

This method of replacing a complex nonmonotonic problem with a simpler monotonic sub-problem is the present basis for the analysis of military electronic equipment component failures. The obvious difficulty with this approach is that it does not address the reality that many component populations do, in fact, demonstrate all three failure periods just as depicted in Figure 1.1. Consequently, by making a simplifying assumption, part of the problem itself has been assumed away. Data, so analyzed are not fully productive and potentially useful information concerning failure cause is unnecessarily lost.

It is proposed that a unified expression capable of combining the entire failure rate curve would overcome the difficulties of present failure rate models. It is further hypothesized that such a model would provide more accurate predictions and that additional information gleaned from present raw failure data by the proposed model would be useful in isolating the underlying causes of component failure. The proposed model will, in all likelihood, be

more complex than are current models, but with the present availability of high speed digital computers this is no longer an important disadvantage.

The thesis is organized such that the early chapters review fundamental reliability theory and provide a basis for the latter applicatory chapters. Chapters 2 through 6 and parts of Chapters 7 and 8 have been extracted from a previous report by the author (2). Portions of Chapters 4, 6 and 8 also appear in a paper, co-authored by Kececioglu, published in the 1971 Transactions of the American Society for Quality Control (3).

CHAPTER 2

FUNCTIONS USED IN LIFE TESTING

2.1 Introduction

If, during a nonreplacement life test of N like items, after a time t , $N_s(t)$ items have survived, we estimate the reliability of any one item at time t to be the ratio of surviving items at time t to the total number of items in test.

$$R(t) = \frac{N_s(t)}{N} \quad (2.1)$$

Similarly, the unreliability is estimated as the ratio of the cumulative number of items failing by time t to the total number of items in test.

$$Q(t) = \frac{N_f(t)}{N} \quad (2.2)$$

Since

$$N = N_f(t) + N_s(t) \quad (2.3)$$

We may write

$$R(t) + Q(t) = 1 \quad (2.4)$$

These expressions are the fundamental definitions of reliability theory. Next we shall examine some basic functions.

2.2 Probability Density Function

In life testing, failure records are maintained on the items in test. The fraction of the total items in test which fail during time Δt , between t and $t + \Delta t$, may be plotted against time, to obtain a failure histogram. If the time increment, Δt , is allowed to approach zero as a limit as N becomes very large, the histogram approaches a smooth curve, called the probability density function, $f(t)$. Probability density functions for three specific distributions are plotted versus time in Figs. 3.1c, 3.2c, and 3.3c. Mathematically, $f(t)$ is written

$$f(t) = \frac{1}{N} \frac{d N_f(t)}{dt} \quad (2.5)$$

The area under $f(t)$ represents the cumulative failures per component in test, which has previously been defined as the probability of failure or unreliability, $Q(t)$. If $f(t)$ is integrated over the limits $-\infty$ to $+\infty$, the cumulative number of items failing will become equal to the total number of items in test and, therefore,

$$\int_{-\infty}^{+\infty} f(t) d(t) = 1 \quad (2.6)$$

By the definition of $f(t)$,

$$f(t) \geq 0 \quad (2.7)$$

for $-\infty < t < \infty$.

Equations (2.6) and (2.7) are the necessary and sufficient conditions for a function to be considered a probability density function (4, p. 10).

The area under the $f(t)$ curve to the left of time t represents the cumulative failures per component which have occurred prior to t ; therefore,

$$Q(t) = \int_{-\infty}^t f(\xi) d\xi \quad (2.8)$$

where ξ is a dummy variable of integration. Since $R(t) = 1 - Q(t)$, equation (2.8) may be written:

$$R(t) = 1 - \int_{-\infty}^t f(\xi) d\xi \quad (2.9)$$

From equations (2.6) and (2.9) it follows that

$$R(t) = \int_{-\infty}^{\infty} f(\xi) d\xi - \int_{-\infty}^t f(\xi) d\xi \quad (2.10)$$

which reduces to

$$R(t) = \int_t^{\infty} f(\xi) d\xi \quad (2.11)$$

Since, by definition $f(\infty) = 0$, we find by differentiation that

$$f(t) = - \frac{d[R(t)]}{dt} \quad (2.12)$$

2.3 Instantaneous Failure Rate Function

It is useful in life testing to construct a failure rate histogram similar to the failure histogram constructed in Section 2.2, but with an all important difference. In this case we plot the fraction of the number of items surviving at t which fail during Δt . If the incremental time, Δt , approaches zero as a limit as N becomes very large, the histogram approaches a smooth curve called the instantaneous failure rate function, $\lambda(t)$. Other names in common usage for this function are hazard rate, force of mortality, and failure rate. The failure rate versus time is plotted for three specific distributions in Figs. 3.1a, 3.2a, and 3.3a. Mathematically, the failure rate is written

$$\lambda(t) = \frac{1}{N_s(t)} \frac{d N_f(t)}{dt} \quad (2.13)$$

Multiplying and dividing equation (2.13) by N gives

$$\lambda(t) = \frac{N}{N_s(t)} \frac{d[N_f(t)/N]}{dt} = \frac{N}{N_s(t)} \frac{d[Q(t)]}{dt} \quad (2.14)$$

or

$$\lambda(t) = - \frac{1}{R(t)} \frac{d[R(t)]}{dt} \quad (2.15)$$

From equation (2.12)

$$- \frac{d[R(t)]}{dt} = f(t)$$

therefore,

$$\lambda(t) = \frac{f(t)}{R(t)} \quad (2.16)$$

2.4 Reliability Function

Equation (2.15) is an ordinary differential equation which can be solved for $R(t)$. Rearranging (2.15)

$$\frac{1}{R(t)} d[R(t)] = - \lambda(t) dt$$

Integrating

$$\int_0^t \frac{d R(\xi)}{R(\xi)} = - \int_0^t \lambda(\xi) d\xi$$

which yields

$$\ln R(\xi) \Big|_0^t = - \int_0^t \lambda(\xi) d\xi$$

If it is assumed that at $t = 0$ no items have failed, the initial condition $R(0) = 1$ is obtained. Therefore,

$$R(t) = e^{-\int_0^t \lambda(\xi) d\xi} \quad (2.17)$$

2.5 Mission Reliability Function

Mission reliability is defined as the probability of survival of an item during a mission of duration T , given that the item or component has not failed prior to the start of the mission at time t .

Bazovsky (5, p. 44) defines the a posteriori probability of failure as

$$Q(t, T) = \frac{Q(t+T) - Q(t)}{R(t)} \quad (2.18)$$

Mission reliability is the complement of $Q(t, T)$,

$$R(t, T) = 1 - \frac{Q(t+T) - Q(t)}{R(t)} \quad (2.19)$$

which may be written

$$R(t, T) = \frac{R(t) - [1 - R(t+T)] + [1 - R(t)]}{R(t)}$$

or after simplifying

$$R(t, T) = \frac{R(t+T)}{R(t)} \quad (2.20)$$

2.6 Summary

It is evident that the functions derived in this section are related to each other in such a way that if an

expression is known for one function, the expression for the other functions can be found directly.

Thus far, the discussion has not been based on any particular distribution. The equations derived in this section are always true regardless of the failure mechanism or type of failure distribution involved. Chapter 3 will be concerned with some of the more common distributions which have been used to represent specific types of failure.

2.7 Symbols Introduced in Chapter 2

$f(t)$	Probability density function
\ln	Natural logarithm
N	Total number of items in test
$N_f(t)$	Cumulative number of items failing by time t
$N_s(t)$	Number of items surviving at time T
$Q(t)$	Unreliability function
$R(t)$	Reliability function
$R(t, T)$	Mission reliability function
T	Mission duration
t	Time variable
Δt	Time increment
$\lambda(t)$	Instantaneous failure rate function
ξ	Dummy variable of integration

CHAPTER 3

DISTRIBUTIONS USED IN LIFE TESTING

3.1 The Exponential Distribution

The exponential distribution has proven to be a representative model for the failure behavior of many electrical components and also for electrical and non-electrical complex systems (6, pp. 113-150). In reliability analysis the exponential distribution is commonly used to evaluate life test data in which failures occur randomly. The distribution is characterized by a constant instantaneous failure rate (Fig. 3.1a).

$$\lambda(t) = \lambda = \text{CONSTANT} \quad (3.1)$$

For the exponential distribution, the mean time between failures is simply

$$\bar{T} = \frac{1}{\lambda} \quad (3.2)$$

The reliability function (Fig. 3.1b) is found from equation (2.17),

$$R(t) = e^{-\int_0^t \lambda(\xi) d\xi} \quad 0 < t < +\infty$$

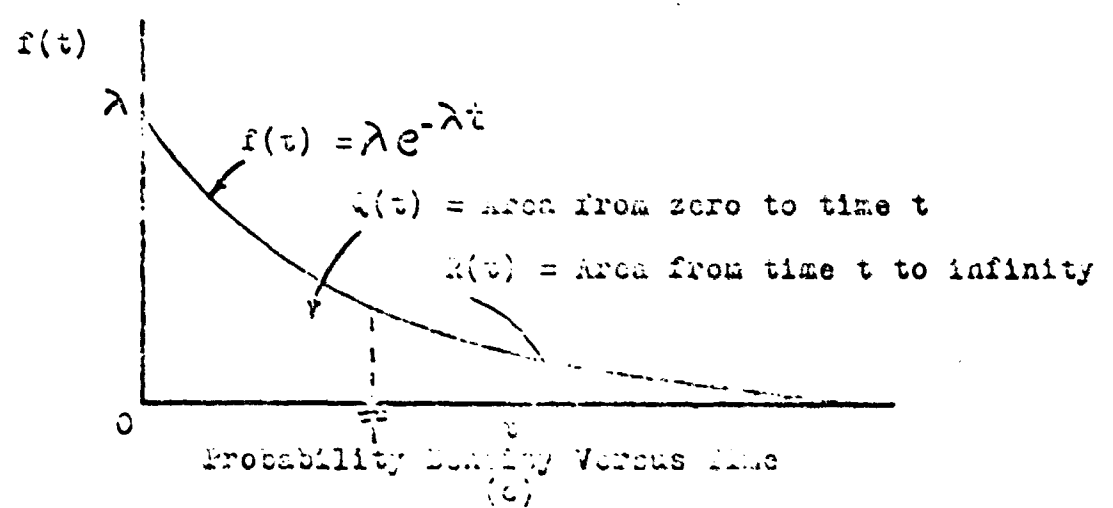
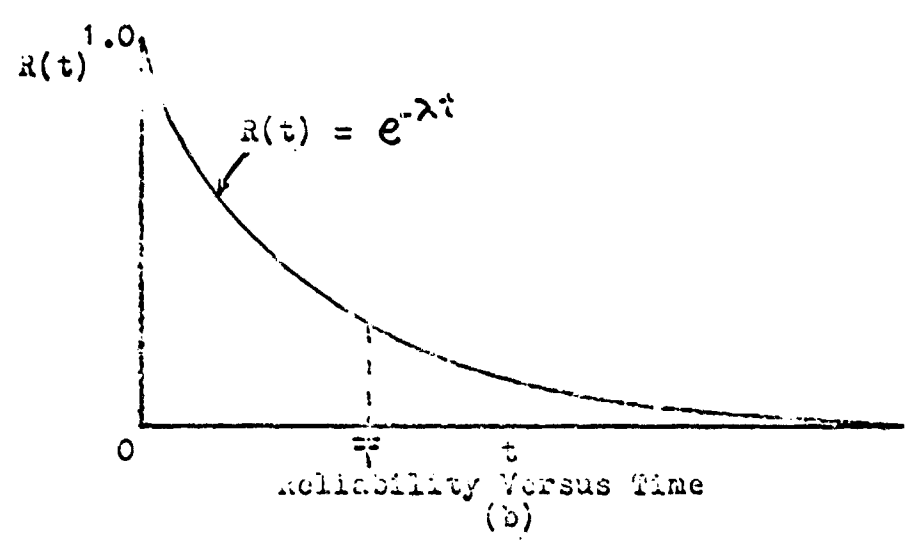
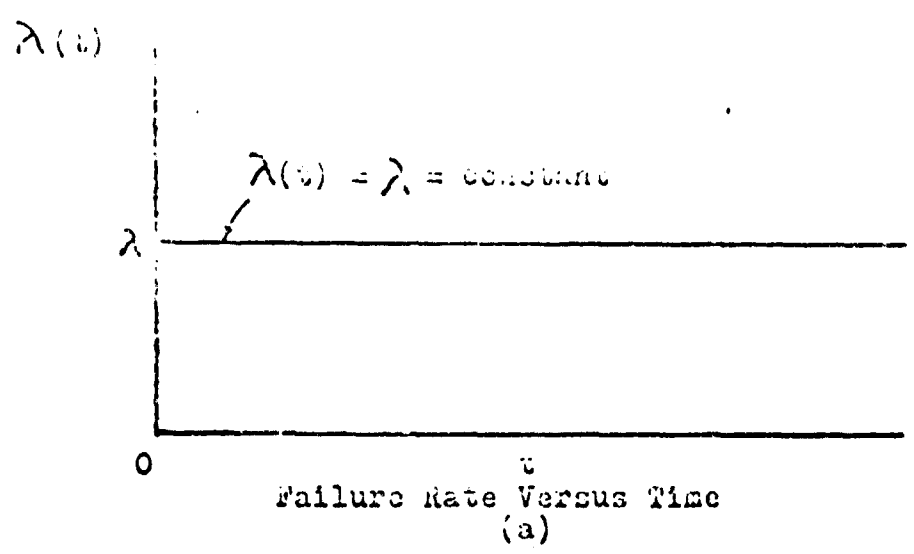


Figure 3.1 Failure Rate, Reliability, and Probability Density Versus Time for Exponentially Distributed Populations

For constant λ

$$R(t) = e^{-\lambda t} \quad 0 < t < +\infty \quad (3.3)$$

The probability density function (Fig. 3.1c) is found by the use of equations (2.16) and (3.3) to be

$$f(t) = \lambda e^{-\lambda t} \quad t \geq 0 \quad (3.4)$$

A preliminary method of determining if failure data follow the exponential distribution is to plot the median rank, which is similar in concept to the cumulative percent failing, versus time on logarithmic paper (Ref. 7, p. 2). The median rank, M.R., in percent is defined as

$$\text{M.R.} = \frac{N_f(t) - 0.3}{N + 0.4} (100) \quad (3.5)$$

If the plotted points closely approximate a straight line the data are assumed to be exponentially distributed. However, since there is no measure of the accuracy of this graphical method, a goodness-of-fit test such as the Chi-Square or the Kolmogorov-Smirnov test should be used as verification. If the data do not fall on a straight line a γ correction can be applied as described in Sec. 3.3 to straighten the curve. If the γ correction does not produce the desired result, other probability papers should be tried.

3.2 The Normal Distribution

Historically, much of the early work with the normal distribution concerned heights and weights of humans and animals, crop yields for different soils and localities, and student examination scores (8, p. 8). Unlike an exponentially distributed population which suffers its greatest losses prior to the mean time \bar{T} , the normally distributed population suffers its greatest loss around the mean time \bar{T} . In life testing it has been observed that failures of the wearout type are often normally distributed about a mean wearout age.

The normal probability density function (Fig. 3.2c) is

$$f(t) = \frac{1}{\sigma \sqrt{2\pi}} e^{-\frac{1}{2} \left(\frac{t - \bar{T}}{\sigma} \right)^2} \quad -\infty < t < \infty \quad (3.6)$$

where \bar{T} is the mean time to failure,

$$\bar{T} = \sum_{i=1}^N (t_i / N) \quad (3.7)$$

and σ is the standard deviation

$$\sigma = \left[\frac{\sum_{i=1}^N (t_i - \bar{T})^2}{N-1} \right]^{1/2} = \left[\frac{\sum_{i=1}^N t_i^2 - N\bar{T}^2}{N-1} \right]^{1/2} \quad (3.8)$$

The reliability function (Fig. 3.2b) is

$$R(t) = \frac{1}{\sigma \sqrt{2\pi}} \int_t^{\infty} e^{-\frac{1}{2} \left(\frac{\xi - \bar{T}}{\sigma}\right)^2} d\xi \quad (3.9)$$

and the failure rate function (Fig. 3.2a) is

$$\lambda(t) = \frac{e^{-\frac{1}{2} \left(\frac{t - \bar{T}}{\sigma}\right)^2}}{\int_t^{\infty} e^{-\frac{1}{2} \left(\frac{\xi - \bar{T}}{\sigma}\right)^2} d\xi} \quad (3.10)$$

A preliminary method of determining if failure data are normally distributed is to plot the Median Ranks (equation (3.5)) versus time on normal or arithmetic probability paper. If the plotted points closely approximate a straight line the data are assumed to be normally distributed. As in the exponential case a goodness-of-fit test should be used for verification. If the data do not fall on a straight line other probability paper should be tried. King (8, p.9) suggests that a concave downward plot on normal probability paper usually suggests a left-skewed distribution and the next step after such a result would be to use extreme value probability paper. He further proposes that a concave upward plot indicates a right skewed distribution and such a result would indicate the use of log-normal probability paper, although extreme value, chi-square, reciprocal, Weibull and log-extreme value probability papers are also possibilities.

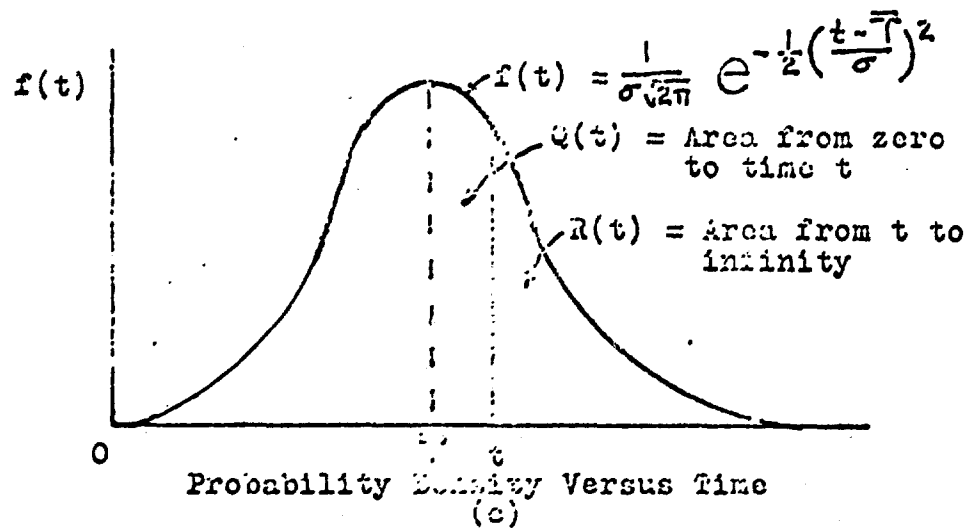
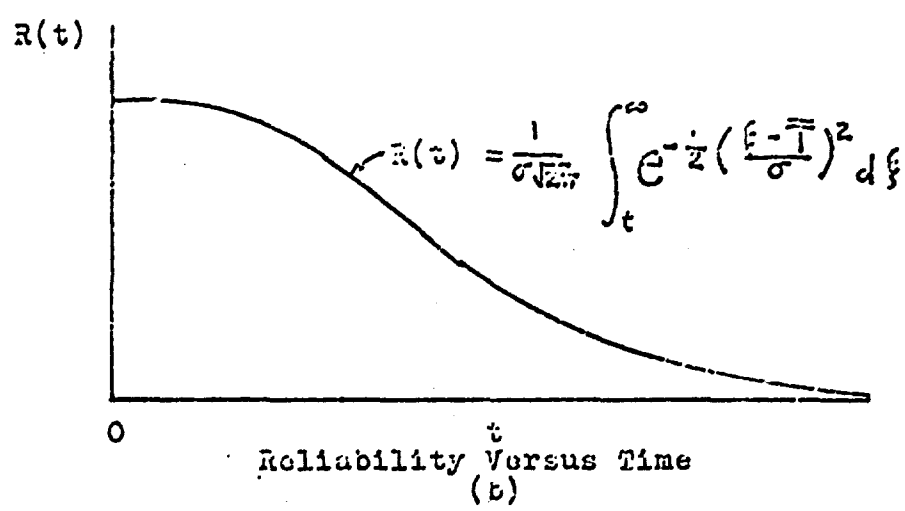
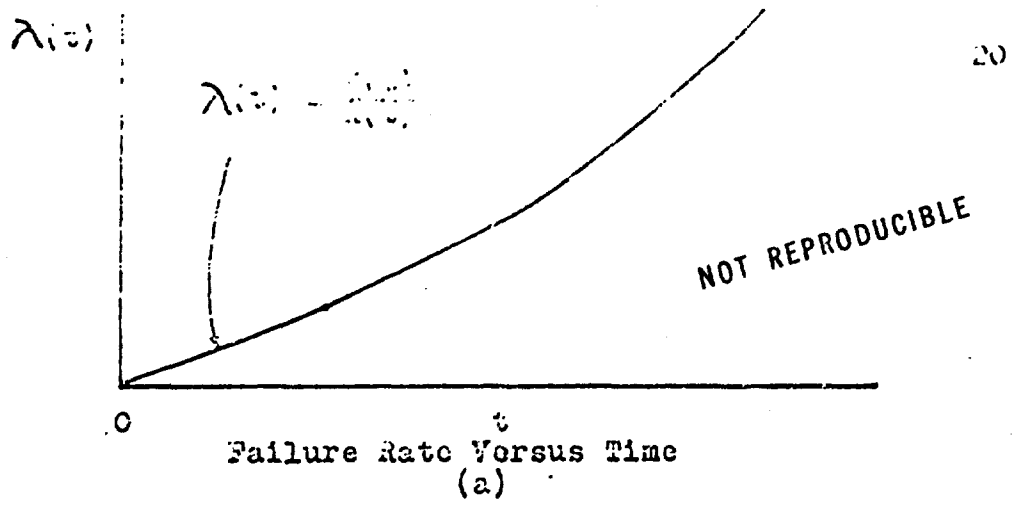


Figure 3.2 Failure Rate, Reliability, and Probability Density Versus Time for Normally Distributed Populations

3.3 The Weibull Distribution

In 1951 Waloddi Weibull published a paper concerning the breaking strength of materials and the size distribution of fly ash (9). Because of the great flexibility of the statistical distribution introduced in this paper the Weibull distribution has been found to be quite useful in other fields including reliability testing. The Weibull probability density function (Fig. 3.3c) is

$$f(t) = \frac{\beta}{\eta} \left(\frac{t-\gamma}{\eta}\right)^{\beta-1} e^{-\left(\frac{t-\gamma}{\eta}\right)^\beta}, \quad t \geq \gamma \quad (3.11a)$$

$$f(t) = 0, \quad t < \gamma \quad (3.11b)$$

where,

β = Shape parameter

$$\beta > 0$$

η = Scale parameter

$$\eta > 0$$

γ = Location parameter

$$-\infty < \gamma < \infty$$

The effect of varying the shape parameter is shown in Fig. 3.3 for $\gamma = 0$ and $\beta = 1/2$, $\beta = 1$, and $\beta = 3$. For β less than 1, the failure rate decreases with time and for β greater than 1, the failure rate increases with time. For $\beta = 1$, the density function becomes that of the exponential case with constant failure rate $\lambda = \frac{1}{\eta}$. For $\beta = 3$, the function approximates the shape of the normal distribution.

The Weibull reliability function (Fig. 3.3b) is

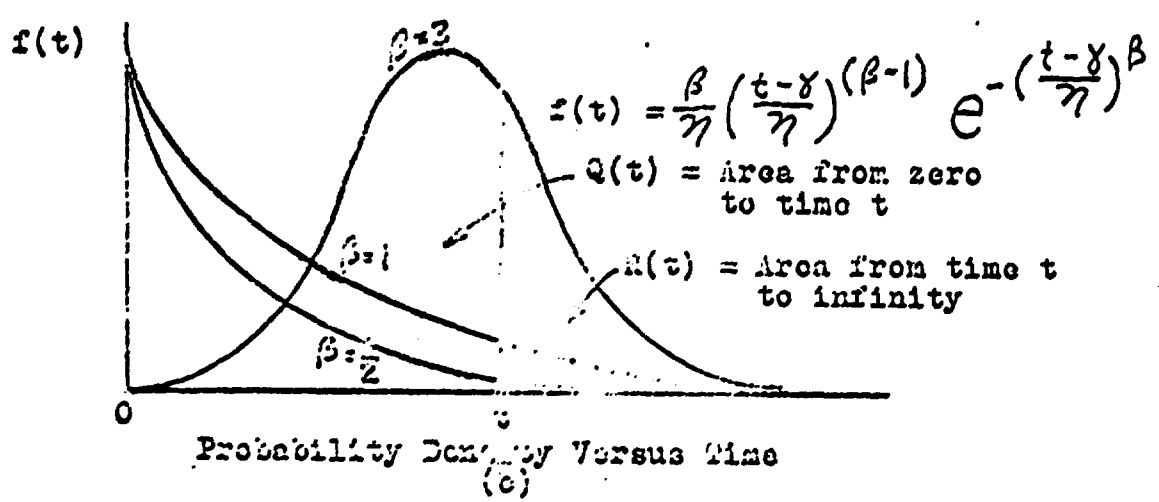
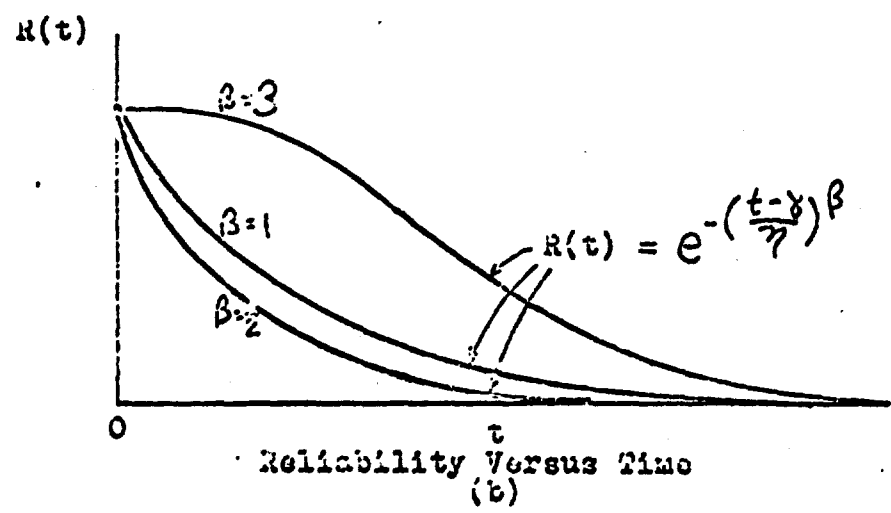
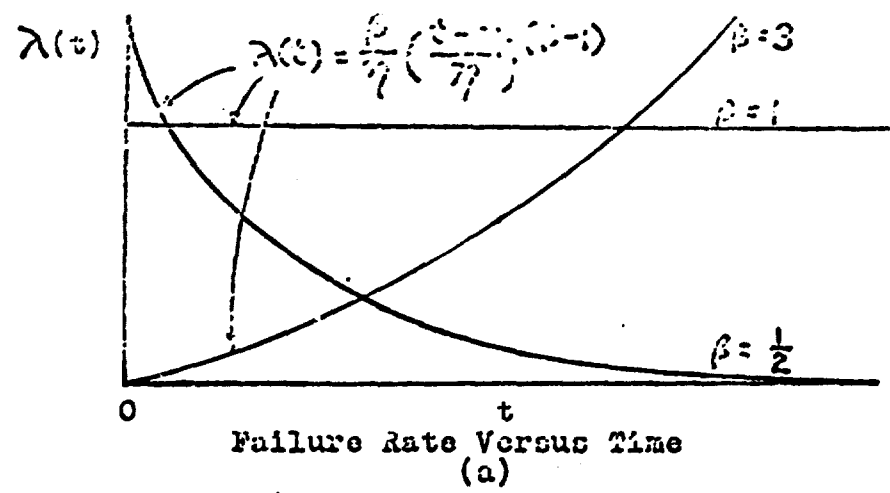


Figure 5.3 failure rate, Reliability, and Probability Density Versus Time for Weibull distributed Populations

$$R(t) = e^{-\left(\frac{t-\gamma}{\eta}\right)^\beta} \quad (3.12)$$

The failure rate function (Fig. 3.3a) is

$$\lambda(t) = \frac{\beta}{\eta} \left(\frac{t-\gamma}{\eta}\right)^{\beta-1} \quad (3.13)$$

Other properties of the Weibull Distribution which are useful in life testing are:

The mean time to failure,

$$\bar{T} = \gamma + \left[\Gamma\left(1 + \frac{1}{\beta}\right)\right] \eta \quad (3.14)$$

where Γ is the Gamma function.

The standard deviation,

$$\sigma = \eta \left[\Gamma\left(1 + \frac{2}{\beta}\right) - \Gamma^2\left(1 + \frac{1}{\beta}\right) \right]^{1/2} \quad (3.15)$$

The modal value of t , that is, the time at which the greatest number of failures occur,

$$\tilde{T} = \gamma + \eta \left(1 - \frac{1}{\beta}\right)^{1/\beta} \quad (3.16)$$

The median value of t , that is, the time at which half the units in test will have failed,

$$\check{T} = \gamma + \eta (\ln 2)^{1/\beta} \quad (3.17)$$

Determining if failure data follow the Weibull distribution is more complicated than the procedure for the normal or exponential distributions. The first step is to find the median rank (equation (3.5)).

Lochner provides a convenient table for median ranks which is good for fifty or fewer items in test (10). Note that if N and $N_f(t)$ are very large,

$$\text{M.R.} \approx 100 Q(t) \quad (3.18)$$

Once the median ranks are determined they are plotted versus the times to failure on Weibull Probability Paper. If the plotted points approximate a straight line it is concluded that the distribution is Weibull and the location parameter γ is equal to zero (Fig. 3.4a). It is far more likely, however, that the plotted points will approximate a curved rather than a straight line on the first trial. If this is the case, γ is not equal to zero and it is necessary to plot the median ranks again; but this time versus $t - t_1$, where t_1 is the time that the first failure was recorded.

Three possible cases may arise:

- Case 1. Both sets of data curve up (Fig. 3.4b). This indicates that $-\infty < \gamma < 0$. Continue plotting the median ranks against $t - \gamma_1$, until a value of γ_1 is found which gives M.R. versus $t - \gamma_1$ as a straight line.
- Case 2. The first set of data curves down and the second set ($t - t_1$) curves up (Fig. 3.4c). This indicates that $0 < \gamma < t_1$. Continue plotting the median ranks against $t - \gamma_1$ for positive values of γ_1 .

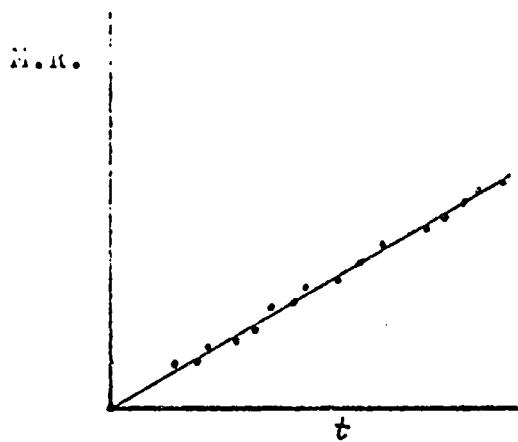
between 0 and t_1 , until a value of γ_i is found which gives M.R. versus $t - \gamma_i$ as a straight line.

Case 3. Both sets of data curve down (Fig. 3.4d). The failure data being analysed do not follow the Weibull distribution and other probability distributions should be considered.

If Case 1 or Case 2 prevails, the data fit the Weibull distribution and γ is equal to the trial γ_i which produces the best straight line approximation.

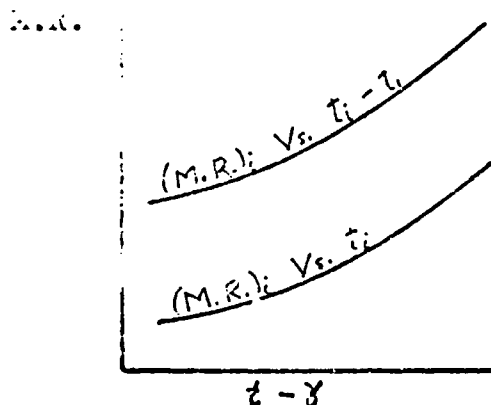
The shape parameter, β , is actually a measure of the slope of the M.R. versus $t - \gamma$ line. Most Weibull papers have an origin through which a line may be drawn parallel to the M.R. versus $t - \gamma$ line. This parallel line will intersect the β scale on the paper and the value of β can be read directly. To find the value of the scale parameter, η , first find the intersection of the M.R. versus $t - \gamma$ line with the horizontal line at M.R. = 63.2%. From this point of intersection drop a vertical line. Read the value of $t - \gamma$ where the vertical line crosses the abscissa. This value of $t - \gamma$ is η .

Since the graphical method gives no measure of the accuracy of the fit of the distribution to the data, it is prudent to verify the graphical procedure by the use of a goodness-of-fit test.



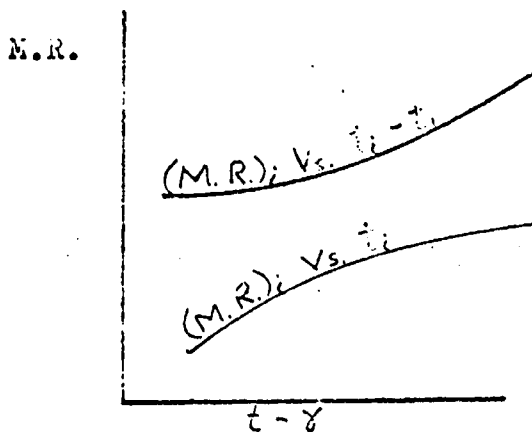
$\gamma = 0$

(a)



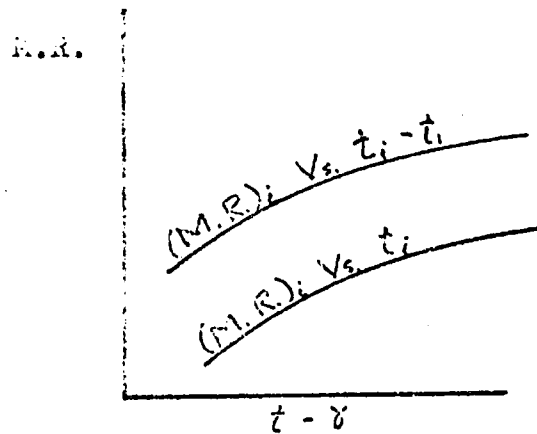
$-\infty < \gamma < 0$

(b)



$0 < \gamma < t_1$

(c)



γ indeterminate

(d)

Figure 3.4 Determination of the γ Parameter for the Weibull Distribution

3.4 Test for Goodness-of-fit

Although there are several valid goodness-of-fit tests available, only the Kolmogorov-Smirnov method will be discussed here since it provides a valid measure of the goodness-of-fit for any distribution and is simple to apply (11, p. 68).

The procedure is to compare the observed unreliability,

$$Q_{\text{obs}}(t_i) = \frac{N_f(t_i)}{N}$$

with the expected unreliability, $Q_{\text{exp}}(t_i)$, as computed by the distribution of interest. The absolute difference, D , between these two cumulative values is noted for each failure time t_i .

$$D_i = |Q_{\text{obs}}(t_i) - Q_{\text{exp}}(t_i)| \quad (3.19)$$

where $i = 1$ for the first failure, 2 for the second failure and finally, $i = N$ for the Nth failure.

The maximum value of D_i is compared with values from the Kolmogorov-Smirnov Table of significance levels (Table 3.1). If the value of the maximum D_i is less than the value given by the Kolmogorov-Smirnov Table for the sample size N and at a specified significance level, we can accept the distribution in question at the specified level of significance. If, on the other hand, the maximum D_i is

greater than the value in the table, the distribution is rejected at the specified significance level.

For example, it is desired to know if the exponential distribution may be used at the .05 level of significance to represent the failure data of 10 items in life test. The D_i 's are calculated at the 10 times to failure. The maximum absolute difference is found to be $D_3 = .45732$. Entering Table 3.1 with N of 10 and a significance level of .05, the maximum allowable value of D at the .05 level of significance is read as .410. Since D_3 is higher than the allowable value the exponential distribution is rejected with a level of significance of .05. Had D_3 been less than .410 the exponential distribution would have been accepted with a significance level of .05. Note that the values of maximum allowable D become more stringent with increasing values of the level of significance. For most purposes and for this paper a level of significance of .05 is considered sufficient to accept a trial distribution.

Table 3.1 D values for the Kolmogorov-Smirnov Goodness-of-fit Test at Various Significance Levels and Sample Sizes (11)

Sample Size (N)	Level of Significance				
	0.20	0.15	0.10	0.05	0.01
1	0.900	0.925	0.950	0.975	0.995
2	0.684	0.726	0.776	0.842	0.929
3	0.565	0.597	0.642	0.708	0.828
4	0.494	0.525	0.564	0.624	0.733
5	0.446	0.474	0.510	0.565	0.669
6	0.410	0.436	0.470	0.521	0.618
7	0.381	0.405	0.438	0.486	0.577
8	0.358	0.381	0.411	0.457	0.543
9	0.339	0.360	0.388	0.432	0.514
10	0.322	0.342	0.368	0.410	0.490
11	0.307	0.326	0.352	0.391	0.468
12	0.295	0.313	0.338	0.375	0.450
13	0.284	0.302	0.325	0.361	0.433
14	0.274	0.292	0.314	0.349	0.418
15	0.266	0.283	0.304	0.338	0.404
16	0.258	0.274	0.295	0.328	0.392
17	0.250	0.266	0.286	0.318	0.381
18	0.244	0.259	0.278	0.309	0.371
19	0.237	0.252	0.272	0.301	0.363
20	0.231	0.246	0.264	0.294	0.356
25	0.21	0.22	0.24	0.27	0.32
30	0.19	0.20	0.22	0.24	0.29
35	0.18	0.19	0.21	0.23	0.27
Over 35	$\frac{1.07}{\sqrt{N}}$	$\frac{1.14}{\sqrt{N}}$	$\frac{1.22}{\sqrt{N}}$	$\frac{1.36}{\sqrt{N}}$	$\frac{1.63}{\sqrt{N}}$

3.5 Symbols Introduced in Chapter 3

D	Absolute difference between expected and observed unreliabilities
e	Base of natural logarithms, $e = 2.71828\dots$
i	Subscript indicates 1,2,3,... in turn
j	Subscript indicates 1,2,3,... in turn
M.R.	Median Rank
$Q_{\text{exp}}(t_i)$	Expected unreliability at time t_i based on a known distribution
$Q_{\text{obs}}(t_i)$	Observed value of unreliability at time t_i
\bar{T}	Median time (half of units in test have failed)
\tilde{T}	Modal time (greatest number of failures occur)
\bar{T}	Mean time (arithmetic average of failure times)
Γ	Gamma function
β	Weibull shape parameter
δ	Weibull location parameter
η	Weibull scale parameter
σ	Standard deviation

CHAPTER 4

THE FAILURE RATE CURVE

4.1 Introduction

In the early 1950's, after plotting failure rate data over a period of years for various electrical and complex mechanical devices, it became evident to researchers that the failure rate curves of many of these unrelated items had certain characteristics in common. It was observed, for example, that in the early portion of component life there was an initially high failure rate which decreased with increasing component age. During the long middle portion of component life the failure rates were observed to level off and become relatively constant. Failures during this period occurred at random intervals not related to component age. Finally, an increasing failure rate was noted as the components became worn. An idealized failure rate curve of the type described above is shown in Fig. 4.1a. The shape of the curve has earned it the name, "bathtub curve." The failure rate curve is of particular

interest in this study because the three failure regions, early, chance, and wearout are more distinct on this curve than on either the $R(t)$ or $f(t)$ curves (Fig. 4.1b,c).

The necessity for separating the failure regions is apparent when it is considered that each failure mode follows a distinct statistical distribution, and, therefore, requires individual mathematical treatment. A second reason for separating the failure regions is that each failure mode requires a different physical technique to improve reliability.

In the next three sections the principle mechanisms accounting for early, chance, and wearout failures will be considered.

4.2 Early Failures

A high incidence of early failures in a component population is an indication of poor quality control and improper debugging and burn-in procedures. Substandard components are initially weaker than the good components in a mixed population and therefore they fail at much lower levels of stress (Fig. 4.2a). As the higher failure rate, substandard items fail and are removed from the population, the population failure rate decreases (12, p. 4).

The Weibull distribution with $\beta < 1$ has been used to represent the early failure period. Mendenhall and

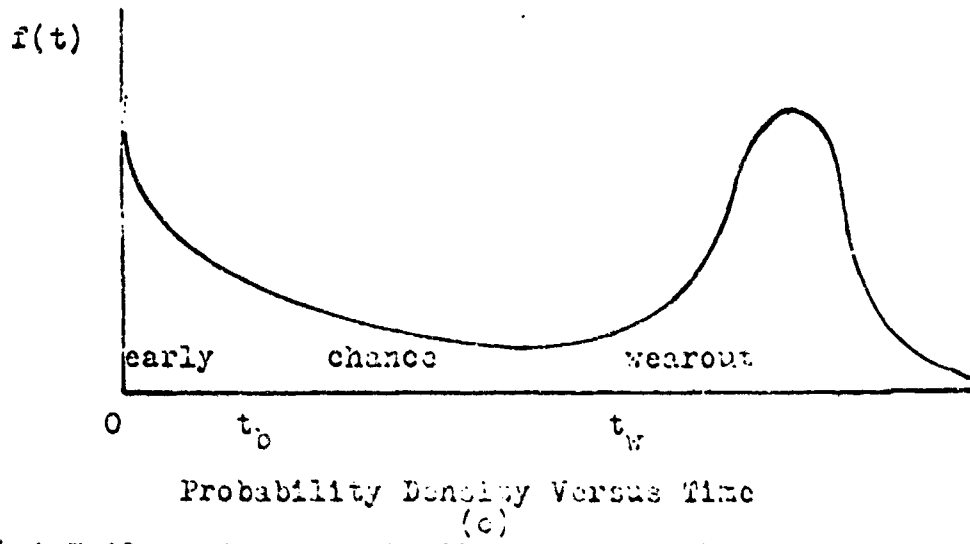
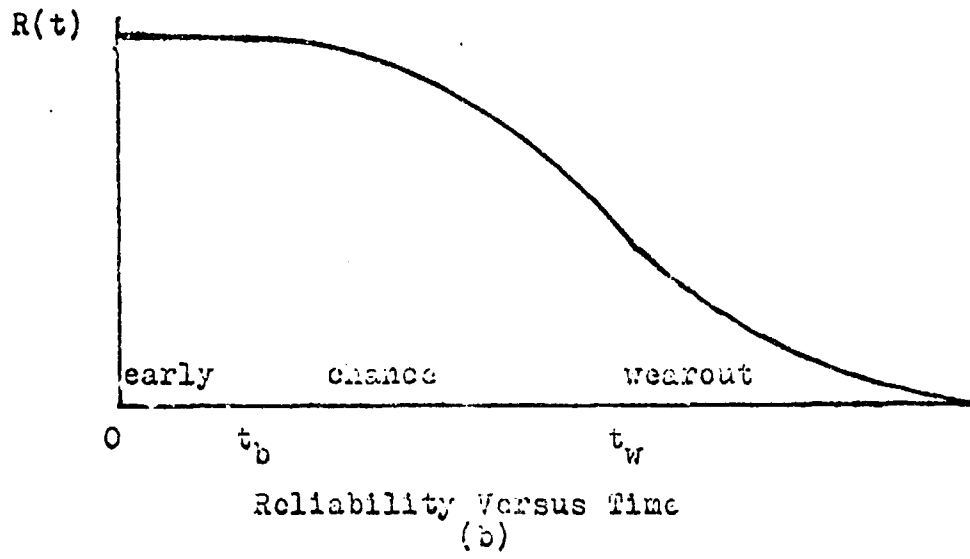
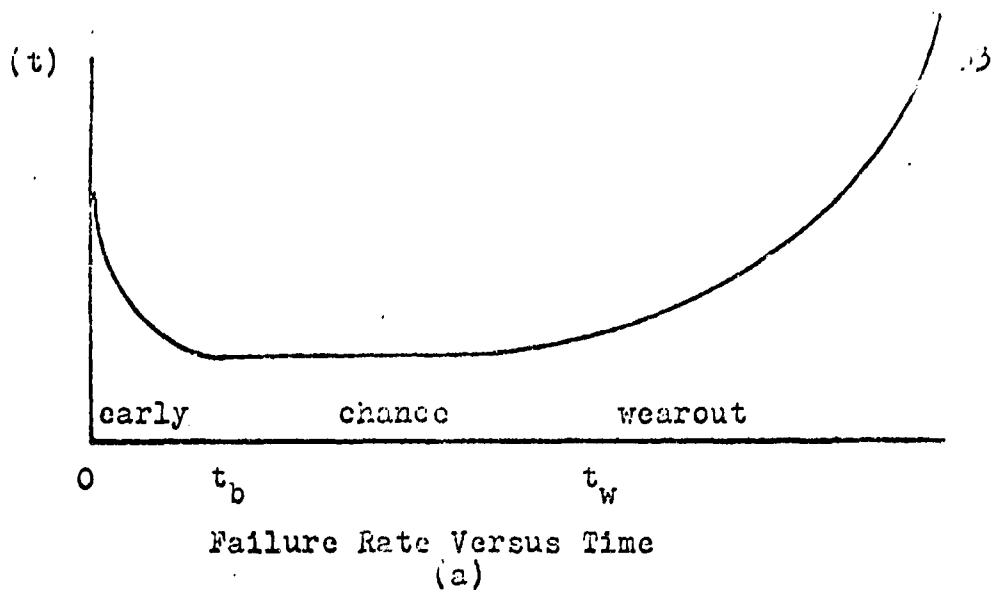


Figure 4.1 Failure Rate, Reliability, and Probability Density Versus Time for a Mixed Failure Population Exhibiting Early, Chance, and Wearout Failures

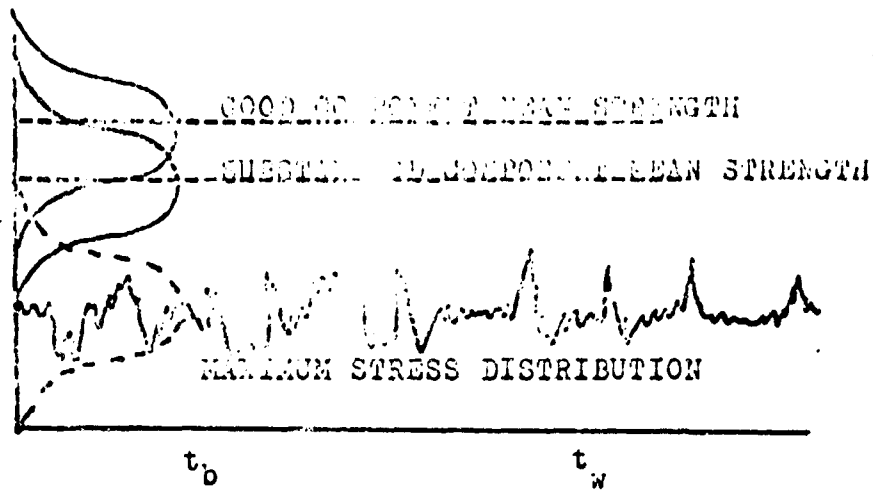
Hader have also shown that a combination of two exponential distributions with different values of λ for the early and chance failure periods will give the characteristic decreasing failure rate of the early period (13).

4.3 Chance Failures

Chance failures occur randomly and are independent of component age; that is, they occur during the entire period that a component is in service and not just during the chance period. In the early period, chance failures occur together with early or substandard failures, and in the wearout phase, chance failures occur with the wearout failures. During the chance failure period it is assumed that only chance failures occur. All the substandard items have already failed and wearout has not yet begun. Chance failures are caused by sudden, unpredictable stress accumulations (Fig. 4.2b).

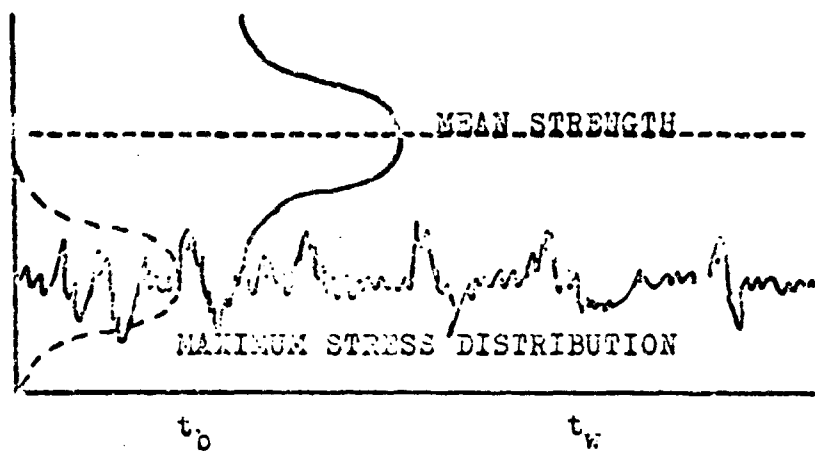
The exponential distribution is most frequently used to model the theoretically constant failure rate which characterizes the chance period of component life. A more flexible model is the Weibull distribution with β approximately equal to 1. This distribution does not require an absolutely constant failure rate in order to have a good fit to observed failure data.

STRENGTH
AND
STRESS



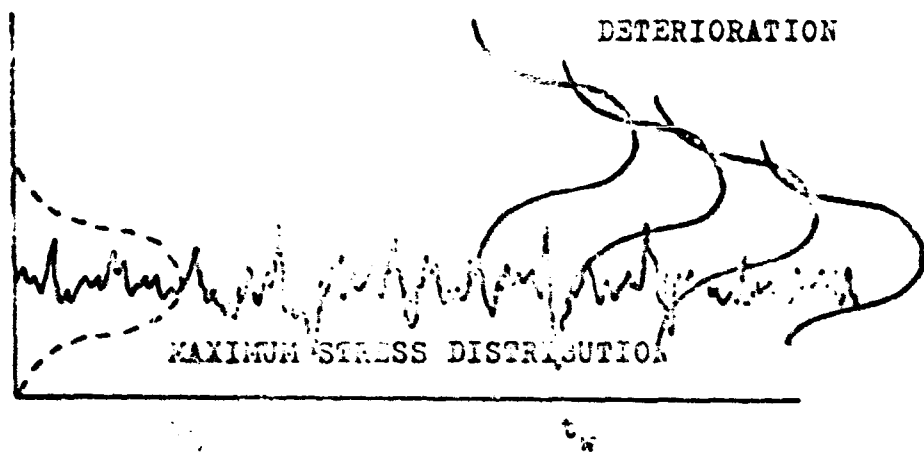
Early Failure Mechanism
(a)

STRENGTH
AND
STRESS



Chance Failure Mechanism
(b)

STRENGTH
AND
STRESS



Wearout Failure Mechanism
(c)

Figure 4.2 Early, Chance, and Wearout Failure Mechanisms

4.4 Wearout Failures

After the chance period of life, component deterioration begins and failures become a function of age. As the surviving components become older they also grow weaker and more subject to failure at lower levels of stress. Thus, deterioration produces the characteristic increasing failure rate of the wearout period (Fig. 4.2c).

Both the normal distribution and the Weibull distribution with β greater than 1 have been successfully used to model the increasing failure rate of the wearout period.

4.5 Summary

In this chapter it has been shown that the individual failure events can be modeled by known statistical distributions. It remains to be shown, however, that the entire bathtub curve including early, chance, and wearout failures can be modeled by a unified mathematical expression derived from accepted reliability theory. The remaining chapters are devoted to finding such an expression.

CHAPTER 5

THE BASIS FOR A UNIFIED EXPRESSION

5.1 Criteria for a Good Model

Curve fitting techniques could be used to fit a mathematical expression to observed failure data, but this would provide very little insight into the mechanics of failure and would not be of great use in reliability improvement. A mathematical model based on the theory of failure would, on the other hand, provide relevant information about failure modes which would be quite useful in analysing failure data and for improving product reliability. For the purpose of this study a good model of the combined failure rate curve is defined as one which meets the following criteria:

- a. The unified model must combine the phenomena of early, chance, and wearout failures.
- b. The number of restrictive assumptions necessary to derive the model should be minimal.
- c. The model should be mathematically simple if at all possible.

- d. The model should correspond to observed failure data at the .05 significance level for the Kolmogorov-Smirnov Goodness-of-fit Test.
- e. The model should be useful for prediction and for theoretical speculation.
- f. The theoretical basis for the model must be consistent with the manner in which the data are generated.

5.2 The Product Rule

If it is assumed that there is a single population of identical components and that the events of early failure, chance failure, and wearout failure are independent, that is to say, that the occurrence of one type of failure in no way alters the probability of occurrence of the other types of failure, then the unified unreliability would be as shown in the Venn diagram (Fig. 5.1). For independent events the joint probability of several events occurring is simply the product of the individual probabilities. The enclosed area of the Venn diagram is

$$\begin{aligned}
 Q_{ecw}(t) = & Q_e(t) + Q_c(t) + Q_w(t) - Q_e(t) Q_c(t) \\
 & - Q_e(t) Q_w(t) - Q_c(t) Q_w(t) \\
 & + Q_e(t) Q_c(t) Q_w(t)
 \end{aligned} \tag{5.1}$$

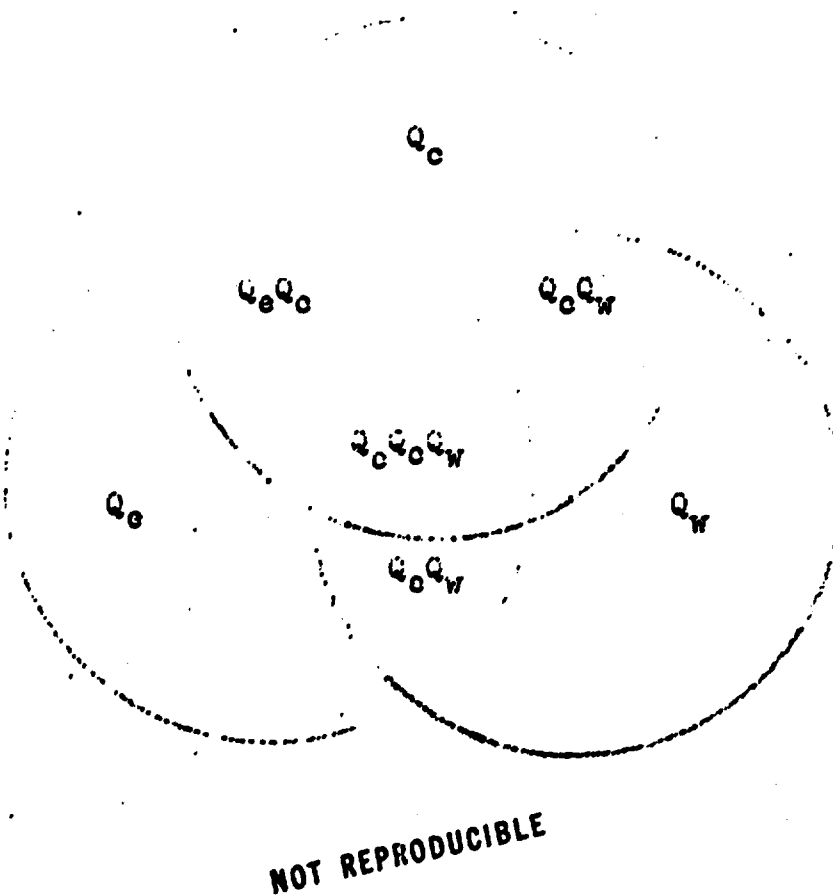


Figure 5.1 Venn Diagram for Early, Chance, and Wearout Failures Considered as Independent Events

where

$$Q_e(t) = \frac{N_{e,f}(t)}{N_e}$$

$$Q_c(t) = \frac{N_{c,f}(t)}{N_c}$$

$$Q_w(t) = \frac{N_{w,f}(t)}{N_w}$$

If each Q term is replaced by its complement, $1 - R$, the reliability product rule is obtained.

$$R_{ecw}(t) = R_e(t) R_c(t) R_w(t) \quad (5.2)$$

where

$$R_e(t) = \frac{N_{e,s}(t)}{N_e}$$

$$R_c(t) = \frac{N_{c,s}(t)}{N_c}$$

$$R_w(t) = \frac{N_{w,s}(t)}{N_w}$$

Equation (5.2) is a potential model of the combined reliability curve and it does meet certain of the specified criteria set forth in Section 5.1. For example, the product rule does combine the effects of the three failure phenomena. There is only one limiting assumption: independent failure events. And the product rule is a very simple expression. The crucial question is whether or not the

product rule corresponds to the observed failure data. To answer this question, consider equation (5.2) with the individual reliabilities replaced by their respective definitions

$$R_{ecw}(t) = \frac{N_{e,s}(t)}{N_e} \times \frac{N_{c,s}(t)}{N_c} \times \frac{N_{w,s}(t)}{N_w} \quad (5.3)$$

At the end of the early period it is assumed that all early failures have occurred, consequently, $N_{e,s}(t_b) = 0$. The result of this is that for all t greater than t_b , the combined reliability given by equations (5.2) and (5.3) is zero. This result is in direct conflict with physical observations of mixed samples which indicate that the reliability at $t = t_b$ is normally quite high. For this reason the product rule which includes early failures as independent failure events in a single population is rejected as a possible model of the combined failure rate curve. The possibility of using the product of reliabilities for chance and wearout failures alone will be considered in Section 5.4.

An interesting sidelight to the product rule is the convenient but incorrect expression

$$\lambda = \lambda_e + \lambda_c$$

which has been used, on occasion, by reliability engineers to represent the combined early and chance failure rate during early life. This simple expression might appear valid after a casual inspection of the failure rate curve (Fig. 4.1a). However, it is derived by the combination of the reasonable assumption that both early and chance failures are of the exponential type with the incorrect assumption that reliability in early life is represented by the product of early and chance reliabilities. Mathematically,

$$R_{ec}(t) = R_e(t) R_c(t)$$

or

$$e^{-\lambda t} = e^{-\lambda_e t} e^{-\lambda_c t}$$

Taking the natural log

$$\lambda = \lambda_e + \lambda_c$$

which is incorrect since it was shown previously that

$$R_{ec}(t) \neq R_e(t) R_c(t)$$

and therefore,

$$\lambda \neq \lambda_e + \lambda_c$$

5.3 The Summation Rule

Consider a hypothetical non-replacement, life test of N components. The components are placed in test at time $t = 0$ without prior burn-in or debugging. As each component fails, the time to failure is recorded and the test is terminated when the last component in test fails. To assist in visualizing the problem, assume that the components are of a type that can be examined after failure and the mode of failure determined, be it early, chance, or wearout. As items fail during the test they are removed from the test population, inspected, and segregated into three lots according to failure type. At the conclusion of the test there will be three subpopulations of N_e , N_c , and N_w failed items, respectively where $N_e + N_c + N_w = N$. If the events of the tests are now reconstructed, it may be theorized that at time $t = 0$ there were actually three separate subpopulations in test each with an individual failure density distribution, even though at time $t = 0$ no failures had yet occurred and therefore the subpopulations were not physically distinguishable. It is not pertinent in making this assumption that the items actually be inspected to determine N_e , N_c , and N_w , as the subpopulations would exist even if these values were unknown or were physically indeterminable. A graphical method for finding

N_e , N_c , and N_w from observed failure data is suggested in Chapter 6.

If the proposition that there are three failure subpopulations is accepted, a mathematical expression combining the effects of the subpopulations may be found directly. The cumulative number of items failing in the mixed population is found from the definition of unreliability

$$N_{ecw,f}(t) = N Q_{ecw}(t) \quad (5.4)$$

Similarly, the number failing from each of the subpopulations is

$$\begin{aligned} N_{e,f}(t) &= N_e Q_e(t) \\ N_{c,f}(t) &= N_c Q_c(t) \end{aligned} \quad (5.5)$$

$$N_{w,f}(t) = N_w Q_w(t)$$

The total number of failures by time t in the mixed population is simply the sum of the failures in the three subpopulations.

$$N_{ecw,f}(t) = N_{e,f}(t) + N_{c,f}(t) + N_{w,f}(t) \quad (5.6)$$

Substituting equations (5.4) and (5.5) into equation (5.6) yields

$$N Q_{ecw}(t) = N_e Q_e(t) + N_c Q_c(t) + N_w Q_w(t) \quad (5.7)$$

or

$$Q_{ecw}(t) = \frac{N_e}{N} Q_e(t) + \frac{N_c}{N} Q_c(t) + \frac{N_w}{N} Q_w(t) \quad (5.8)$$

This expression could also have been derived directly from Bayes' Theorem (14, p. 57), which, for this example, says that the unreliability of a component drawn at random from a mixed population composed of three failure subpopulations is the summation of three terms: the probability that the component is from the early subpopulation times its unreliability if it is from the early subpopulation, plus the probability that the component is from the chance subpopulation, times its unreliability if it is from the chance subpopulation, plus the probability that the component is from the wearout subpopulation times its unreliability if it is from the wearout subpopulation. This may be written mathematically as

$$Q_{ecw}(t) = \frac{N_e}{N} Q_e(t) + \frac{N_c}{N} Q_c(t) + \frac{N_w}{N} Q_w(t)$$

which is identical to equation (5.8).

If in equation (5.8) each of the unreliability terms is replaced by its complement, $Q = 1 - R$, a unified reliability expression is obtained as follows:

$$1 - R_{ecw}(t) = \frac{N_e}{N} [1 - R_e(t)] + \frac{N_c}{N} [1 - R_c(t)] + \frac{N_w}{N} [1 - R_w(t)]$$

$$1 - R_{ecw}(t) = \frac{N_e}{N} - \frac{N_e}{N} R_e(t) + \frac{N_c}{N} - \frac{N_c}{N} R_c(t) + \frac{N_w}{N} - \frac{N_w}{N} R_w(t)$$

since

$$N_e + N_c + N_w = N$$

or

$$\frac{N_e}{N} + \frac{N_c}{N} + \frac{N_w}{N} = 1$$

it follows that

$$1 - R_{ecw}(t) = 1 - \frac{N_e}{N} R_e(t) - \frac{N_c}{N} R_c(t) - \frac{N_w}{N} R_w(t)$$

This reduces to the unified reliability function

$$R_{ecw}(t) = \frac{N_e}{N} R_e(t) + \frac{N_c}{N} R_c(t) + \frac{N_w}{N} R_w(t) \quad (5.9)$$

which is also called the reliability summation rule.

The other functions of interest are found by applying the equations of Chapter 2 to equation (5.9).

From equation (2.12) it is known that

$$f_{ecw}(t) = - \frac{d}{dt} [R_{ecw}(t)] \quad (5.10)$$

For the summation model this becomes

$$f_{ecw}(t) = \frac{N_e}{N} \left[- \frac{d}{dt} R_e(t) \right] + \frac{N_c}{N} \left[- \frac{d}{dt} R_c(t) \right] + \frac{N_w}{N} \left[- \frac{d}{dt} R_w(t) \right]$$

which reduces to

$$f_{ecw}(t) = \frac{N_e}{N} f_e(t) + \frac{N_c}{N} f_c(t) + \frac{N_w}{N} f_w(t) \quad (5.11)$$

This equation is also given by K. L. Wong (4, p.19) as representing the combined probability density function when early, chance, and wearout failures are present. Applying

equation (2.11) to equation (5.9) it is shown that

$$\lambda_{ecw}(t) = \frac{f_{ecw}(t)}{R_{ecw}(t)} \quad (5.12)$$

or,

$$\lambda_{ecw}(t) = \frac{\frac{N_e}{N} f_e(t) + \frac{N_c}{N} f_c(t) + \frac{N_w}{N} f_w(t)}{\frac{N_e}{N} R_e(t) + \frac{N_c}{N} R_c(t) + \frac{N_w}{N} R_w(t)} \quad (5.13)$$

The mission reliability for a mission of duration T starting at time t with a surviving component is found by use of equation (2.20)

$$R_{ecw}(t, T) = \frac{R_{ecw}(t + T)}{R_{ecw}(t)} \quad (5.14)$$

which expands to

$$R_{ecw}(t, T) = \frac{\frac{N_e}{N} R_e(t + T) + \frac{N_c}{N} R_c(t + T) + \frac{N_w}{N} R_w(t + T)}{\frac{N_e}{N} R_e(t) + \frac{N_c}{N} R_c(t) + \frac{N_w}{N} R_w(t)} \quad (5.15)$$

A cursory check of the criteria for a good model given in Section 5.1 shows that the summation rule does meet certain of the specified criteria. The Phenomena of early, chance, and wearout failures are combined. The single assumption required for this model is that the mixed population be composed of three individual failure subpopulations. The model is mathematically simple and if the above assumption is correct, this model would be useful for prediction

and theoretical speculation. The correspondence of the model to observed failure data cannot be shown as simply as the other criteria considered here and, therefore, this will be considered in detail as a separate subject in Chapters 7, 8, and 9. Conclusions concerning the validity of the summation rule as a model for component reliability are held in abeyance until further examination is provided.

5.4 Combined Product and Summation Rules

It was shown in Section 5.2 that early failures could not be combined with chance or wearout failures by use of the product rule because the unified reliability would go to zero at the end of the early life period. In Section 5.3 it was shown that this problem did not occur when the summation rule was used as the unified reliability model. A third possible combination of reliabilities exists and there is ample theoretical basis for its consideration as will be shown.

In Section 5.3 it was theorized that wearout failures and chance failures could be considered as separate failure subpopulations. A re-examination of Fig. 4.2 would cast some doubt on this. Figure 4.2a clearly shows two subpopulations, the substandard and the good. The substandard subpopulation contributes the early failures,

whereas, the good subpopulation contributes both the chance and the wearout failures (Fig. 4.2b,c). It was noted in Section 4.3 that in the early period both early (substandard) and chance failures occur. This means that in the early period two subpopulations are in test and the summation rule may be applied. In the chance and wearout periods, however, only the good subpopulation is in test, the substandard items having already failed. The good subpopulation provides both the chance and wearout failures. For a good component to survive during the chance and wearout periods it must survive both types of hazard, chance failure and wearout (deterioration) failures. This is a serial arrangement of reliabilities to which the product rule must be applied.

The unified reliability of a component drawn at random from a population containing good and substandard components is found directly from Bayes' Theorem to be the sum of two terms: the probability that the component is substandard times its reliability if it is substandard, plus the probability that the component is good times its reliability if it is good (14, p. 57).

Mathematically,

$$R_{ecw}(t) = \frac{N_e}{N} R_e(t) + \frac{N_c + N_w}{N} R_e(t) R_w(t) \quad (5.16)$$

where $N_c + N_w$ is equal to the number of good components in test, N_G . The other functions of interest are found by applying the general equations developed in Chapter 2 and in Section 5.3 of this chapter to equation (5.16). From equation (5.10)

$$f_{ecw}(t) = - \frac{d}{dt} [R_{ecw}(t)]$$

For the combined model this is

$$f_{ecw}(t) = \frac{N_e}{N} \left\{ - \frac{d}{dt} R_e(t) \right\} + \frac{N_c + N_w}{N} \left\{ - \frac{d}{dt} [R_c(t) R_w(t)] \right\}$$

which may be written

$$f_{ecw}(t) = \frac{N_e}{N} \left\{ - \frac{d}{dt} R_e(t) \right\} + \frac{N_c + N_w}{N} \left\{ R_c(t) \left[- \frac{d}{dt} R_w(t) \right] + R_w(t) \left[- \frac{d}{dt} R_c(t) \right] \right\}$$

Therefore, the combined probability density function is

$$f_{ecw}(t) = \frac{N_e}{N} f_e(t) + \frac{N_c + N_w}{N} [R_c(t) f_w(t) + R_w(t) f_c(t)] \quad (5.17)$$

From equation (5.12)

$$\lambda_{ecw}(t) = \frac{f_{ecw}(t)}{R_{ecw}(t)}$$

which gives the combined failure rate

$$\lambda_{ecw}(t) = \frac{\frac{N_e}{N} f_e(t) + \frac{N_c + N_w}{N} [R_c(t) f_w(t) + R_w(t) f_c(t)]}{\frac{N_e}{N} R_e(t) + \frac{N_c + N_w}{N} R_c(t) R_w(t)} \quad (5.18)$$

The mission reliability for a mission of duration T starting at time t is found from equation (5.14) to be

$$R_{ecw}(t, T) = \frac{\frac{N_e}{N} R_e(t+T) + \frac{N_c + N_w}{N} R_c(t+T) R_w(t+T)}{\frac{N_e}{N} R_e(t) + \frac{N_c + N_w}{N} R_c(t) R_w(t)} \quad (5.19)$$

A check of the criteria for a good model given in Section 5.1 shows that the combined product and summation rule does meet certain of the specified criteria. The phenomena of early, chance, and wearout failures are combined. The single restricting assumption is that there are two failure subpopulations, one exhibiting only early failures and the other exhibiting both chance and wearout failures. The model is mathematically simple and if the assumption above is correct the model would be useful for prediction and theoretical speculation. Of the three potential models considered in this section, two still remain and require further analysis.

5.5 Comparison of Different Models

Thus far in this chapter three potential unified reliability models have been considered: the reliability product model, the reliability summation model, and a combined product and summation model. The product model was eliminated because it went to zero at the end of the

early period. Therefore it is prudent, before going to Chapter 6, to compare the two remaining models at several critical time periods during component life to insure that the models are valid during the entire lifetime and to provide a comparison of the two equations during the different periods. The equations which will be compared are equation (5.9), the reliability summation rule, and equation (5.16), the combined product and summation rule.

At time $t = 0$ no components have failed, and, therefore, $R_e = R_c = R_w = 1$.

SUMMATION RULE ($t = 0$)

$$R_{ecw}(0) = \frac{N_e}{N} (1) + \frac{N_c}{N} (1) + \frac{N_w}{N} (1)$$

or

$$R_{ecw}(0) = \frac{N_e + N_c + N_w}{N}$$

Since $N_e + N_c + N_w = N$,

$$R_{ecw}(0) = \frac{N}{N} = 1 \quad (5.20)$$

COMBINED RULE ($t = 0$)

$$R_{ecw}(0) = \frac{N_e}{N} (1) + \frac{N_c + N_w}{N} (1)$$

or,

$$R_{ecw}(0) = \frac{N_e + N_c + N_w}{N} = \frac{N}{N} = 1 \quad (5.21)$$

Hence, both rules give the desired result for $t = 0$.

Next consider the period $0 \leq t \leq t_w$. The individual

reliabilities are $R_e = R_e(t)$, $R_c = R_c(t)$, and $R_w = 1$ since wearout does not begin prior to t_w .

$$\begin{array}{c} \text{SUMMATION RULE } (0 \leq t \leq t_w) \\ \hline R_{ecw}(t) = \frac{N_e}{N} R_e(t) + \frac{N_c}{N} R_c(t) + \frac{N_w}{N} \end{array} \quad (5.22)$$

$$\begin{array}{c} \text{COMBINED RULE } (0 \leq t \leq t_w) \\ \hline R_{ecw}(t) = \frac{N_e}{N} R_e(t) + \frac{N_c + N_w}{N} R_c(t) \end{array} \quad (5.23)$$

Equations (5.22) and (5.23) vary by the amount,

$\frac{N_w}{N} [1 - R_c(t)]$. In tests in which wearout is not considered, $N_w = 0$ and both equations (5.22) and (5.23) reduce to

$$R_{ecw}(t) = \frac{N_e}{N} R_e(t) + \frac{N_c}{N} R_c(t) \quad (5.24)$$

Equation (5.24) is given by Dietrich (15, p. 15), Wong (4, p. 19), Polovko (16, p. 94), and Mendenhall and Hader (13, p. 505).

In the time period $t_b \leq t < \infty$ the individual reliabilities are $R_e = 0$, $R_c = R_c(t)$, and $R_w = R_w(t)$.

$$\begin{array}{c} \text{SUMMATION RULE } (t_b \leq t < \infty) \\ \hline R_{ecw}(t) = \frac{N_c}{N} R_c(t) + \frac{N_w}{N} R_w(t) \end{array} \quad (5.25)$$

COMBINED RULE ($t_b \leq t < \infty$)

$$R_{ecw}(t) = \frac{N_c + N_w}{N} R_c(t) R_w(t) \quad (5.26)$$

Although equations (5.25) and (5.26) are dissimilar, forms of both have been referenced in the literature for the time period after burn-in. Equation (5.25) is given by Polovko (16, p. 95) and by Wong (4, p. 19). Equation (5.26) is given when $N_e = 0$ and therefore $\frac{N_c + N_w}{N} = 1$ by Bazovsky (5, p. 52) and by Pieruschka (17, p. 73).

The two models have now been considered and compared for three critical periods of time during component life and neither has been eliminated. To be of use, however, the parameters of the models must be obtainable. In Chapter 6 a method will be given for obtaining the parameters of the summation rule. The combined model offers a different problem in parameter determination and although considerable effort was expended to find an analytical method for the determination of $R_c(t)$ and $R_w(t)$, no satisfactory method was developed. The only practical technique found for applying equation (5.16) without prior knowledge of $R_c(t)$ and $R_w(t)$ is to eliminate one of the parameters by combining the quantity $R_c(t) * R_w(t)$ into a single term $R_G(t)$. The result of this combination is to reduce the

combined summation-product model to an ordinary summation model with two subpopulations

$$R_{ecw}(t) = \frac{N_e}{N} R_e(t) + \frac{N_G}{N} R_G(t) \quad (5.27)$$

where $N_e + N_G = N$. An expression of this form is used by Kao (18, p. 397) to describe electron tube failures. If the life test is truncated before wearout, equation (5.27) is equivalent to equation (5.24). One method of parameter determination for equation (5.27) is given by Kao (18) and another is given in Chapter 6 of this report. The final choice as to which model to use, equation (5.9) or equation (5.27), must be based on the data itself. A graphical aid to assist in determining the number of underlying subpopulations is suggested in Chapter 6. In cases in which both equation (5.9) and equation (5.27) appear to apply, equation (5.9) is preferred because with its additional parameters it is the more powerful expression.

5.6 Symbols Introduced in Chapter 5

$f_e(t)$	Early probability density function
$f_c(t)$	Chance probability density function
$f_w(t)$	Wearout probability density function
$f_{ecw}(t)$	Unified probability density function
N	Total items in test, $N = N_e + N_c + N_w$
N_e	Total items failing in early mode (substandard)
N_c	Total items failing in chance mode
N_w	Total items failing in wearout mode
N_G	Total good items in test, $N_G = 1 - N_e = N_c + N_w$
$N_{e,f}(t)$	Items failing in early mode by time t
$N_{c,f}(t)$	Items failing in chance mode by time t
$N_{w,f}(t)$	Items failing in wearout mode by time t
$N_{ecw,f}(t)$	Items failing in all modes combined by time t
$N_{e,s}(t)$	Items in early subpopulation surviving by time t
$N_{c,s}(t)$	Items in chance subpopulation surviving by time t
$N_{w,s}(t)$	Items in wearout subpopulation surviving by time t
$Q_e(t)$	Early unreliability $N_{e,f}(t)/N_e$
$Q_c(t)$	Chance unreliability $N_{c,f}(t)/N_c$
$Q_w(t)$	Wearout unreliability $N_{w,f}(t)/N_w$
$Q_{ecw}(t)$	Unified unreliability function

$R_e(t)$	Early (substandard) reliability $N_{e,s}(t)/N_e$
$R_c(t)$	Chance reliability $N_{c,s}(t)/N_c$
$R_w(t)$	Wearout reliability $N_{w,s}(t)/N_w$
$R_G(t)$	Reliability of all good components regardless of failure mechanism
$R_{ecw}(t)$	Unified reliability function
t_b	Time at end of the early period
t_w	Time at beginning of wearout period
$\lambda_{ecw}(t)$	Unified failure rate function

CHAPTER 6

TECHNIQUE FOR APPLYING THE RELIABILITY SUMMATION MODEL

6.1 Introduction

If the early, chance, and wearout failure periods are each modeled by an individual Weibull Distribution, equation (5.9) may be written as

$$R_{ecw}(t) = \frac{N_e}{N} e^{-\left(\frac{t-\gamma_e}{\eta_e}\right)^{\beta_e}} + \frac{N_c}{N} e^{-\left(\frac{t-\gamma_c}{\eta_c}\right)^{\beta_c}} + \frac{N_w}{N} e^{-\left(\frac{t-\gamma_w}{\eta_w}\right)^{\beta_w}} \quad (6.1)$$

where the subscripts e, c, and w indicate individual Weibull parameters for the early, chance, and wearout subpopulations, respectively. In order to use equation (6.1) to compute component reliability it is necessary to find the three subpopulation sizes N_e , N_c , and N_w and the nine Weibull parameters, γ_e , β_e , η_e , γ_c , β_c , η_c , γ_w , β_w , and η_w .

The subpopulation sizes may be determined by analytical means or by physical failure analysis, but the analytical method is preferred for several reasons:

1. Analytical methods are usually less expensive

and are less time consuming than physical inspection.

2. The components may not lend themselves to physical inspection without sophisticated and expensive test equipment, and the expenditure of much time.
3. The failure data may be old and the components no longer available for inspection.
4. The components may be destroyed upon failure, thus making it impossible to conduct a failure analysis.
5. The components may be in remote or otherwise inaccessible equipment.

Kao (18) suggests a graphical method for separating the subpopulations and finding five Weibull parameters for a mixed population consisting of two subpopulations. For the purpose of this report an attempt was made to extend Kao's original method so that it would apply to the case of three subpopulations, but the effort was abandoned for reasons which are fully discussed in Appendix A.

A graphical method for subpopulation separation is recommended in Section 6.2 and illustrative examples are given in Chapters 7, 8, and 9.

6.2 Parameter Determination

The following steps provide a method for separating a mixed Weibull population into its constituent subpopulations and then of finding the parameters γ , n , and β for each of the subpopulations. The steps are:

1. Compute median ranks for the mixed failure data and plot median ranks versus time on Weibull probability paper.

2. By visual inspection fit straight lines to the plotted data points. For the case of early, chance, and wearout subpopulations there will be three relatively straight line segments on the Weibull plot of the mixed failure data. Points falling closest to the lower line are in the early subpopulation, points falling closest to the middle line are in the chance subpopulation, and points falling closest to the upper line are in the wearout subpopulation.

3. N_e is calculated as the cumulative number of failures represented by the points along the early (lower) line, N_c is calculated as the cumulative number of failures represented by the points along the chance (middle) line. N_w is calculated as the cumulative number of failures represented by the points along the wearout (upper) line.

4. Compute new median ranks for each subpopulation based on sample sizes N_e , N_c and N_w , respectively.

5. Replot each subpopulation on individual Weibull paper and determine δ , η , and β for each subpopulation by the method described in Section 3.3.

Using the above graphical procedures, all of the unknown quantities in equation (6.1) may be estimated. The method described in this chapter will be applied to raw data in the next three chapters. Human mortality is considered for illustrative purposes in Chapter 7 while Chapters 8 and 9 deal with Klystron and Magnetron failures respectively.

CHAPTER 7

APPLICATION OF THE RELIABILITY SUMMATION MODEL TO HUMAN MORTALITY

7.1 The Data to be Analysed

If mortality is plotted versus time for a large sample of humans, the resulting curve provides a classic example of a mixed population exhibiting infantile, chance, and deterioration failures or, in this case, deaths. Experience has shown that the observed failure data of some electrical and complex mechanical systems is similar to that of human mortality. For this reason and because the data are familiar, human mortality has been selected as the subject for this first application of the reliability summation model. A sample population of 1000 Americans has been assumed and the mortality data for this population are given in Table 7.1. The sample data are based upon survival probabilities given by Reference 19. The data of Table 7.1 are grouped into twenty, 5-year class intervals and the mortality and force of mortality histograms are plotted in Figs. 7.1 and 7.2

Table 7.1 Mortality Table for 1000 Americans

Age At Class Interval End Point	Probability of Survival at Beginning of 5-Year Period	Number Dying During 5-Year Period	Proba- bility Density Function	Proba- bility of Death at End of 5-Year Period	Force of Mortal- ity $\frac{f_{ecw}(t)}{R_{ecw}(t)}$
t	$R_{ecw}(t)$	Deaths	$f_{ecw}(t)$	$Q_{ecw}(t)$	$\lambda_{ecw}(t)$
5	1.000	13	.013	.013	.013
10	.987	6	.006	.019	.006
15	.981	6	.006	.025	.006
20	.975	8	.008	.033	.008
25	.967	9	.009	.042	.009
30	.958	10	.010	.052	.012
35	.948	11	.011	.063	.012
40	.937	13	.013	.076	.014
45	.924	19	.019	.095	.021
50	.905	29	.029	.124	.032
55	.876	43	.043	.167	.049
60	.833	63	.063	.230	.076
65	.770	90	.090	.320	.117
70	.680	121	.121	.441	.178
75	.559	146	.146	.587	.261
80	.413	150	.150	.737	.363
85	.283	132	.132	.869	.466
90	.131	84	.084	.953	.640
95	.047	37	.037	.990	.789
100	.010	10	.010	1.000	1.000

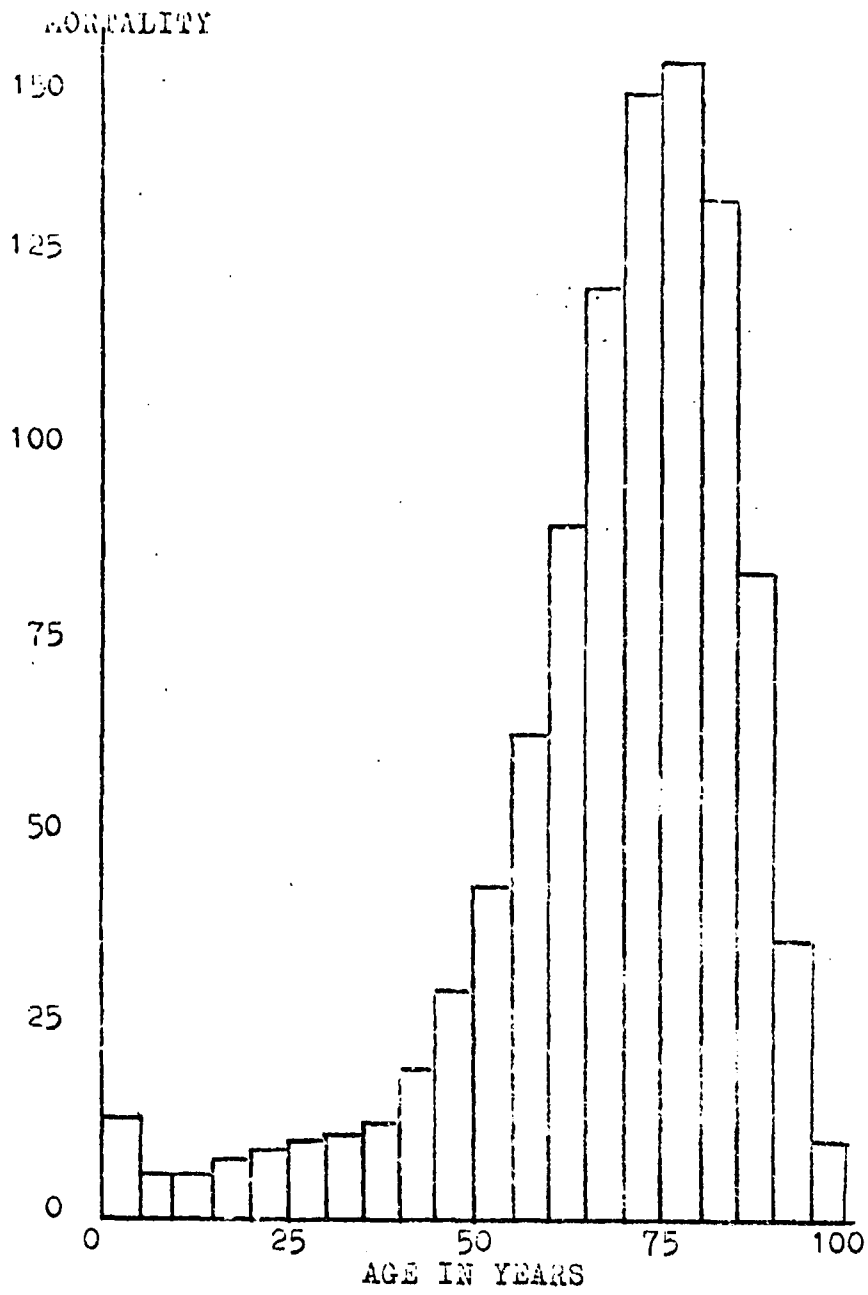


Figure 7.1 Mortality Histogram for 1000 Americans



Figure 7.2 Force of Mortality Histogram for 1000 Americans

7.2 Parameter Determination

The example data are prepared for plotting by computing the median rank for each class interval. In this case the sample was so large that the median ranks were considered equal to the cumulative percent failing. The median ranks and class interval end points are tabulated in Table 7.2 and the data are plotted on Weibull probability paper in Fig. 7.3. The median ranks have been plotted at the class interval end points rather than at the mid-points as suggested by some authors, because the failure data are actually accumulated up to the class interval end point and therefore this would seem to be the more logical location for the median ranks. Three straight lines are fitted amongst the points plotted in Fig. 7.3, and it is determined by visual inspection that points 1 and 2 fall along the line representing the early subpopulation. Points 4 through 9 are identified with the chance subpopulation and points 11 through 20 are placed in the wearout subpopulation. Points 3 and 10 each fall close to two lines and the final determination as to which subpopulation the questionable points should be identified with is not made until after the points have been included in both possible subpopulations and the subpopulations replotted on Weibull paper. This was done and the best straight line approximation occurred when

Table 7.2 Mortality Data Prepared for Plotting

Point Number	Age	Median Rank
1	5	1.3
2	10	1.9
3	15	2.5
4	20	3.3
5	25	4.2
6	30	5.2
7	35	6.3
8	40	7.6
9	45	9.5
10	50	12.4
11	55	16.7
12	60	23.0
13	65	32.0
14	70	44.1
15	75	58.7
16	80	73.7
17	85	86.9
18	90	95.3
19	95	99.0
20	100	100.0

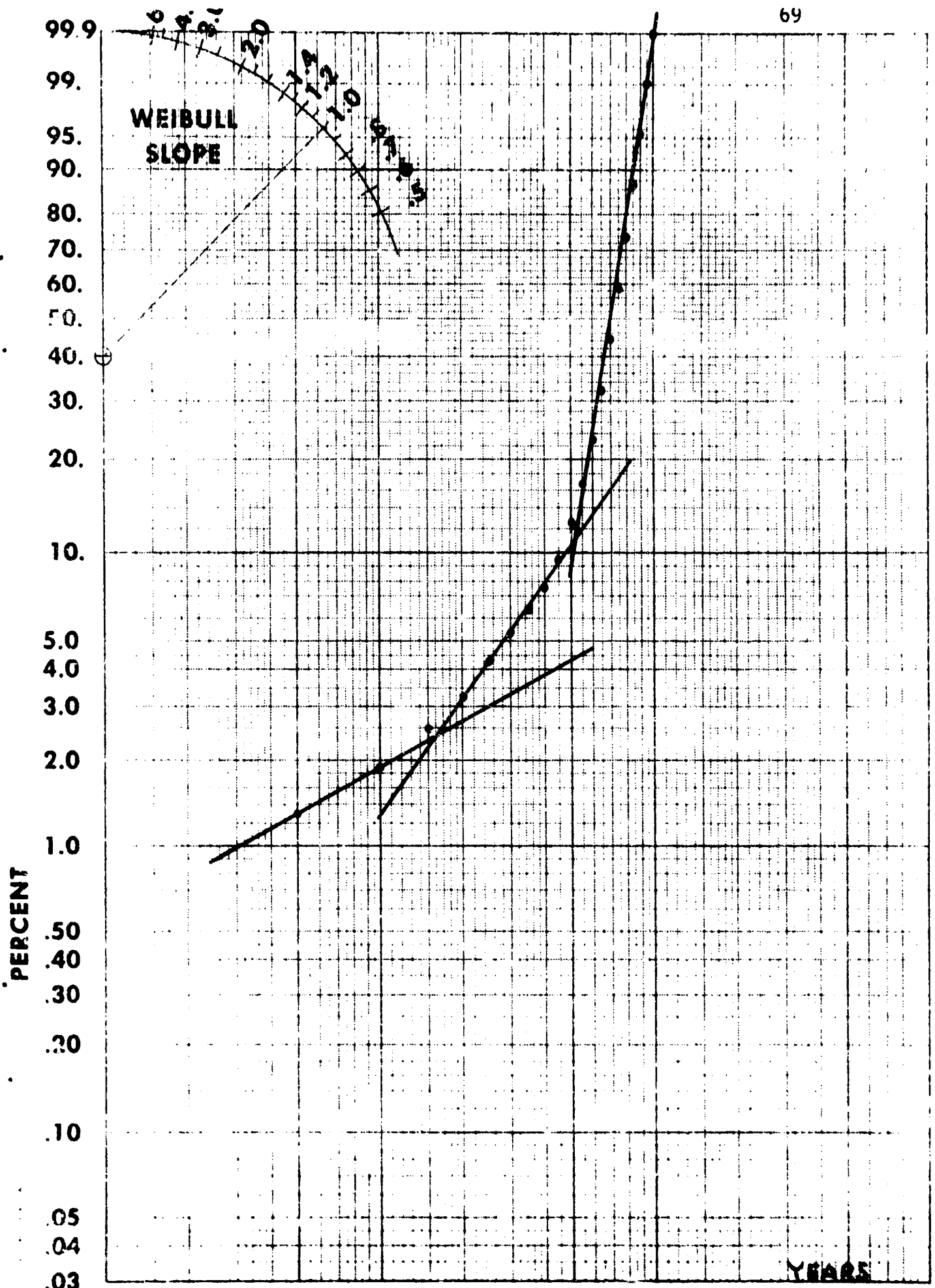


Figure 7.3 Weibull Plot of Human Mortality Mixed Population
 WEIBULL PROBABILITY PAPER

point 3 was included in the chance subpopulation and when point 10 was placed in the wearout subpopulation. All of the points have now been identified with a particular subpopulation. The subpopulation sizes are determined by the total failures represented by the points which fall in the particular subpopulation. Thus

$$N_e = 19$$

$$N_c = 76$$

$$N_w = 905$$

New median ranks are calculated for subpopulation replotting by considering each of the subpopulations as an individual population. The new median ranks are tabulated in Table 7.3 and the subpopulations are replotted individually in Figs. 7.4, 7.5, and 7.6. From these replots, the following Weibull parameters are determined:

Figure 7.4

$$\gamma_e = 0$$

$$\beta_e = 1.60$$

$$\eta_e = 4.85$$

Figure 7.5

$$\gamma_c = 0$$

$$\beta_c = 2.81$$

$$\eta_c = 35.9$$

Table 7.3 Mortality Data Prepared for Subpopulation Replot

	Point Number	Age	Subpopu- lation $N_f(t)$	Median Rank
Early Subpopulation ($N_e = 19$)	1	5	13	65.5
	2	10	19	96.4
Chance Subpopulation ($N_c = 76$)	3	15	6	7.46
	4	20	14	17.95
	5	25	23	29.7
	6	30	33	42.7
	7	35	44	57.3
	8	40	57	74.2
	9	45	76	99.2
Wearout Subpopulation ($N = 905$)	10	50	29	3.17
	11	55	72	7.92
	12	60	135	14.89
	13	65	225	24.8
	14	70	346	38.2
	15	75	492	54.3
	16	80	642	71.0
	17	85	774	85.5
	18	90	858	94.7
	19	95	895	98.7
	20	100	905	99.9

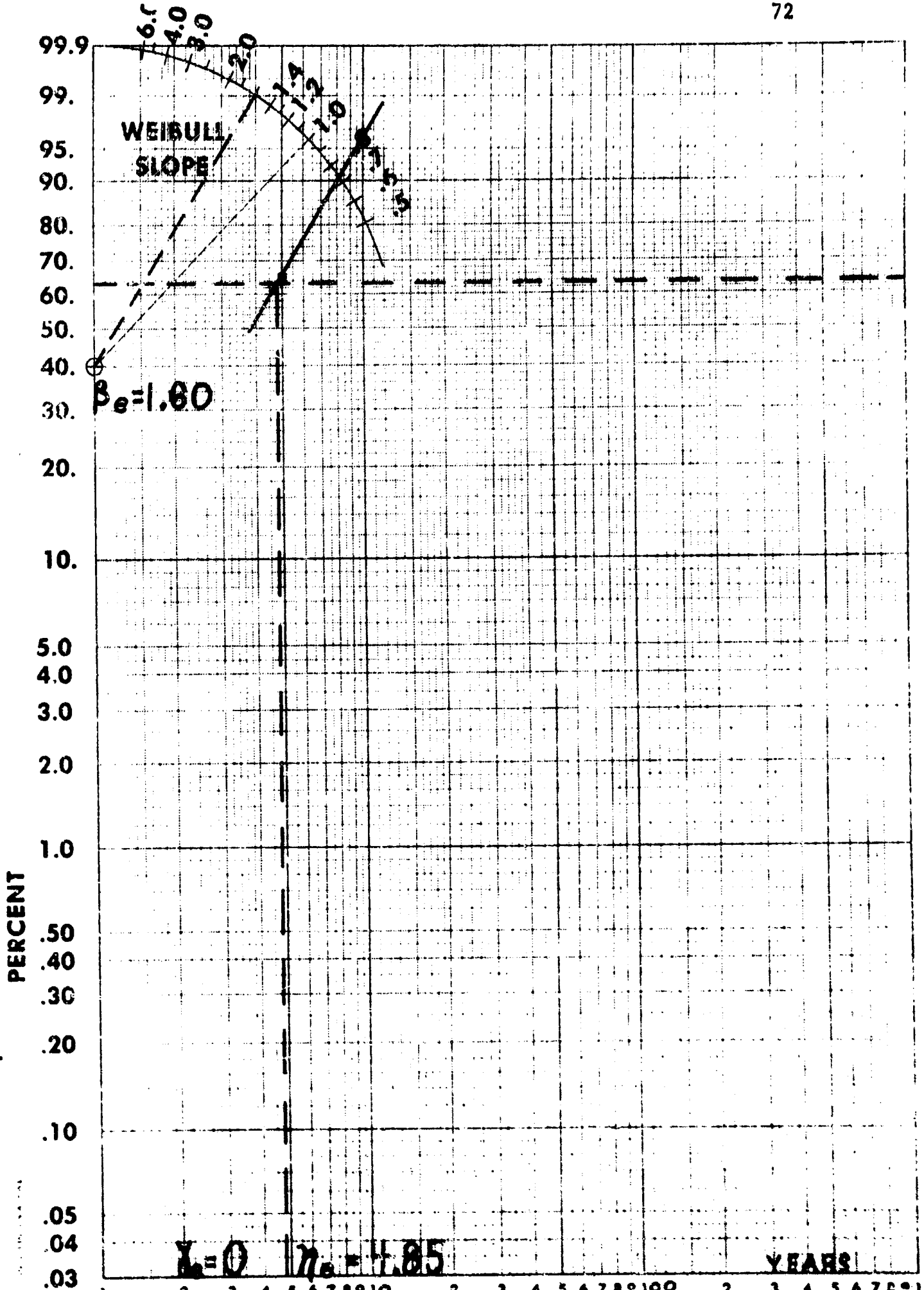
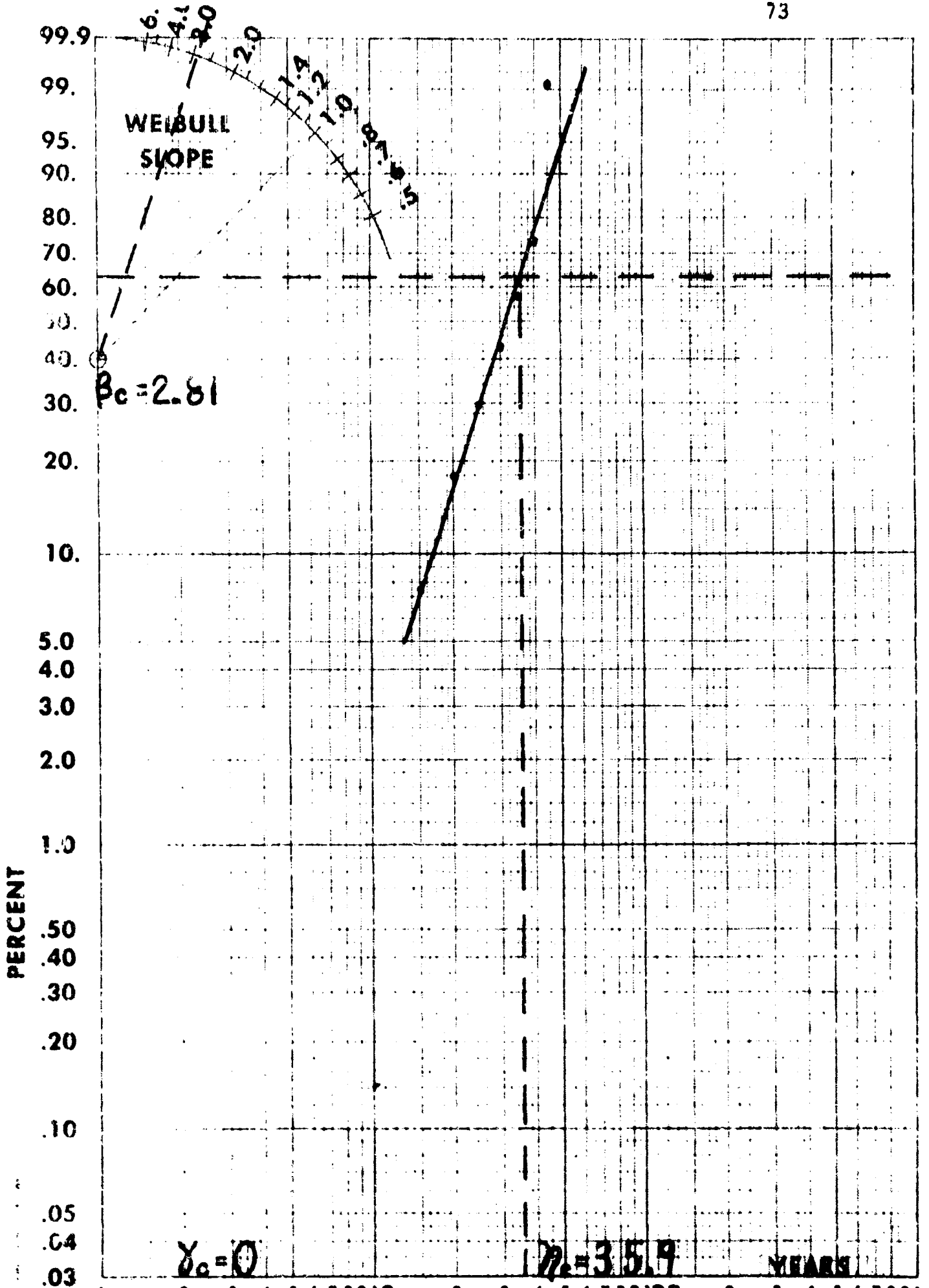


Figure 7.4 Mortality Early Subpopulation Replot

Standard 1950

WEIBULL PROBABILITY PAPER



Figures 7.5 Mortality Chance Subpopulation Replot
 1 2 3 4 5 6 7 8 9 10 2 3 4 5 6 7 8 9 10 2 3 4 5 6 7 8 9 10
 WEIBULL PROBABILITY PAPER

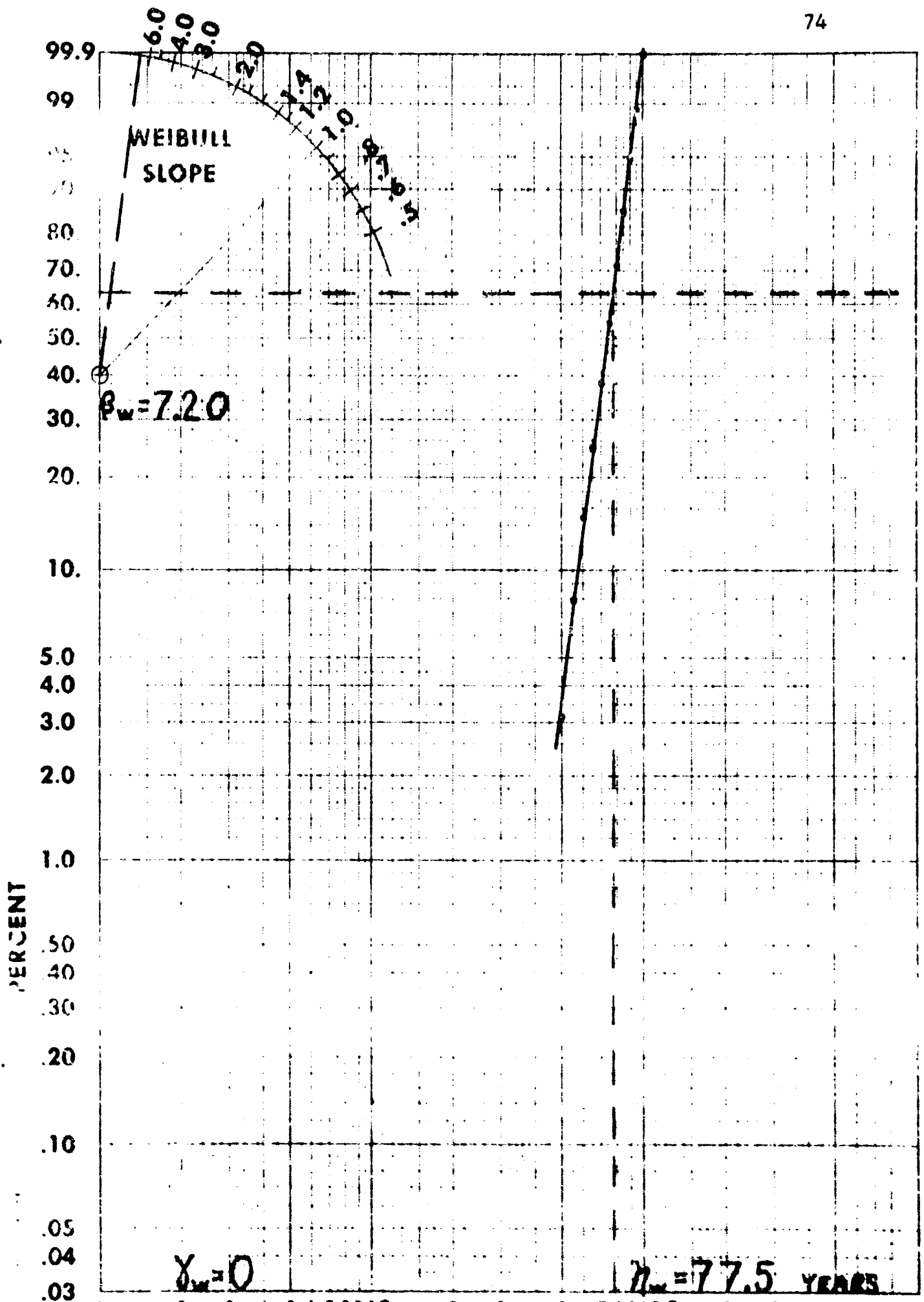


FIGURE 7.6 Mortality Wearout Subpopulation Replot

Figure 7.6

$$\gamma_w = 0$$

$$\beta_w = 7.20$$

$$\eta_w = 77.5$$

All parameters necessary to use equation (6.1) have been determined and the equation may now be used to find reliability, or in this case the probability of living, for all positive values of t . For example, consider $t = 30$ years. Equation (6.1) is

$$R_{ecw}(t) = \frac{N_e}{N} e^{-\left(\frac{t-\gamma_e}{\eta_e}\right)^{\beta_e}} + \frac{N_c}{N} e^{-\left(\frac{t-\gamma_c}{\eta_c}\right)^{\beta_c}} + \frac{N_w}{N} e^{-\left(\frac{t-\gamma_w}{\eta_w}\right)^{\beta_w}}$$

Substituting numerical values for each of the parameters gives

$$\begin{aligned} R_{ecw}(t) &= \frac{19}{1000} e^{-\left(\frac{30-0}{4.85}\right)^{1.6}} + \frac{76}{1000} e^{-\left(\frac{30-0}{35.9}\right)^{7.81}} + \frac{905}{1000} e^{-\left(\frac{30-0}{77.5}\right)^{7.2}} \\ &= .019(.962 \cdot 10^{-8}) + .076(.547) + .905(.999) \\ &= .946 \end{aligned}$$

If this sample of 1000 is representative and if equation (6.1) is valid, a human, randomly selected at birth, can be expected to have a 94.6% chance of surviving to age 30. Conversely, the expected probability of dying before age 30 would be

$$Q_{ecw}(30) = 1 - R_{ecw}(30) = 1 - .946$$

$$Q_{ecw}(30) = .054$$

7.3 Goodness-of-Fit

For the purpose of comparison the observed value of $Q_{ecw}(30)$ from the sample of 1000 is found to be .052. The value of the absolute difference between the expected $Q_{ecw}(30)$ and the observed $Q_{ecw}(30)$ is

$$D_{30} = .054 - .052 = .002$$

From the Kolmogorov-Smirnov Table (Table 3.1) for N greater than 35, the asymptotic equations are used to find the maximum allowable value of D at the .05 significance level

$$D = \frac{1.36}{N} = \frac{1.36}{1000} = .00136 \approx .0014$$

To fully test the proposed model for goodness-of-fit, it is necessary to find D_i at each class interval to insure that no value of D_i is greater than .043. This has been done and the values of Q_{ecw} Expected, Q_{ecw} observed, and D_i are tabulated for each class interval in Table 7.4. The maximum D_i is found to be .007. Since .007 is less than the allowable maximum difference of .043 it is concluded that the summation model for three subpopulations does meet the criteria established in Section 5.1 for a good model. The expected and the observed cumulative failure distributions are

Table 7.4 Absolute Difference Between Expected and Observed Cumulative Mortality Data (Summation Model)

Age	Observed	Expected	Absolute Difference
t	$Q_{ecw}(t)$	$Q_{ecw}(t)$	D_i
5	.013	.013	.000
10	.019	.020	.001
15	.025	.025	.000
20	.033	.032	.001
25	.042	.042	.000
30	.052	.054	.002
35	.063	.068	.005
40	.076	.083	.007*
45	.095	.010	.005
50	.124	.127	.003
55	.167	.166	.001
60	.230	.226	.004
65	.320	.317	.003
70	.441	.440	.001
75	.587	.589	.002
80	.737	.742	.005
85	.869	.871	.002
90	.953	.952	.001
95	.990	.988	.002
100	1.000	.998	.002

* Maximum absolute difference

Allowable absolute difference at the .05 significance level is found from Table 3.1 to be

$$\frac{1.36}{\sqrt{N}} = \frac{1.36}{\sqrt{1000}} = .043$$

plotted for visual comparison in Fig. 7.7. The excellent correlation between the observed and the expected data clearly indicates that the reliability summation model is capable of accurately representing the reliability of mixed populations.

7.4 Analysis of Underlying Failure Causes-Early Failures

In Chapter 4 it was shown that the characteristic decreasing failure rate of the early failure period may be produced by a combination of subpopulations, none of which individually exhibits a decreasing failure rate. An interesting example of the phenomenon is provided by the 1958 Commissioner's Standard Ordinary Mortality Table (19). In this case each of the three subpopulations to be combined exhibits a monotonic increasing failure rate (force of mortality) as indicated by the subpopulation shape parameters each being greater than unity. Yet, when these subpopulations are combined into a heterogeneous population the combined failure rate is initially decreasing. This phenomenon may be explained by considering the interaction of the three subpopulations. Table 7.3 indicates that the early subpopulation is composed of only 19 of the 1000 individuals being considered. Because the early subpopulation exhibits a very high failure rate in contrast to the useful and wearout subpopulations it causes an initially high overall failure rate for the heterogeneous

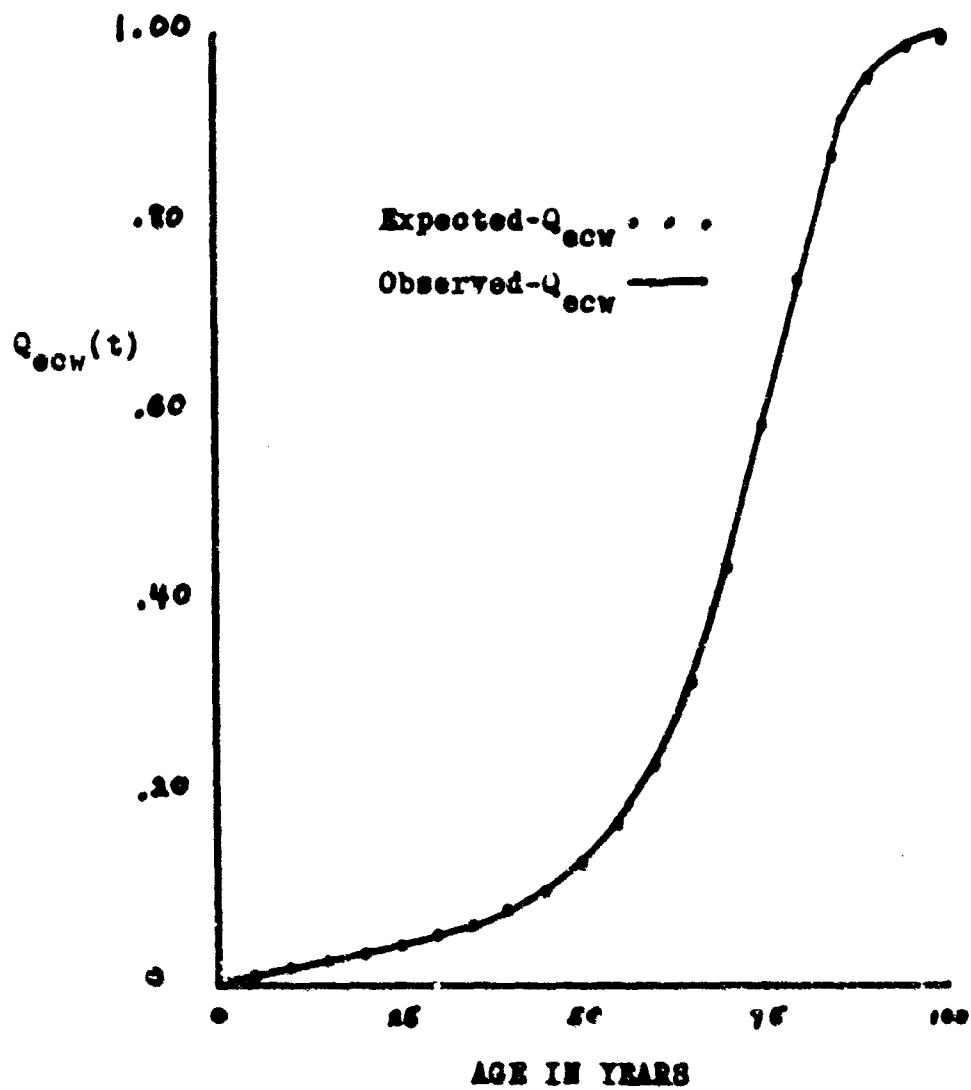


Figure 7.7 Plot of Expected and Observed Cumulative Mortality Versus Time (Summation Model)

population. During the first 5 years after birth 13 of the 19 members of the early subpopulation die and, therefore, the future impact of this subpopulation on the overall failure rate is diminished. After ten years all 19 members of the early subpopulation have died and the failure rate of the heterogeneous population has decreased to its lowest point, thus ending the early failure period.

A mathematical explanation of the decreasing failure rate phenomenon during the early portion of human life is provided by the failure rate model, equation (5.13). The subpopulation values for probability density function and reliability have been determined from individual Weibull models for each subpopulation.

$$\lambda_{ecw}(t) = \frac{\frac{N_e}{N} f_e(t) + \frac{N_c}{N} f_c(t) + \frac{N_w}{N} f_w(t)}{\frac{N_e}{N} R_e(t) + \frac{N_c}{N} R_c(t) + \frac{N_w}{N} R_w(t)} \quad (5.13)$$

At $t = 5$ years the failure rate equation after multiplying and dividing by 1000 yields

$$\lambda_{ecw}(5) = \frac{19 (.650) + 76 (.004) + 905(0)}{19 (.350) + 76 (.996) + 905(1)}$$

The first term in the numerator and denominator represents that portion of the heterogeneous failure rate caused by the early subpopulation. The arithmetic is done in detail below to demonstrate this effect at age five.

$$\lambda_{ecw}^{(5)} = \frac{12.3 + .3 + 0}{6.7 + 75.6 + 905} = .013$$

Note that 97 per cent of the contribution to failure rate is produced by the early subpopulation at age 5 years.

At age 10

$$\lambda_{ecw}^{(10)} = \frac{19(.309) + 76(.023) + 905(0)}{19(.041) + 76(.973) + 905(1)}$$

This reduces to

$$\lambda_{ecw}^{(10)} = \frac{5.86 + 1.75 + 0}{.8 + 74 + 905} = .008$$

The contribution to failure rate by the early subpopulation is now only 77 per cent and the failure rate has decreased from its previous value. Consider age $t = 15$.

$$\lambda_{ecw}^{(15)} = \frac{19(.039) + 76(.056) + 905(0)}{19(.002) + 76(.917) + 905(1)}$$

This reduces to

$$\lambda_{ecw}^{(15)} = \frac{.741 + 4.26 + 0}{.038 + 69.7 + 905} = .005$$

The contribution of the early subpopulation is now only 15 per cent and the trend in failure rate is no longer decreasing thus indicating that the early failure period has ended.

Useful Life Failures

Examination of Figure 7.2 reveals that the chance

or useful life failure period starts at 10 years of age and extends to approximately 50 years at which time wearout becomes the dominant mode of failure. The slight increase in failure rate prior to 50 years is attributed to the interaction between wearout and chance failure mechanisms. An accident which causes the death of an older person might only cause injury to a younger individual. Thus, even though the mechanism of failure or death is essentially of the chance variety the force of mortality is not strictly independent of age as it is in the ideal case.

Wearout

The delineation between the chance and wearout periods is not as distinct in Figure 7.2 as it is in the theoretical curve of Figure 1.1, because in the present illustration both periods exhibit an increasing failure rate. However when the cumulative failures are plotted on Weibull probability paper, as in Figure 7.3, the delineation between the chance and wearout periods is clearly shown to occur at 50 years of age. Human mortality, of course, is quite dissimilar from the failure of mechanical or electrical components. This example has served the purpose of placing failure phenomena and the reliability summation model on a more familiar plane. It is time now to apply the model to actual military equipment component failure data.

CHAPTER 8

APPLICATION OF THE RELIABILITY SUMMATION MODEL TO KLYSTRON FAILURES

8.1 The Data to be Analysed

In a paper titled, "High-Power High-Frequency Reliability Techniques," Doyon and Siegman (20) have presented some klystron failure data exhibiting early, chance, and wearout failures. Their data for 92 klystrons tested to failure are the basis for this second example. Table 8.1 is a tabulation of pertinent failure data for the 92 klystrons in test. The data have been grouped into twenty-seven 600 hour class intervals.

8.2 Parameter Determination

The class interval end points together with their respective median ranks are tabulated in Table 8.2 and plotted on Weibull probability paper in Fig. 8.1. Three straight lines are drawn amongst the points and by inspection it is determined that points 1 through 4 are in the early subpopulation, points 5 through 11 are in the

Table 8.1 Raw Failure Data for 92 Klystrons

Time at Class Interval End Point	Reliability at Beginning of Class Interval	Failures During Class Interval	Probability Density Function	Unreliability at End of Class Interval	Failure Rate
t	$R_{ecw}(t)$	Failures	$f_{ecw}(t)$	$Q_{ecw}(t)$	$\lambda_{ecw}(t)$
600	1.000	23	.2500	.250	.2500
1200	.750	9	.0980	.348	.1305
1800	.652	2	.0218	.370	.0334
2400	.630	3	.0326	.402	.0517
3000	.598	11	.1200	.521	.2010
3600	.479	6	.0650	.587	.1360
4200	.413	3	.0326	.619	.0790
4800	.381	6	.0650	.684	.1705
5400	.316	4	.0453	.728	.1375
6000	.272	3	.0326	.761	.1200
6600	.239	4	.0435	.804	.1820
7200	.196	8	.0870	.891	.4440
7800	.109	3	.0326	.924	.2990
8400	.076	0	.0000	.924	.0000
9000	.076	1	.0109	.935	.1436
9600	.065	2	.0218	.956	.3359
10200	.044	2	.0218	.980	.4960
10800	.020	0	.0000	.980	.0000
11400	.020	0	.0000	.980	.0000
12000	.020	0	.0000	.980	.0000
12600	.020	0	.0000	.980	.0000
13200	.020	0	.0000	.980	.0000
13800	.020	0	.0000	.980	.0000
14400	.020	1	.0109	.990	.5450
15000	.010	0	.0000	.990	.0000
15600	.010	0	.0000	.990	.0000
16200	.010	1	.0109	1.000	1.0900

Table 8.2 Klystron Failure Data Prepared for Plotting

Point Number	Age	Median Rank
1	600	24.6
2	1200	34.4
3	1800	36.5
4	2400	39.7
5	3000	51.7
6	3600	58.2
7	4200	61.4
8	4800	68.0
9	5400	72.3
10	6000	75.5
11	6600	79.8
12	7200	88.5
13	7800	91.7
	8400	
14	9000	92.9
15	9600	95.0
16	10200	97.2
	10800	
	11400	
	12000	
	12600	
	13200	
	13800	
17	14400	98.4
	15000	
	15600	
18	16200	99.4

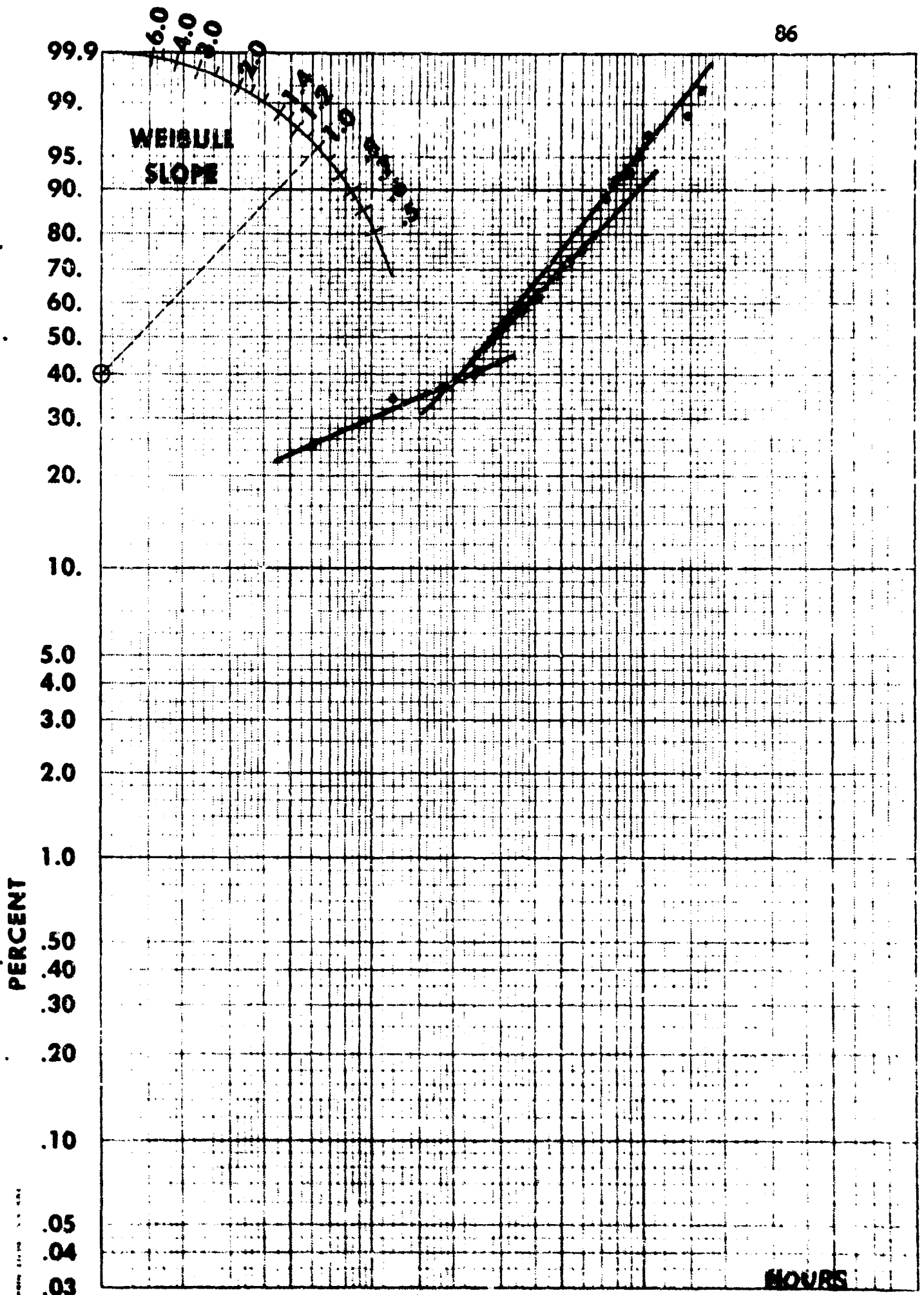


Figure 8.1 Weibull Plot of Klystron Mixed Failure Population

1980

WEIBULL PROBABILITY PAPER

chance subpopulation, and points 12 through 18 are in the wearout subpopulation. No importance is attached to the fact that the three lines in this case intersect at a common point, as the only purpose of the mixed population plot is to identify and separate the three subpopulations. By totaling the failures represented by each of the points falling in a particular subpopulation, the subpopulation sizes are found to be

$$N_e = 37$$

$$N_c = 37$$

$$N_w = 18$$

New median ranks are calculated based on these subpopulation sizes and these data are tabulated in Table 8.3. The subpopulations are individually replotted in Figs. 8.2, 8.3, and 8.4 and the following Weibull parameters are determined:

Figure 8.2

$$\gamma_e = 0$$

$$\beta_e = .92$$

$$\eta_e = 650$$

Figure 8.3

$$\gamma_c = 0$$

$$\beta_c = 2.65$$

$$\eta_c = 4390$$

Figure 8.4

$$\begin{aligned}\gamma_w &= 0 \\ \beta_w &= 3.00 \\ \eta_w &= 8900\end{aligned}$$

All parameters necessary to use equation (6.1) have been found. The equation can now be used to determine the expected reliability, at a given time, of a klystron randomly drawn from a mixed population which is represented by the tested sample. For example, consider $t = 4800$ hours.

Equation (6.1) is

$$R_{ecw}(t) = \frac{N_e}{N} e^{-\left(\frac{t-\gamma_e}{\eta_e}\right)^{\beta_e}} + \frac{N_c}{N} e^{-\left(\frac{t-\gamma_c}{\eta_c}\right)^{\beta_c}} + \frac{N_w}{N} e^{-\left(\frac{t-\gamma_w}{\eta_w}\right)^{\beta_w}}$$

Substituting numerical values for all parameters

$$\begin{aligned}R_{ecw}(4800) &= \frac{37}{92} e^{-\left(\frac{4800-0}{650}\right)^{.92}} + \frac{37}{92} e^{-\left(\frac{4800-0}{4390}\right)^{2.65}} \\ &\quad + \frac{18}{92} e^{-\left(\frac{4800-0}{8900}\right)^{3.00}} \\ &= .402(.00185) + .402(.282) + .196(.855) = .282\end{aligned}$$

If the sample of 92 is representative and if equation (6.1) is valid, a klystron randomly drawn at time $t = 0$ can be expected to have a 28.2% chance of surviving 4800 hours of operation. Conversely, the expected probability of failing before 4800 hours of operation is

$$Q_{ecw}(4800) = 1 - R_{ecw}(4800) = 1 - .282 = .718$$

Table 8.3 Klystron Failure Data Prepared for Subpopulation Replot

	Point Number	Age	Subpopu- lation $N_f(t)$	Median Rank
Early Subpopulation ($N_e = 37$)	1	600	23	60.7
	2	1200	32	84.7
	3	1800	34	90.1
	4	2400	37	98.1
Chance Subpopulation ($N_c = 37$)	5	3000	11	28.6
	6	3600	17	44.6
	7	4200	20	52.6
	8	4800	26	68.8
	9	5400	30	79.4
	10	6000	33	87.5
	11	6600	37	98.1
Wearout Subpopulation ($N_w = 18$)	12	7200	8	41.8
	13	7800	11	58.1
	14	9000	12	63.6
	15	9600	14	74.5
	16	10200	16	85.4
	17	14400	17	90.9
	18	16200	18	96.3

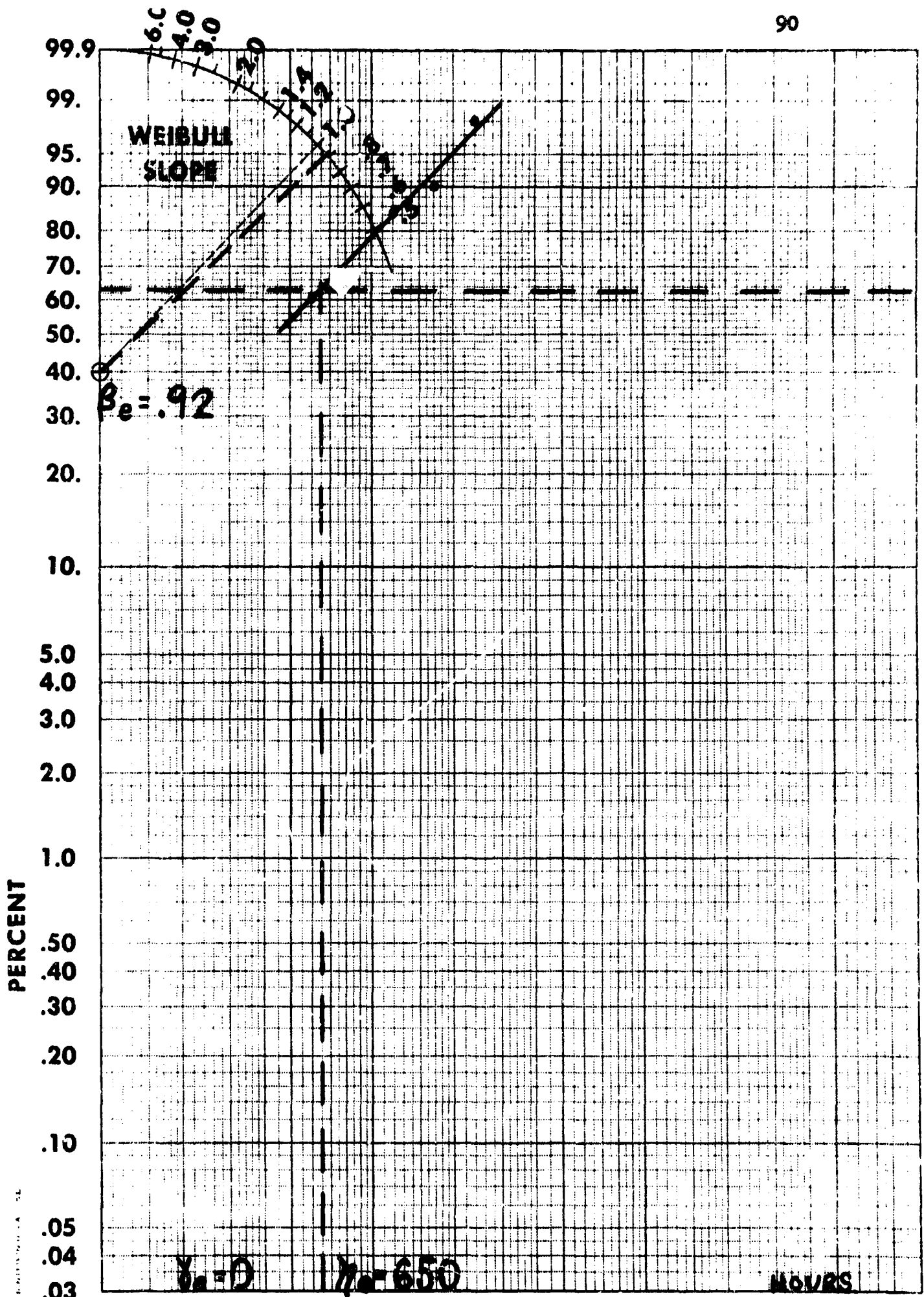


Figure 8.2 Klystron Failure Early Subpopulation Replot



JAN 1950

WEIBULL PROBABILITY PAPER

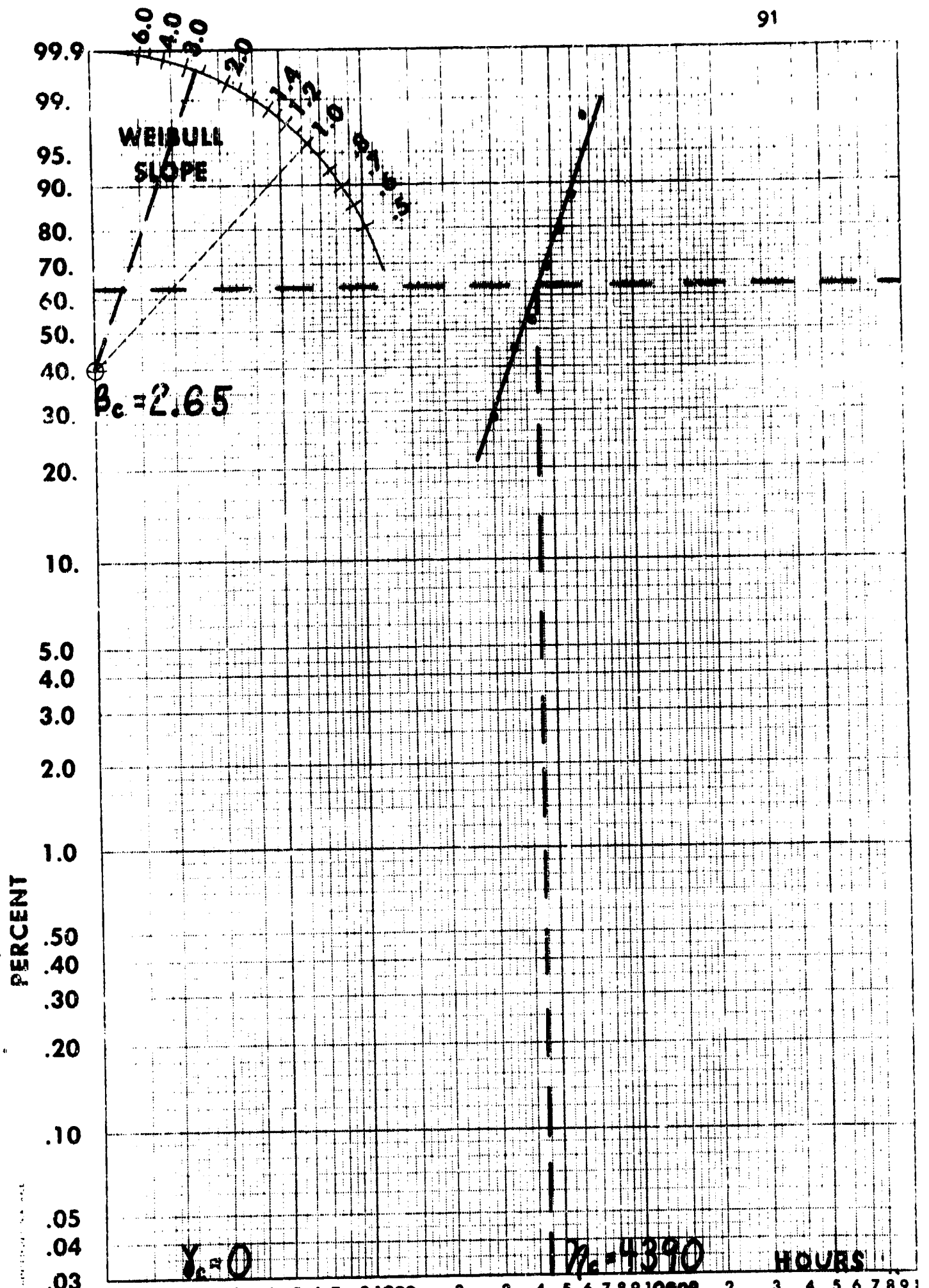


Figure 8.3 Klystron Failure Chance Subpopulation Replot

Ford JAN 1950

WEIBULL PROBABILITY PAPER

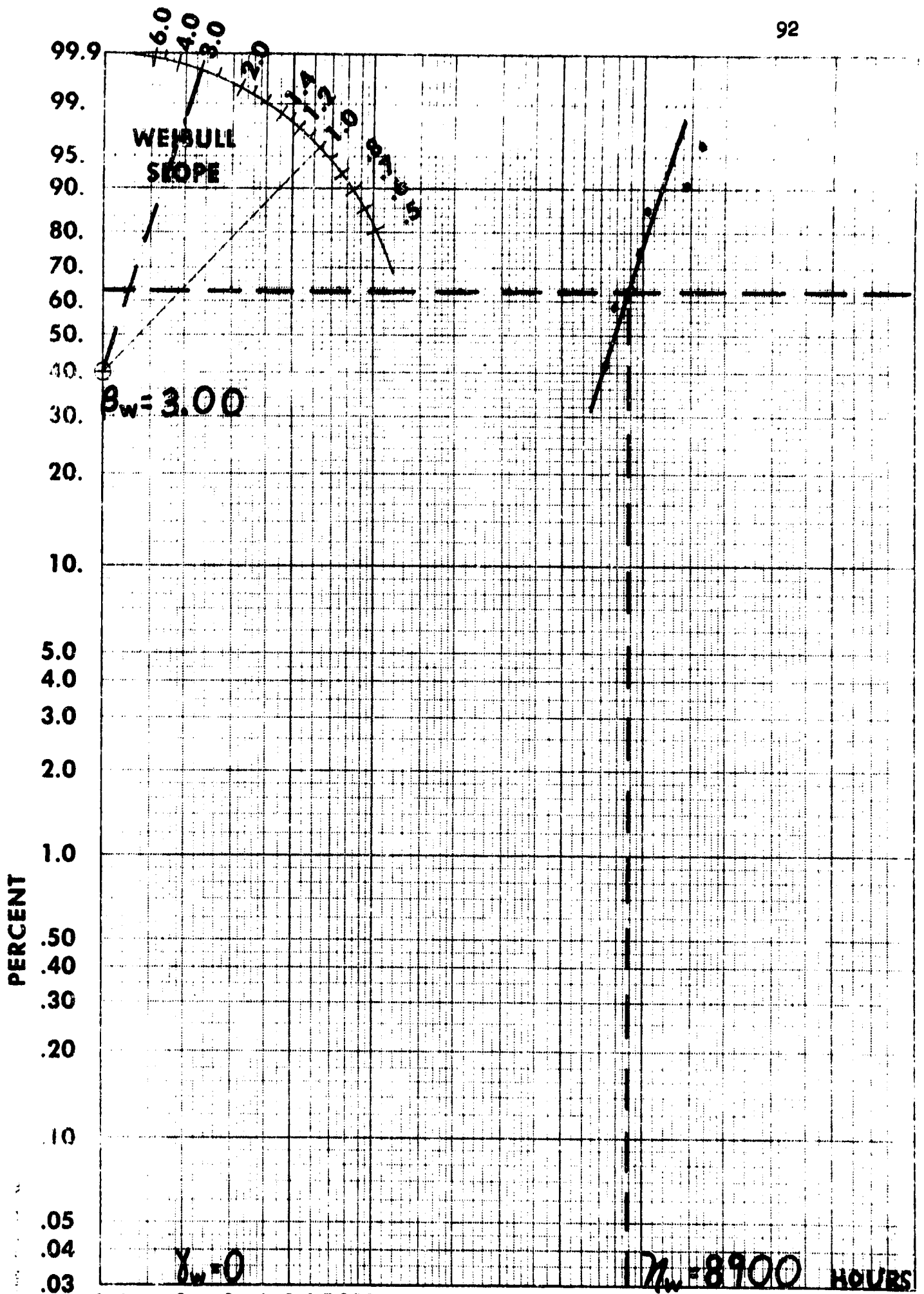


Figure 8.4 Klystron Failure Wearout Subpopulation Replot

50re JAN 1950

8.3 Goodness-of-Fit

For the purpose of comparison, the observed value of $Q_{ecw}(4800)$ from the tested sample of 92 klystrons is .684 (Table 8.1). The absolute difference between the observed and the expected values is

$$D_{4800} = .718 - .684 = .034$$

From the Kolmogorov-Smirnov Table (Table 3.1) for N greater than 35, the asymptotic equations are used to find the maximum allowable value of D at the .05 significance level.

$$D = \frac{1.36}{\sqrt{N}} = \frac{1.36}{\sqrt{92}} = .1415$$

To fully test the proposed model for goodness-of-fit, it is necessary to find D_i at each class interval to insure that no value of D_i is greater than .1415. This has been done and the values of Q_{ecw} expected, Q_{ecw} observed, and D_i are tabulated for each class interval in Table 8.4. The maximum D_i is found to be .063. Since .063 is less than the allowable maximum difference of .1415 it is concluded that the summation model for three failure subpopulations does meet the criteria established in Section 5.1 for a good model. The expected and the observed cumulative failure distributions are plotted for visual comparison

Table 8.4 Absolute Difference Between Expected and Observed Cumulative Klystron Failures (Summation Model)

Time	Observed	Expected	Absolute Difference
t	$Q_{ecw}(t)$	$Q_{ecw}(t)$	D_i
600	.250	.245	.005
1200	.348	.346	.002
1800	.370	.408	.038
2400	.402	.465	.063*
3000	.521	.525	.004
3600	.587	.591	.004
4200	.619	.657	.038
4800	.684	.718	.034
5400	.728	.772	.044
6000	.761	.815	.054
6600	.804	.848	.044
7200	.891	.875	.016
7800	.924	.896	.028
8400	.924	.914	.010
9000	.935	.930	.005
9600	.956	.944	.012
10200	.980	.956	.024
10800	.980	.967	.013
11400	.980	.976	.004
12000	.980	.983	.003
12600	.980	.989	.009
13200	.980	.992	.012
13800	.980	.995	.015
14400	.990	.997	.007
15000	.990	.998	.008
15600	.990	.999	.009
16200	1.000	1.000	0.000

*Maximum absolute difference

Allowable absolute difference at the .05 significance level is found from Table 3.1 to be

$$\frac{1.36}{\sqrt{N}} = \frac{1.36}{\sqrt{92}} = .1415$$

in Fig. 8.5. In this example there is a good correlation between the observed and the expected data and it may be concluded, as it was in Chapter 7, that the reliability summation model with parameters determined by the graphical method given in Chapter 6, accurately models the reliability of mixed failure mode populations.

8.4 Analysis of Underlying Failure Causes-Early Failures

In Fig. 8.1 the four points which fall in the early subpopulation represent 37 klystron failures or 40 per cent of the heterogeneous klystron population. This large early subpopulation indicates that there are a large number of substandard items in the mixed population. Unfortunately the exact number of substandard klystrons cannot be determined mathematically because the early subpopulation is composed of chance as well as substandard failures. The effect of this combination is to produce a decreasing failure rate until 2400 hours of operation. See Fig. 8.6. After 2400 hours the klystron population is completely burned in.

Useful Life Failures

In Fig. 8.6 the useful life period which extends from 2400 hours to 7200 hours is seen to be nonmonotonic as a result of the interaction of the three sub-

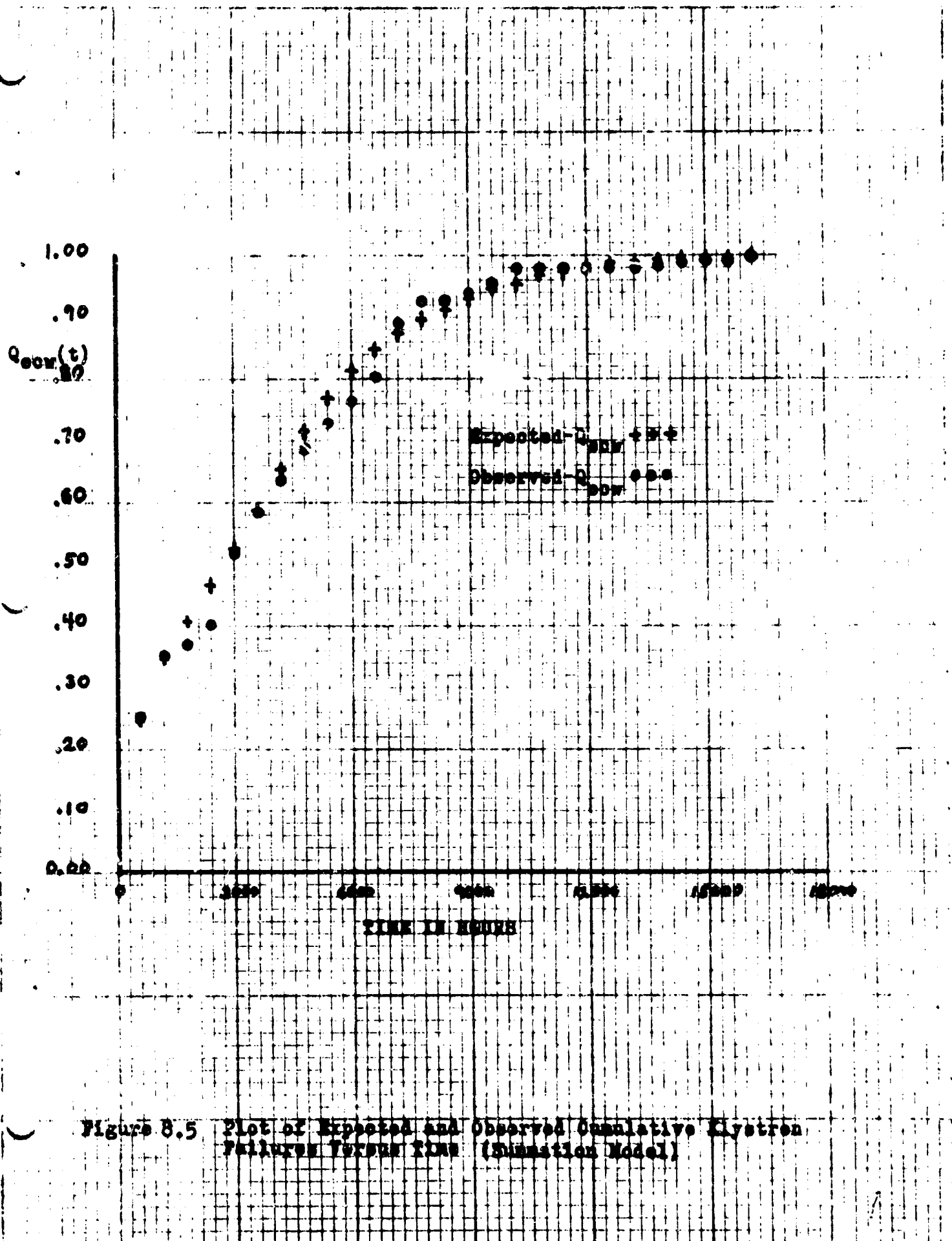


Figure 8.5 Plot of Expected and Observed Cumulative Klystron Failures Versus Time (Sustation Model)

populations which each have an impact on failure rate during the period. An additional 49% of the klystron population fails during the useful life period leaving only 18 klystrons to fail in wearout.

Wearout Failures

Although wearout begins after 7200 hours of operation, the wearout failure rate does not exceed the maximum useful life failure rate until after 9000 hours of operation. From Fig. 8.6 it is seen that 20 per cent of klystrons with greater than 9600 hours may be expected to fail within the next 600 hours.

Conclusion of Analysis

1. The large size of the early subpopulation suggests that improved quality control measures are in order for future klystron production of the type analysed.

2. Because of the high failure rate exhibited during useful life, a burn-in period of only 600 hours during early life would be sufficient to reduce population failure rate to that of the useful life period. During the 600 hour burn-in approximately 20% of the klystrons may be expected to fail as compared to 40% failures if the burn-in test is run for the 2400 hour duration of early life.

3. Operational reliability of klystrons could be

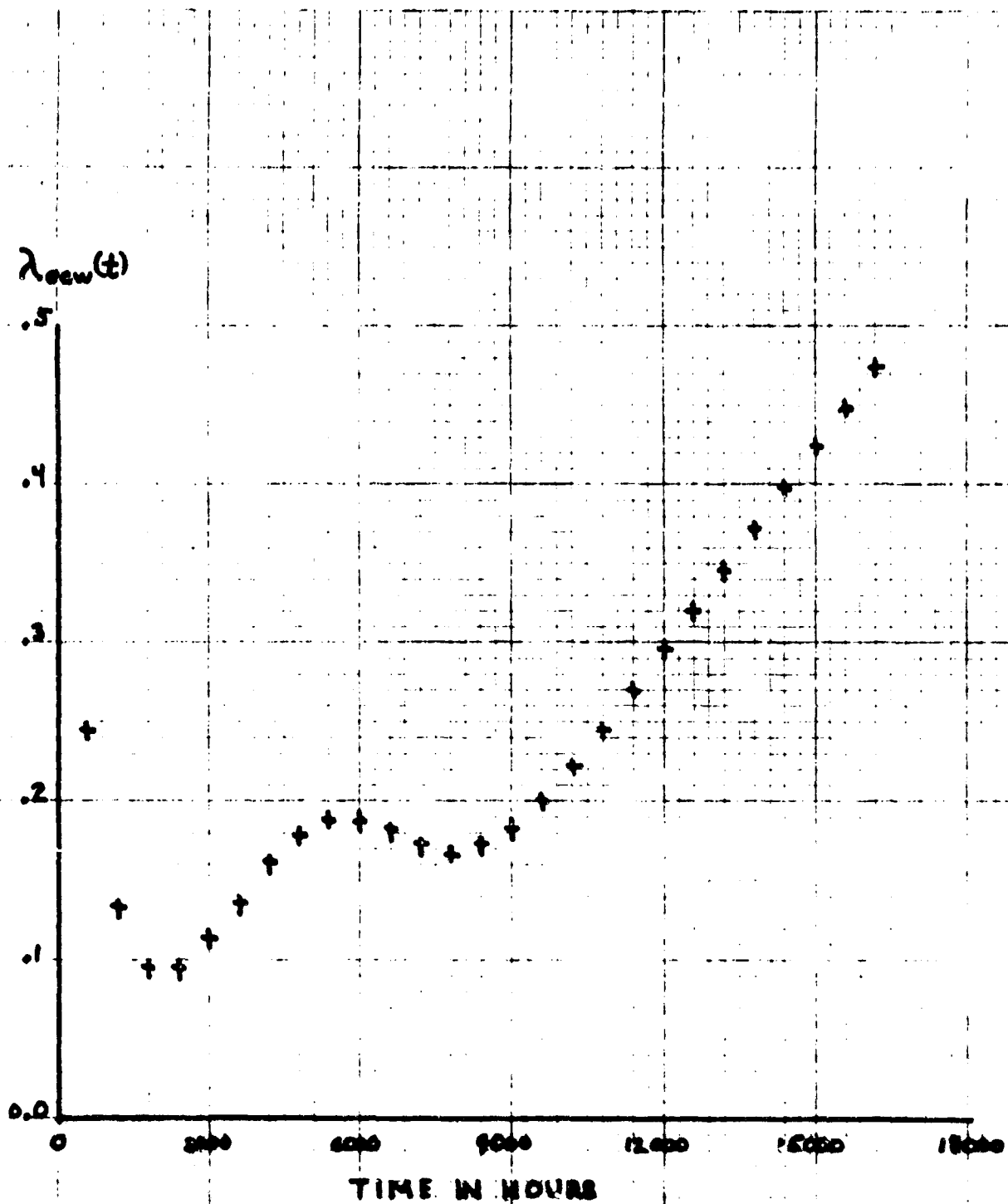


Figure 8.6 Plot of Expected Klystron Failure Rate Versus Time

maintained at specified levels by controlling the number of hours the klystrons are permitted to operate. For example, it might be specified that all klystrons in operation must have an 80 per cent chance of survival during any 600 hour interval. In this case a 600 hour burn-in prior to operational employment of the klystrons should reduce the population failure rate below 20 per cent at an estimated cost of 20 per cent of the total klystron population.

Next, klystrons surviving 8400 hours of use could be removed from operation prior to failure at a cost of an additional 8 per cent of the klystrons. The result is that by selectively discarding 28 per cent of the klystron population the remaining klystrons would have an 80 per cent chance of surviving during any 600 hour mission.

CHAPTER 9

APPLICATION OF THE RELIABILITY SUMMATION MODEL TO MAGNETRON FAILURES

9.1 The Data to be Analysed

Table 9.1 contains failure information for a population of 38 magnetrons during operational use. The information was provided by the U.S. Army Missile Command located at Redstone Arsenal, Alabama. The accuracy and the analytical power of the proposed model will be examined in this chapter. In Chapter 10 the results obtained in this chapter will be compared with those obtained using present reliability modeling techniques.

9.2 Parameter Determination

The median rank and age at failure for each failed magnetron is tabulated in Table 9.2 and plotted on Weibull probability paper in Figure 9.1. Three straight lines are drawn amongst the points and by inspection it is determined that points 1 through 10 are in the early subpopulation, points 11 through 35 are in the chance or useful life

Table 9.1 Raw Failure Data (38 Magnetrons)

Time at failure	Cumulative Failing at Time = t	Cumulative % Failing at Time = t
t	Failures	$Q_{ecw}(t)$
0.0	1	.026
1.0	2	.053
1.5	3	.079
1.7	4	.105
8.3	5	.132
10.0	6	.158
15.0	7	.184
15.5	8	.210
28.0	9	.237
36.7	10	.263
73.6	11	.290
95.0	12	.316
116.0	13	.342
120.0	14	.368
130.0	15	.395
153.5	16	.421
165.0	17	.447
226.4	18	.474
332.3	19	.500
363.0	20	.526
405.4	21	.551
409.0	22	.579
431.0	23	.605
439.0	24	.631
525.0	25	.658
541.7	26	.684
577.9	27	.710
677.0	28	.736
739.0	29	.763
873.0	30	.790
937.0	31	.798
1144.0	32	.844
1169.0	33	.849
1297.0	34	.868
1630.0	35	.898
2088.9	36	.924
2340.9	37	.975
2343.0	38	.976

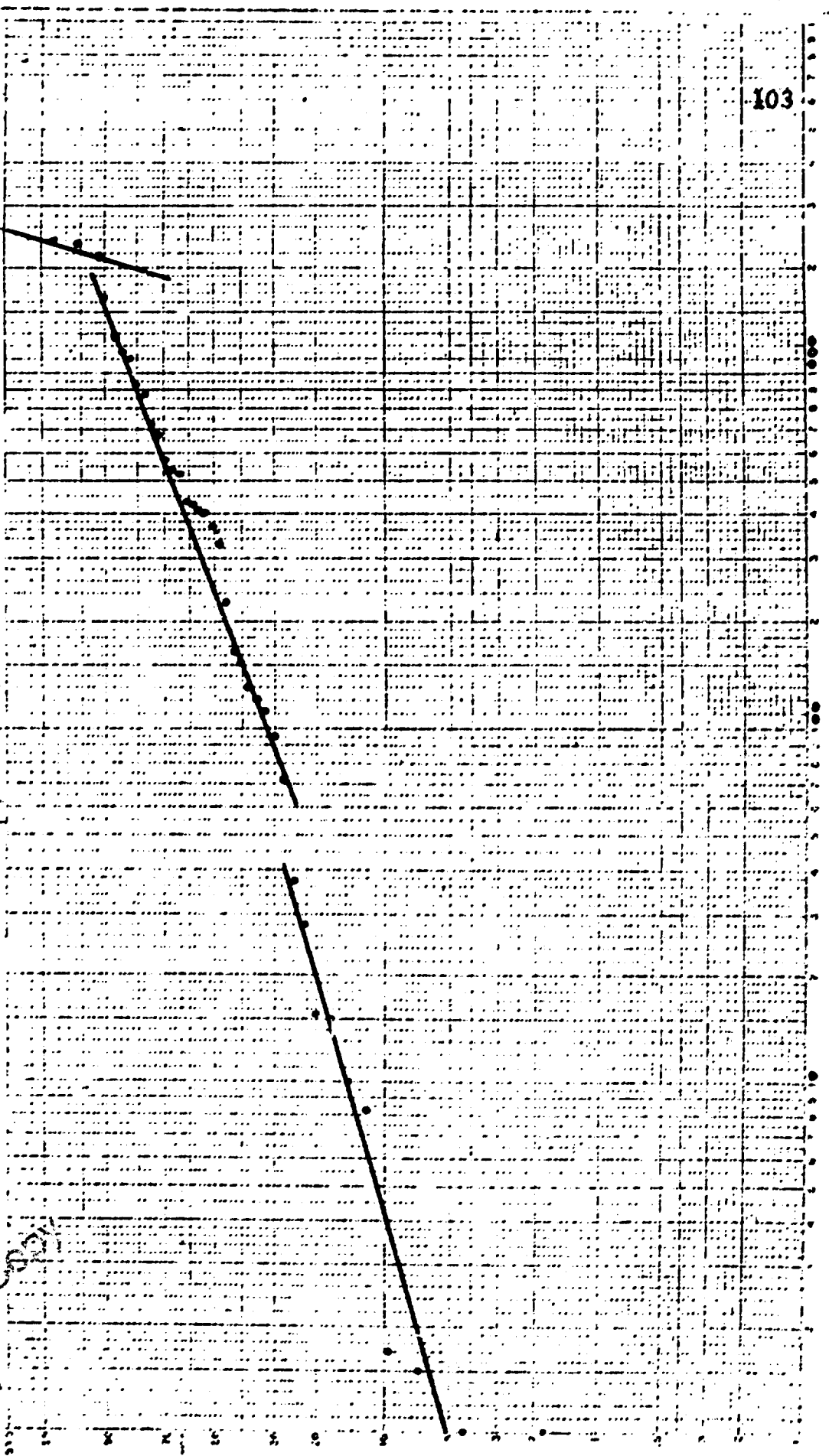
Table 9.2 Magnetron Failure Data Prepared for Plotting

Point Number	Age	Median Rank
1	0.0	1.82
2	1.0	4.42
3	1.5	7.04
4	1.7	9.64
5	8.3	12.20
6	10.0	14.85
7	15.0	17.45
8	15.5	20.3
9	28.0	22.6
10	36.7	25.3
11	73.6	27.9
12	95.0	30.4
13	116.0	33.1
14	120.0	35.6
15	130.0	38.3
16	153.5	40.9
17	165.0	43.5
18	226.4	46.1
19	332.3	48.6
20	363.0	51.4
21	405.4	53.9
22	409.0	56.5
23	431.0	59.0
24	439.0	61.6
25	525.0	64.4
26	541.7	67.0
27	577.9	69.5
28	677.0	72.0
29	739.0	74.6
30	873.0	77.4
31	937.0	80.0
32	1144.0	82.5
33	1169.0	85.2
34	1297.0	87.7
35	1630.0	90.4
36	2088.9	93.0
37	2340.9	95.6
38	2343.0	98.2

WEIBULL PROBABILITY CHART

WEIBULL PROBABILITY CHART

Sample Size	10	Sample Size	10
Shape	2.0	Shape	2.0
Characteristic Life	1000	Characteristic Life	1000
Minimum Life	100	Minimum Life	100
Maximum Life	10000	Maximum Life	10000



Best Available Copy

Figure 9.1. Weibull Plot of Magnetron Mixed Failure Population

subpopulation, and points 36, 37, and 38 are in the wear-out subpopulation. Since the data are not grouped each point represents a single failure and the subpopulation sizes are found to be

$$N_e = 10$$

$$N_c = 25$$

$$N_w = 3$$

New median ranks are calculated based on these subpopulation sizes and the median ranks are tabulated in Table 9.3. The subpopulations are individually replotted in Figures 9.2, 9.3, and 9.4 and the following Weibull parameters are determined:

Figure 9.2

$$\gamma_e = 0$$

$$\beta_e = 0.69$$

$$\eta_e = 12.1$$

Figure 9.3

$$\gamma_c = 0$$

$$\beta_c = 1.25$$

$$\eta_c = 620$$

Figure 9.4

$$\gamma_w = 0$$

$$\beta_w = 20$$

$$\eta_w = 2310$$

All parameters necessary to use equation (6.1) have been found. The equation can now be used to determine the ex-

Table 9.3 Magnetron Failure Data Prepared for Subpopulation Replot

	Failure Number	Age	Median Rank
Early Subpopulation ($N_e = 10$)	1	0.0	6.7
	2	1.0	16.3
	3	1.5	26.0
	4	1.7	35.6
	5	8.3	45.1
	6	10.0	54.8
	7	15.0	64.4
	8	15.5	74.0
	9	28.0	83.6
	10	36.7	93.4
Useful Life Subpopulation ($N_c = 25$)	11	73.6	2.8
	12	95.0	6.7
	13	116.0	10.6
	14	120.0	14.5
	15	130.0	18.5
	16	153.5	22.4
	17	165.0	26.4
	18	226.4	30.3
	19	332.3	34.2
	20	363.0	38.2
	21	405.4	42.1
	22	409.0	46.0
	23	431.0	50.0
	24	439.0	54.0
	25	525.0	58.0
Wearout Subpopulation ($N_w = 3$)	26	541.7	61.9
	27	577.9	65.7
	28	677.0	69.6
	29	739.0	73.6
	30	873.0	77.5
	31	937.0	81.5
	32	1144.0	85.5
	33	1169.0	89.5
	34	1297.0	93.4
	35	1630.0	97.3
	36	2088.9	20.6
	37	2340.9	50.0
	38	2343.0	79.4

WEIBULL PROBABILITY CHART

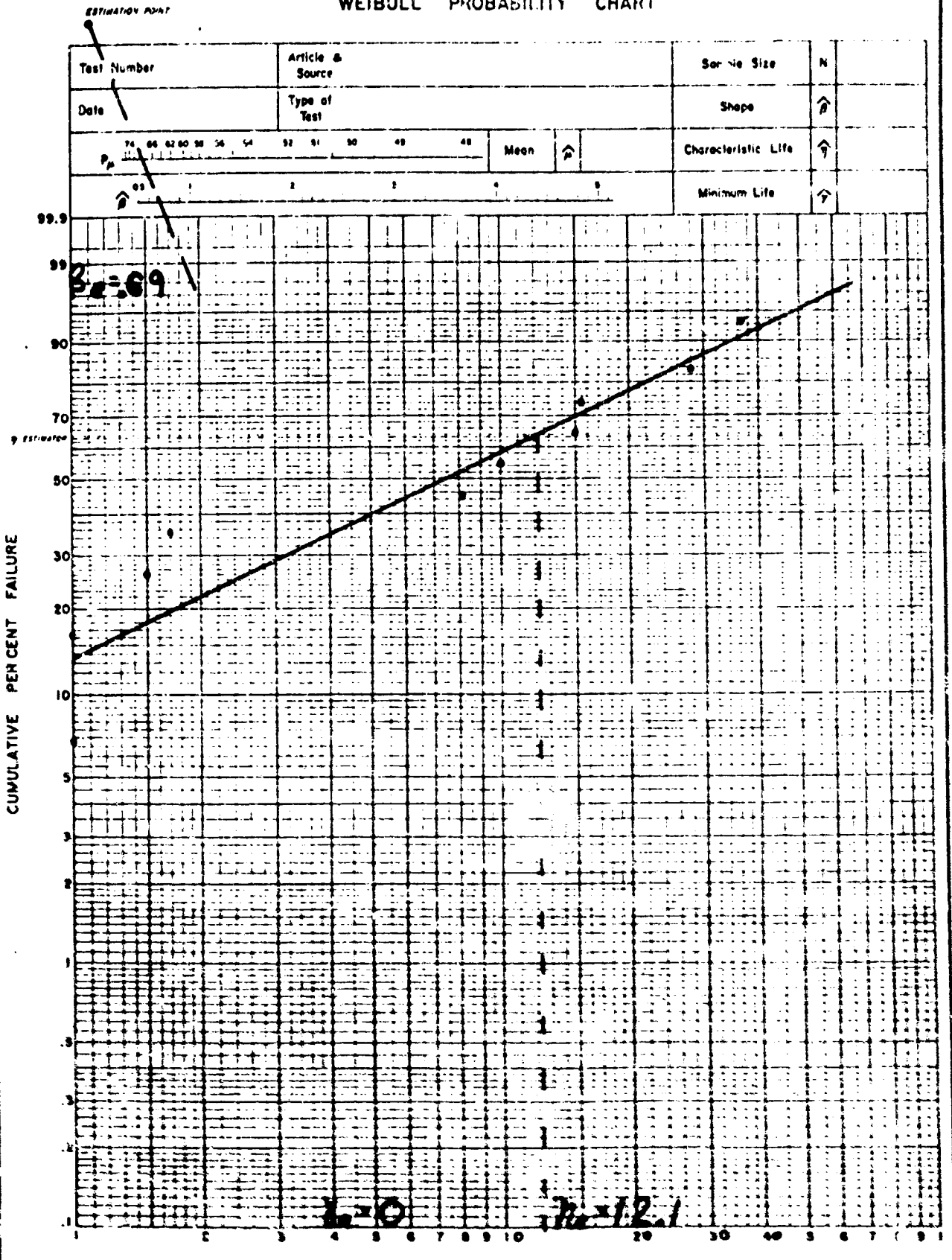
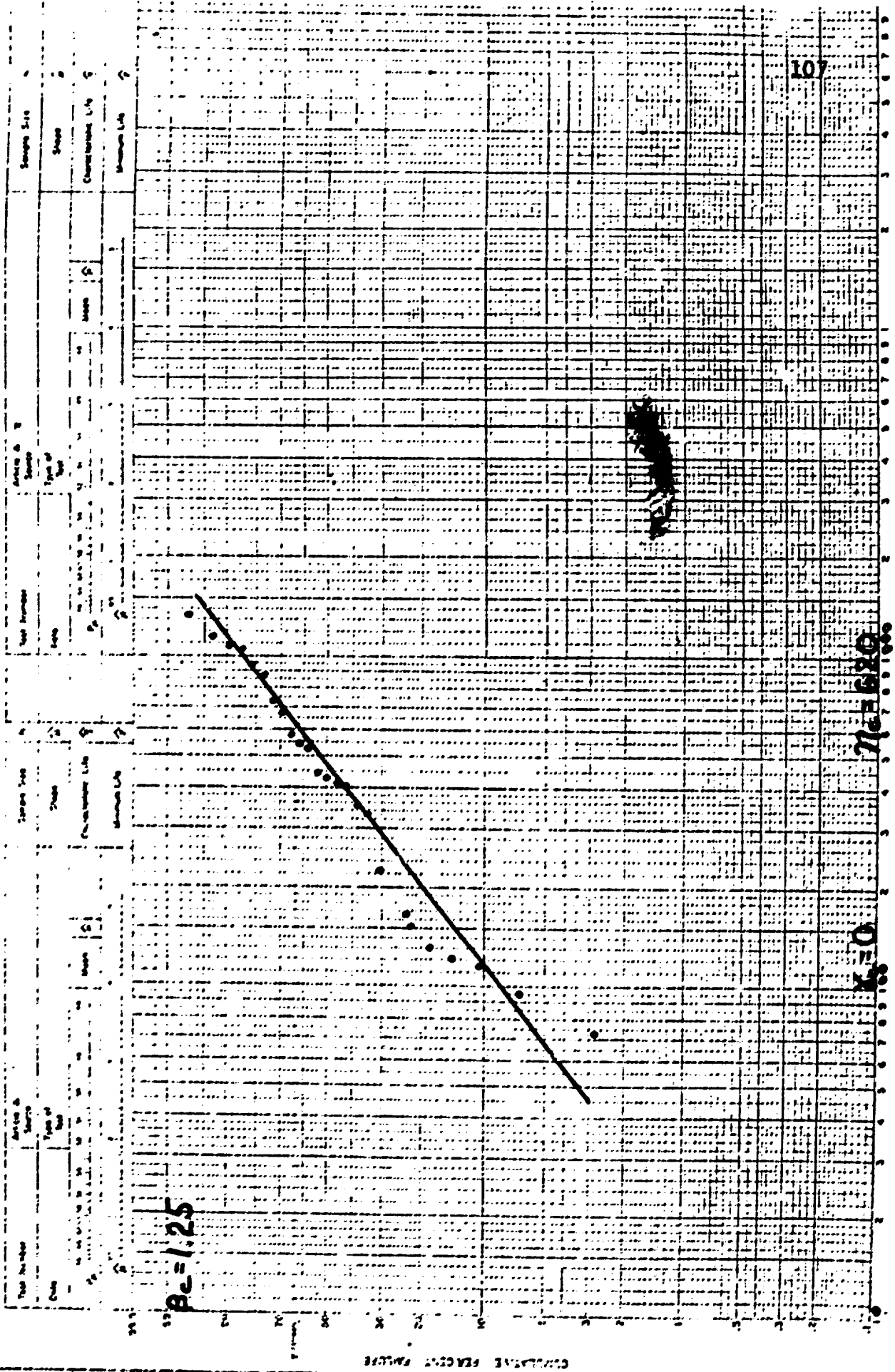


Figure 9.2 Magnetron Failure Early Subpopulation Replot

WEIBULL PROBABILITY CHART

WEIBULL PROBABILITY CHART



AGE AT FAILURE
 AGE AT FAILURE
 Figure 9.3 Magnetron Failure Chance Subpopulation Replot

Not Available Copy

WEIBULL PROBABILITY CHART

ESTIMATION POINT

Test Number	Article & Source	Sample Size	N
Date	Type of Test	Shape	$\hat{\beta}$
P_M 74 66 62 60 58 56 54 52 51 50 49 48		Mean	$\hat{\mu}$
$\hat{\beta}$ 0.5 1 2 3 4 5		Characteristic Life	$\hat{\eta}$
		Minimum Life	$\hat{\gamma}$

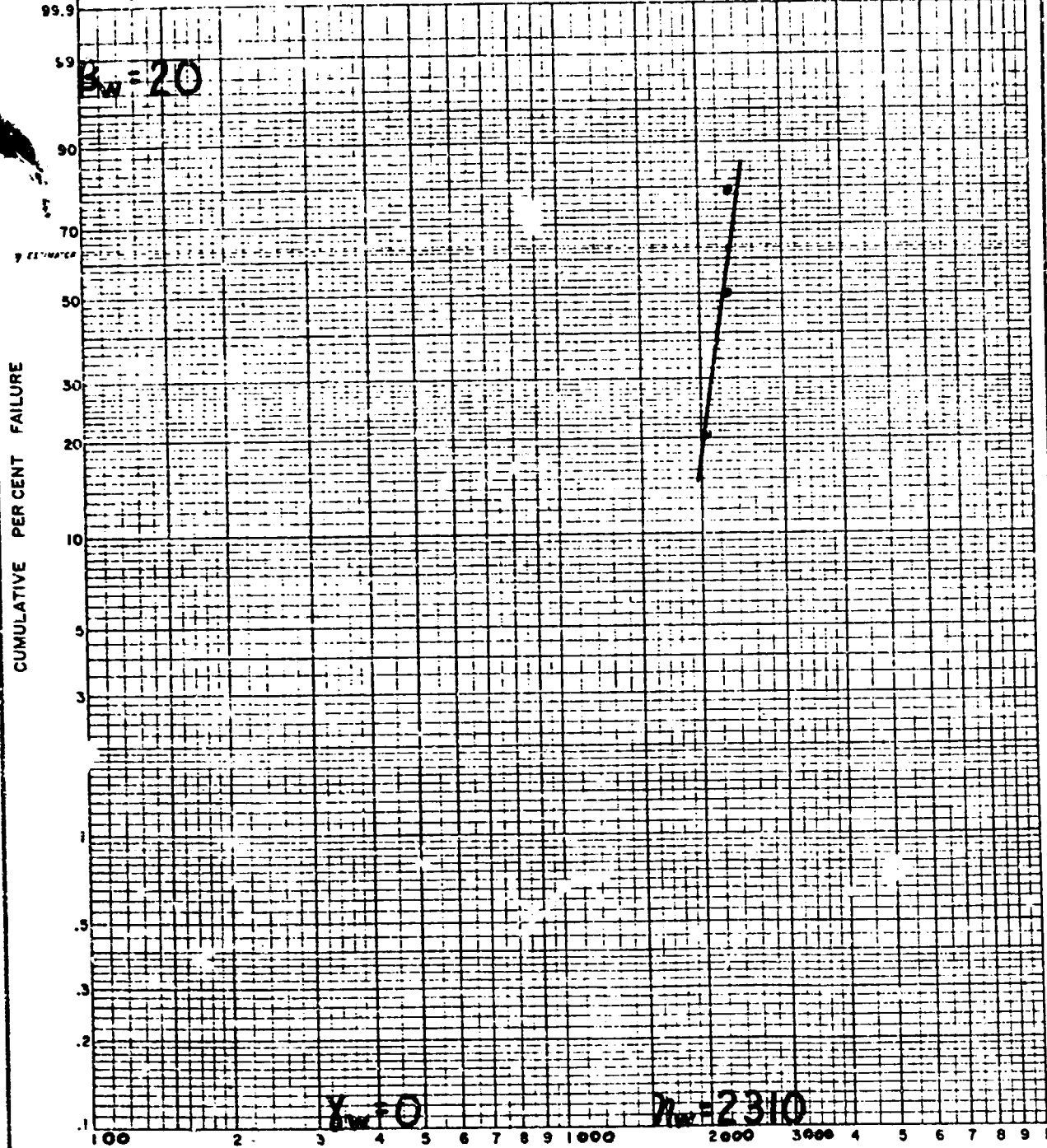


Figure 9.4 Magnetron Failure Wearout Subpopulation Replot

pected reliability, at a given time, of a magnetron randomly drawn from a mixed population which is represented by the observed sample. For example, consider $t = 28$ hours. Substituting numerical values for all parameters into equation (6.1) yields:

$$R_{ecw}(t) = \frac{10}{38} e^{-\left(\frac{28-0}{12.1}\right)^{.69}} + \frac{25}{38} e^{-\left(\frac{28-0}{620}\right)^{1.25}} + \frac{3}{38} e^{-\left(\frac{28-0}{2310}\right)^{20}}$$

$$= .263(.168) + .658(.979) + .079(1.000) = .767$$

If the sample of 38 magnetrons is representative and if equation (6.1) is valid, a magnetron randomly drawn at time $t = 0$ can be expected to have a 76.7 per cent chance of surviving 28 hours of radiate time. Conversely, the expected probability of failing before 28 hours of operation is

$$Q_{ecw}(28) = 1 - R_{ecw}(28) = 1 - .767 = .233$$

9.3 Goodness-of-Fit

At time $t = 28$ hours the observed value of unreliability, $Q_{ecw}(28)$, from the tested sample of 38 magnetrons is .237 (Table 9.1). The absolute difference between the observed and the expected values of unreliability is

$$D_{28} = .237 - .233 = .004$$

From the Kolmogorov-Smirnov Table (Table 3.1) for N greater than 35, the asymptotic equations are used to find the maximum allowable value of D at the .05 significance level.

$$D = \frac{1.36}{\sqrt{N}} = \frac{1.36}{\sqrt{38}} = .220$$

To fully test the proposed model for goodness-of-fit, it is necessary to find D_i at each class interval to insure that no value of D_i is greater than .220. This has been done and the values of Q_{ecw} expected, Q_{ecw} observed, and D_i are tabulated for each failure time in Table 9.4. The maximum D_i is found to be .070. Since .070 is less than the allowable maximum difference of .220 it is concluded that the summation model for three failure subpopulations does meet the criteria established in Section 5.1 for a good model. The expected and observed cumulative failure distributions are plotted for visual comparison in Fig. 9.5. The excellent correlation between the observed and the expected data clearly indicates that the reliability summation model is capable of accurately representing the reliability of mixed populations.

9.4 Analysis of Underlying Failure Causes-Early Failures

Fig. 9.6 is a superposition of the subpopulation failure rates based on the expected failures from the reliability summation model. The early

Table 9.4 Absolute Difference Between Expected and Observed Cumulative Magnetron Failures (Summation Model)

Time	Observed	Expected	Absolute Difference
t	$Q_{ecw}(t)$	$Q_{ecw}(t)$	D_i
0.0	.026	.000	.026
1.0	.053	.043	.010
1.5	.079	.056	.023
1.7	.105	.060	.045
8.3	.132	.144	.012
10.0	.158	.157	.001
15.0	.184	.187	.003
15.5	.210	.189	.021
28.0	.237	.233	.004
36.7	.263	.251	.012
73.6	.290	.299	.009
95.0	.316	.319	.003
116.0	.342	.337	.005
120.0	.368	.340	.028
130.0	.395	.349	.046
153.5	.421	.368	.053
165.0	.447	.377	.070*
226.4	.474	.426	.048
332.3	.500	.505	.005
363.0	.526	.577	.001
405.4	.551	.556	.005
409.0	.579	.558	.021
431.0	.605	.572	.033
439.0	.631	.577	.054
525.0	.658	.629	.029
541.7	.684	.638	.046
577.9	.710	.658	.052
677.0	.736	.706	.030
739.0	.763	.732	.031
873.0	.790	.779	.011
973.0	.815	.798	.017
1144.0	.841	.844	.003
1169.0	.869	.849	.020
1297.0	.895	.868	.027
1630.0	.921	.898	.023
2088.9	.947	.924	.023

(continued)

Table 9.4 Continued

Time	Observed	Expected	Absolute Difference
t	$Q_{ecw}(t)$	$Q_{ecw}(t)$	D_i
2340.9	.975	.975	.000
2343,9	1.000	.976	.024

*Maximum absolute difference

Allowable absolute difference at the .05 significance level is found from Table 3.1 to be

$$\frac{1.36}{\sqrt{N}} = \frac{1.36}{\sqrt{38}} = .220$$

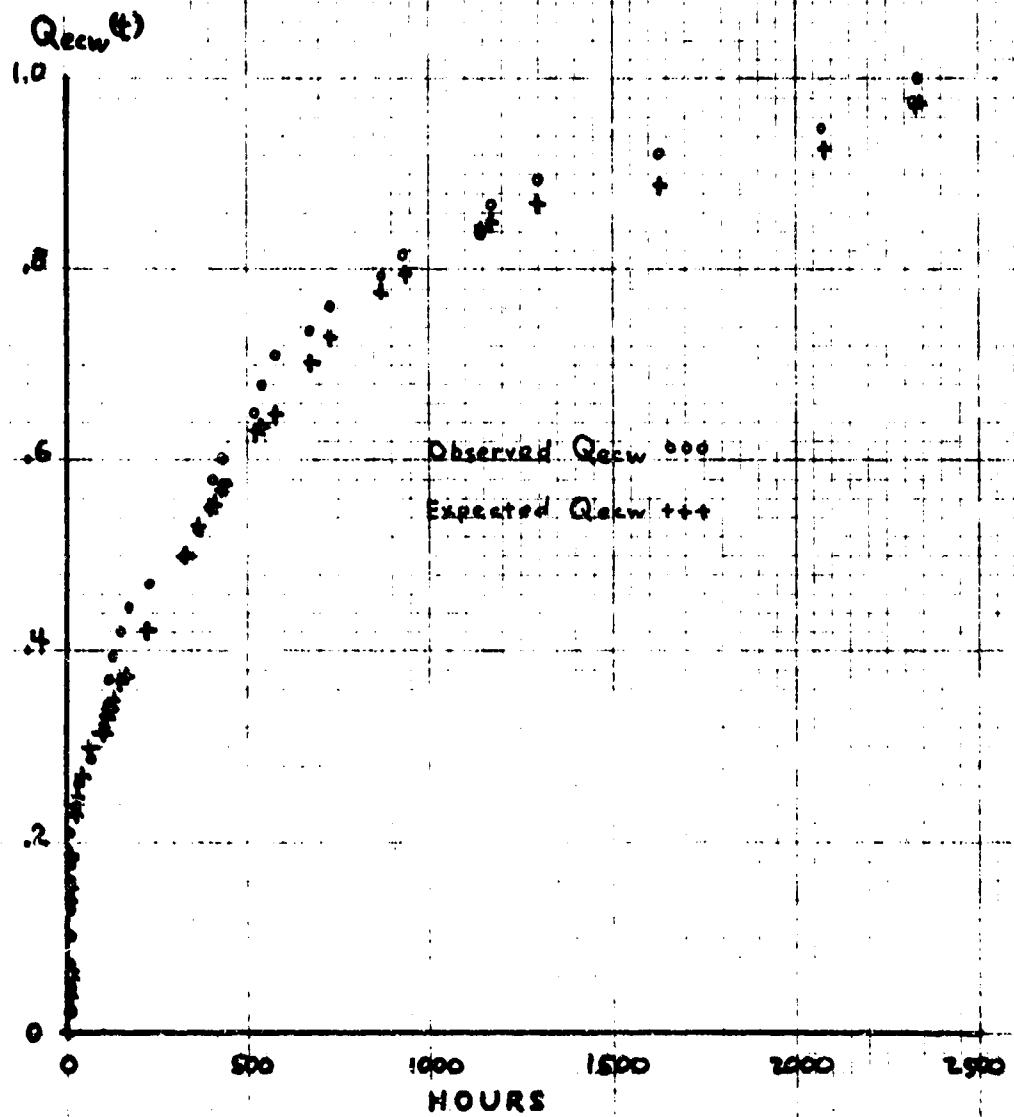


Figure 9.5 Plot of Expected and Observed Cumulative Magnetron Failures Versus Time in Hours (Summation Model)

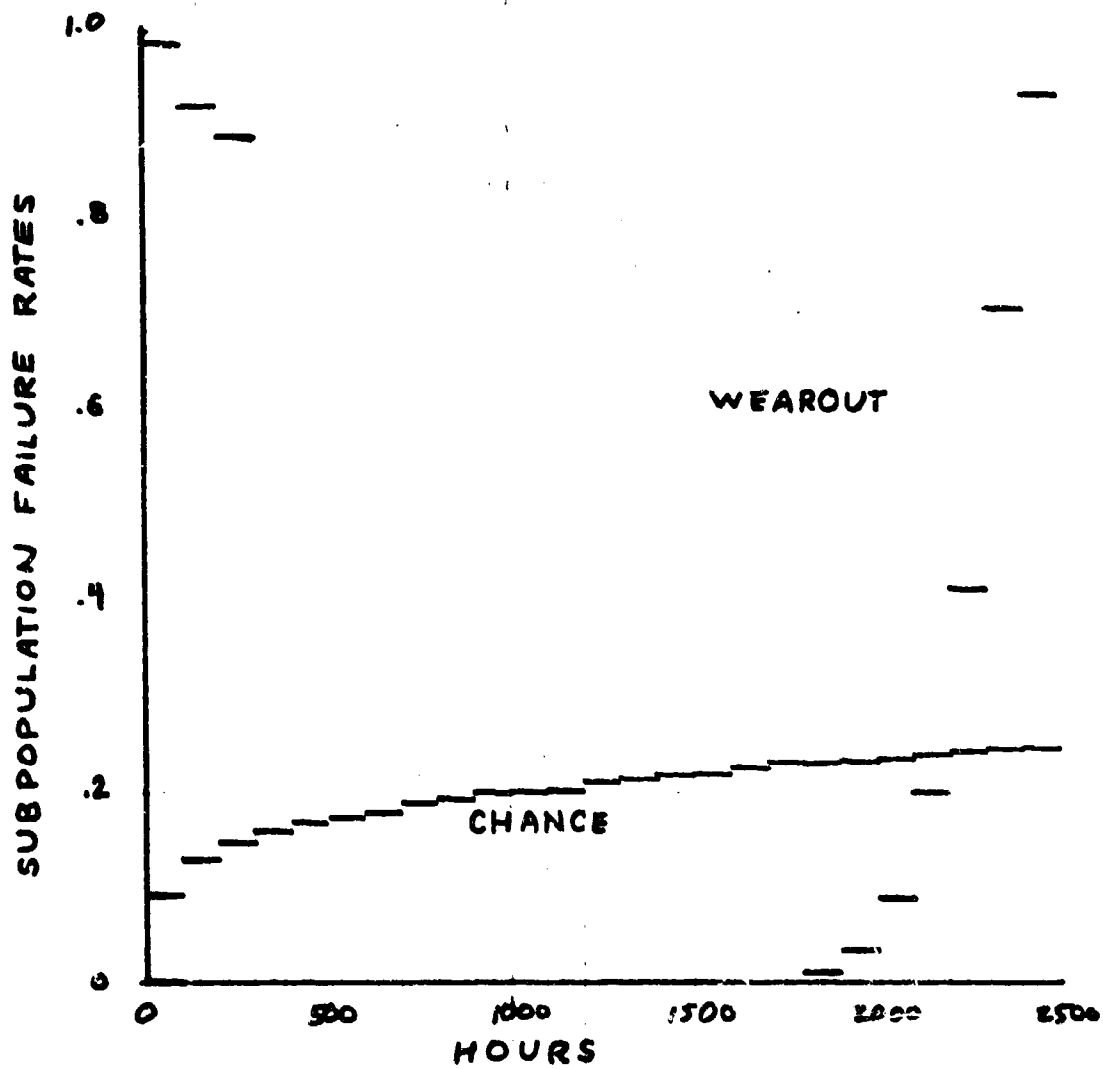


Figure 9.6 Plot of Expected Magnetron Subpopulation Failure Rates Versus Time in Hours

subpopulation exhibits a monotonic decreasing failure rate. This is reflected in the heterogeneous population as a decreasing failure rate during the first 100 hours of operation. See Fig. 9.7. The non-grouped data of Fig. 9.1 more accurately pinpoints the end of the early failure period at 36.7 hours. Therefore, a required burn-in period of approximately 40 hours as part of the manufacturer's quality control program would eliminate the early failure period prior to placing the magnetrons into the Army supply system. The advantages to the Army of such an arrangement are three fold:

1. Radar down time due to faulty magnetrons would be greatly reduced with a subsequent increase in operational readiness.
2. Fewer magnetrons would be handled in the supply and maintenance systems.
3. The number of magnetrons of this type required by the Army would be reduced by approximately one fourth, a significant savings.

Useful Life Failures

The useful life failure period extends from 40 hours to 2000 hours and unlike the theoretical, chance failure period it is not a purely constant failure rate period.

$\lambda_{av}(t)$

1.0

.8

.6

.5

.3

500

1000

1500

2000

2500

HOURS

Figure 9.7 Plot of Magnetron Failure Rate Versus Time in Hours

Figure 9.7 shows the failure rate during useful life to vary from a high of .14 to a low of .048 failures per 100 hours. This indicates that the useful life failure mechanism is not strictly random but is a combination of two or more failure mechanisms. A simple explanation of this dependence is provided by a hypothetical and highly simplified illustrative life test of automobile tires. During the life test those tires which throw their tread are considered substandard; those which fail as a result of punctures are considered chance failures; and those which fail as a result of tread wear are considered wearout failures. Theoretically, the failure rate of the tires undergoing the life test is initially expected to decrease as the high failure rate substandard tires fail and are removed from test. The population is then expected to exhibit a constant failure rate during useful life as the sole failure mechanism during this period is random punctures; finally, as the tires become bald the failure rate increases until all the remaining tires have failed. An actual test would vary from the theoretical example above during useful life because the puncture failure mechanism is not, in reality, independent of tire wear. As the tread becomes worn, it loses thickness and increasingly smaller objects will be able to penetrate and cause punctures; therefore, the

puncture failure mechanism is not strictly random but is also dependent upon tire wear.

It may be speculated that a similar type of dependence causes the useful life of the magnetrons to exhibit a nonmonotonic failure rate. The magnetron case is even more complex than the tire example because both early and wearout mechanisms have an impact during useful life.

Wearout Failures

Wearout begins at approximately 2000 hours. The wearout subpopulation is extremely small and only 3 magnetrons of 38 failed during the wearout period.

Conclusion of Analysis

Approximately one fourth of the magnetrons will fail prior to forty hours of operation. An obvious savings would accrue to the Army in time, money, material, and manpower if these early failures could be isolated prior to being placed in supply and maintenance channels or into radars. This could be accomplished by requiring the manufacturer to provide a forty hour burn-in period before releasing magnetrons for operational use.

CHAPTER 10

COMPARISON OF PRESENT AND PROPOSED MODELS

10.1 Weibull Model of Magnetron Failures

In the past it has been expedient to model observed failure rate data with simple expressions capable of portraying only monotonic failure rates. Inherent in this measure is the assumption that a component population will not exhibit both decreasing and increasing failure rates during the span of population life. In the case of the magnetron data presented in Chapter 9 both government and industry have accepted the Weibull distribution with $\beta = .63$, $\alpha = 520$, and $\gamma = 0$ as an appropriate model (Figure 10.1). Since β is less than unity, a monotonic decreasing failure rate is indicated during the entire magnetron life. This state of affairs is contradictory to classic reliability theory and defies either practical or theoretical explanation. Nevertheless, the Weibull model with the indicated parameters can be shown to fit the observed failure data at the .05 significance level using the Kolmogorov-Smirnov Test for goodness-of-fit (Table 10.1).

ENCLOSURE (2) to RAYTHEON MEMO JDM:iem:7199:W2293

Dated 25 June 1970

Page 9 of 9

WEIBULL PROBABILITY CHART

WEIBULL PROBABILITY CHART

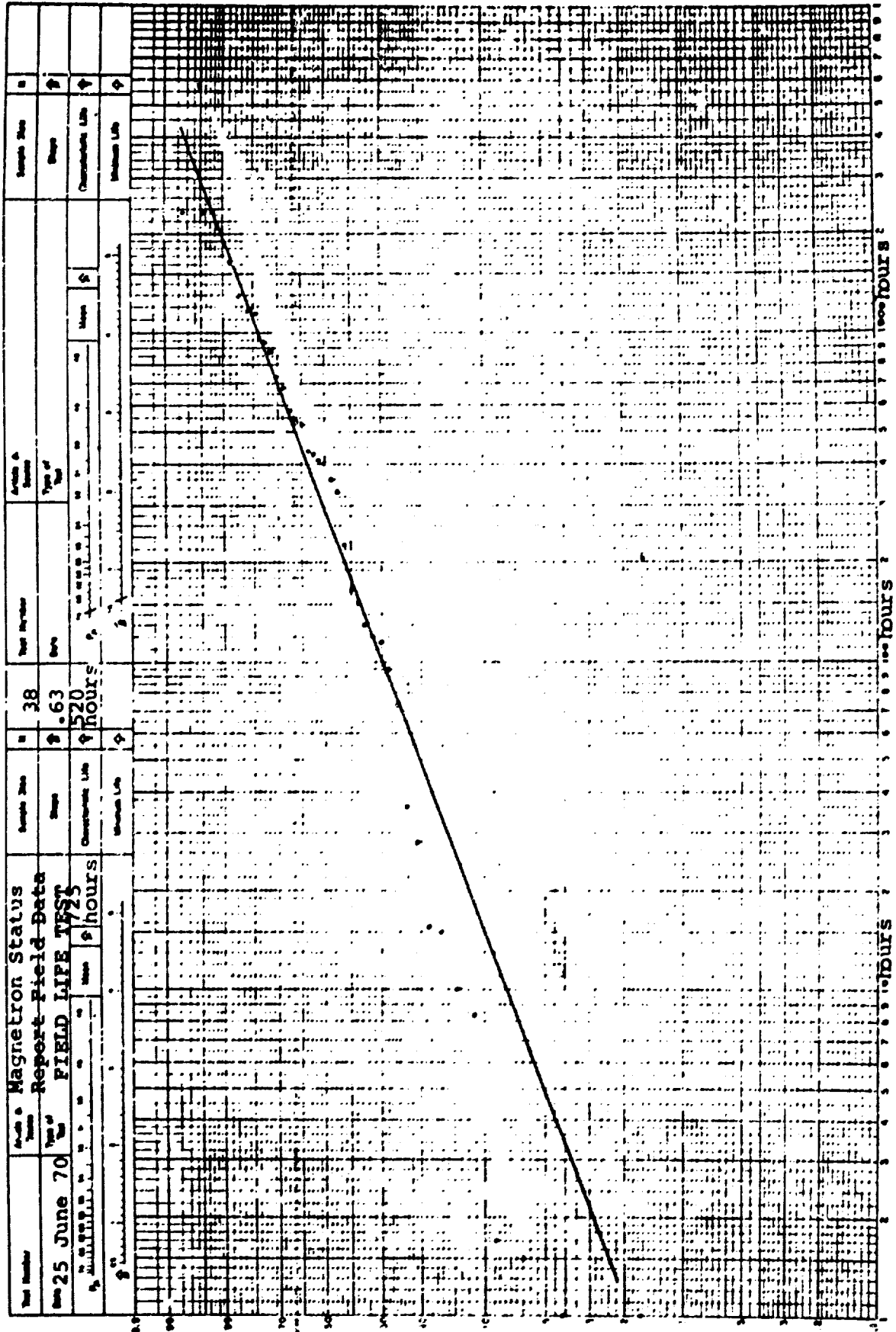


Figure 10.1 Weibull Plot of Magnetron Failures from Assumed Homogeneous Population

Table 10.1 Absolute Difference Between Expected and Observed Cumulative Magnetron Failures (Weibull Distribution)

Time	Observed	Expected	Absolute Difference
t	Q (L)	Q(L)	D _i
0.0	.026	.000	.026
1.0	.053	.019	.034
1.5	.079	.025	.054
1.7	.105	.027	.078
8.3	.132	.071	.061
10.0	.158	.080	.078
15.0	.184	.102	.082
15.5	.210	.104	.106*
28.0	.237	.147	.090
36.7	.263	.172	.091
73.6	.290	.253	.037
95.0	.316	.290	.026
116.0	.342	.322	.020
120.0	.368	.328	.040
130.0	.395	.341	.054
153.5	.421	.371	.050
165.0	.447	.384	.063
226.4	.474	.447	.027
332.3	.500	.530	.030
363.0	.526	.549	.023
405.4	.551	.575	.024
409.0	.579	.577	.002
431.0	.605	.589	.016
439.0	.631	.593	.038
525.0	.658	.634	.024
541.7	.684	.642	.042
577.9	.710	.657	.053
677.0	.736	.693	.043
739.0	.763	.713	.050
873.0	.790	.750	.040
937.0	.815	.765	.050
1144.0	.841	.807	.034
1169.0	.869	.811	.058
1297.0	.895	.831	.064
1630.0	.921	.871	.050
2088.9	.947	.909	.038
2340.9	.975	.924	.051
2343.0	1.000	.924	.076

*Maximum absolute difference .106

Allowable absolute difference at the .05 significance level is found from Table 3.1 to be

$$\frac{1.36}{\sqrt{N}} = \frac{1.36}{\sqrt{38}} = .220$$

Thus, the Weibull distribution is demonstrated to be a satisfactory expression for fitting a curve to the observed magnetron failure data. However, the model provides little insight into the mechanics of failure and would not be of great use in either reliability improvement or theoretical speculation because of its inexplicable monotonic decreasing failure rate.

10.2 Comparison of Goodness-of-Fit

Figure 10.2 provides a comparison of the expected cumulative failures as determined by both the proposed and the standard Weibull models. As might be expected, because of the larger number of parameters the proposed model fits the observed data more closely than does the standard Weibull distribution. While the Weibull data is seen to fall below the observed cumulative data after 500 hours of radiate time the summation model closely approximates the observed data throughout the entire span of component life. The maximum absolute difference between expected and observed cumulative failures is .070 (Table 9.4) for the proposed summation model and .106 (Table 10.1) for the Weibull distribution. The allowable maximum difference at the .05 significance level for the Kolmogorov-Smirnov goodness-of-fit test is .220. This indicates that both models are adequate at the .05 significance level

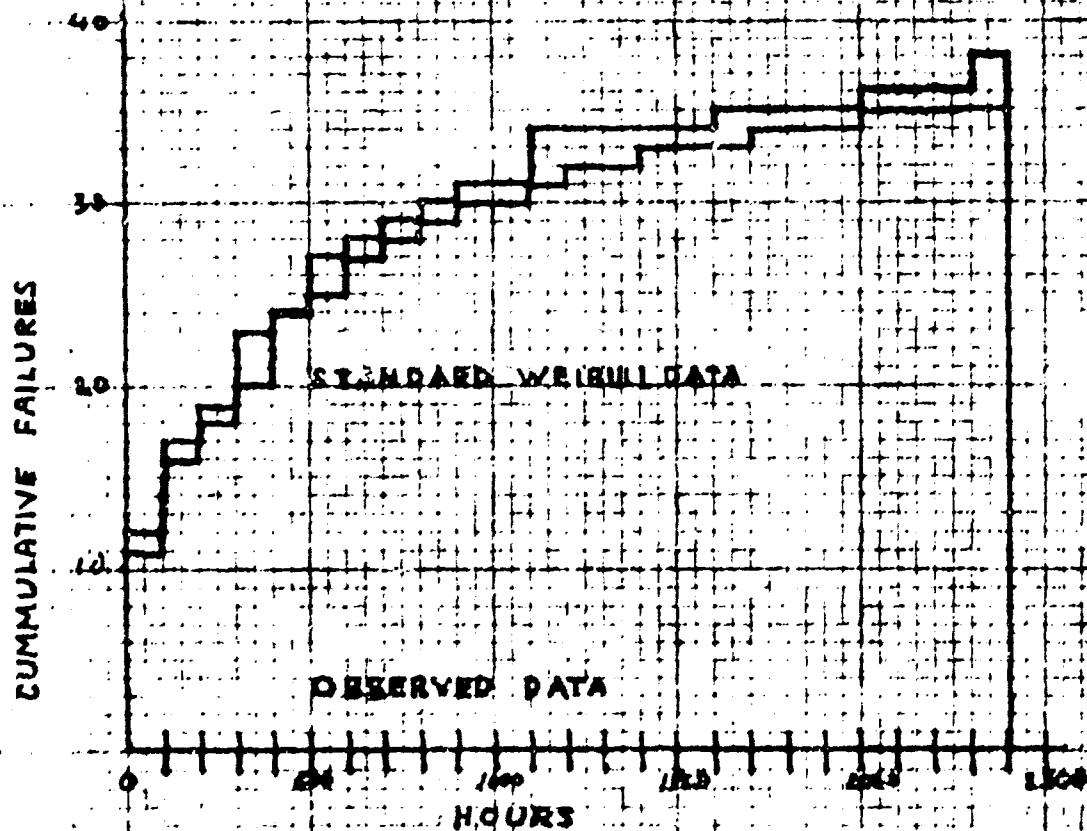


Figure 10.2 Comparison of Weibull and Summation Model
Cumulative Failures Versus Time in Hours

for curve fitting purposes, although the proposed model is the more accurate of the two.

10.3 Comparison of Failure Rate

At this point one might question the use of a complex model to gain unrequired accuracy when the more simple Weibull distribution has been shown to be sufficient. The answer lies in the analysis of the failure rate curves of the two expressions. The Weibull failure rate is monotonic decreasing (Figure 10.3) which is inconsistent with reliability theory. The proposed model failure rate is, on the other hand, nonmonotonic: first decreasing, then showing a slight increase and decrease, followed by a dramatic increase which continues to the end of component life (Figure 10.3). Since the proposed model has been shown to be a more accurate model of observed data it is logical to assume that the failure rate behavior described by the summation model is also more accurate. Since the failure rate of the summation model relates fairly well to reliability theory, the model becomes useful for theoretical speculation concerning failure cause.

10.4 Comparison of Analytical Power

Figure 10.1 is the standard method of plotting failure data and obtaining a straight line fit. The fact that

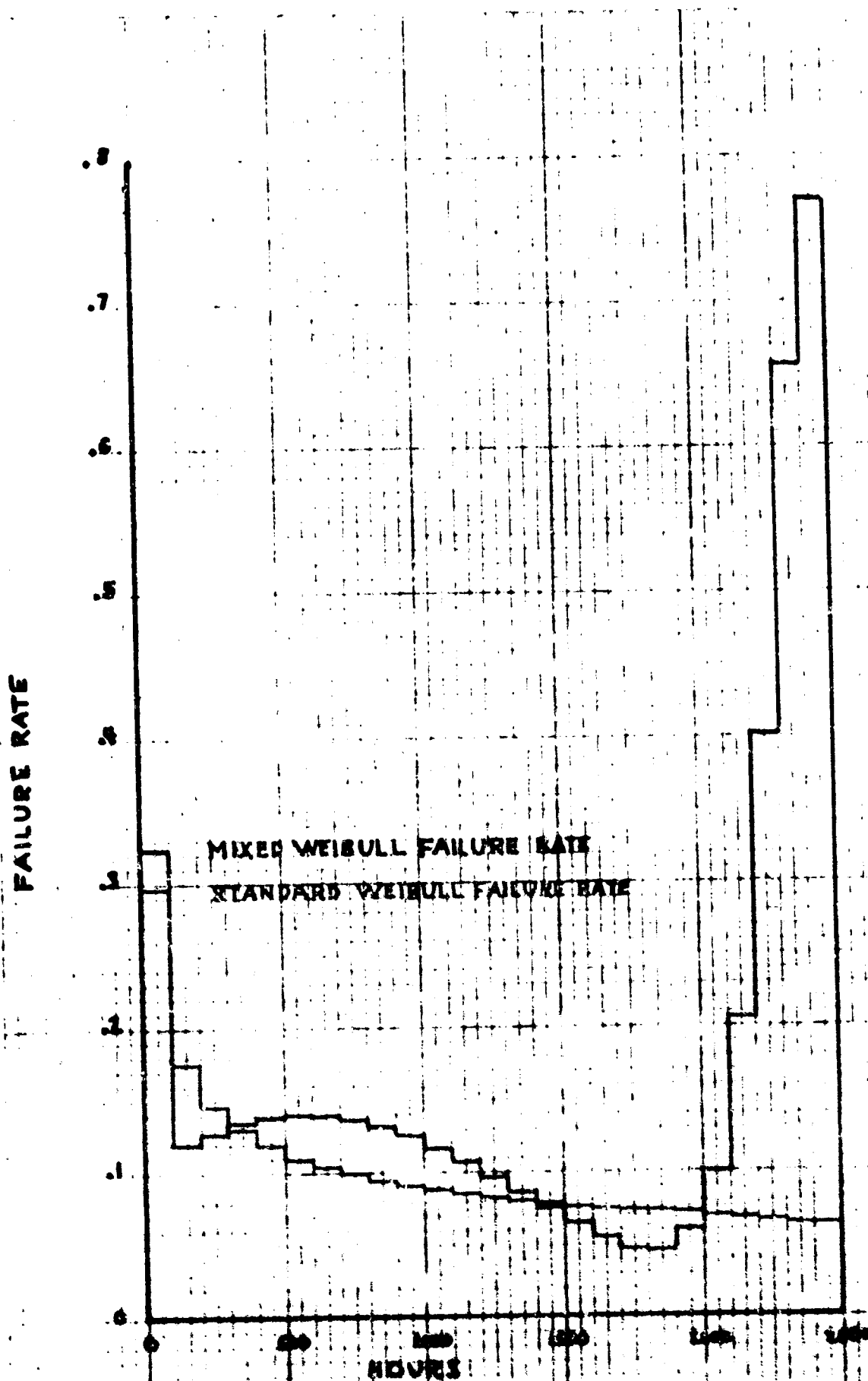


Figure 10.3 Comparison of Weibull and Summation Model Failure Rates Versus Time in Hours.

the straight line does not fit well at the tails of the data is usually ignored or considered inconsequential as it was in this case. Figure 9.1 is the same failure data, but this time with three straight lines fit to it. The theoretical basis for the three lines was established in Section 5.3. The advantages of using the reliability summation rule rather than the commonly used monotonic failure rate distributions are:

1. The proposed expression models failure data more accurately than expressions currently being used for this purpose.
2. The proposed technique is sufficiently flexible to model data that cannot be modeled by the usual statistical methods. Human mortality is an example of this.
3. The proposed model yields information about failure cause which is obscured by present methods. For example, no wearout was evident in the Weibull plot of magnetron failures; whereas, the summation model indicates a wearout period extending from 2000 to 2500 hours. Furthermore the Weibull plot gives no indication of when the burn-in or early period ends since the entire Weibull failure rate curve is monotonic decreasing. The summation model, on the other hand, definitely indicates that burn-in is terminated after 1000 hours of operation. This is important.

information for managers as well as theoreticians and it is totally obscured by present modeling techniques.

CHAPTER 11

SUMMARY AND RECOMMENDATIONS

11.1 Summary

In this report three unified expressions have been considered to see which best describes the reliability of components drawn randomly from a population of components exhibiting failures of the early, chance, and wearout type. The product model,

$$R_{ecw}(t) = R_e(t) R_c(t) R_w(t) \quad (5.2)$$

was eliminated because it indicates incorrectly that the unified reliability is zero after the population is burned in.

The combined summation and product model

$$R_{ecw}(t) = \frac{N_e}{N} R_e(t) + \frac{N_c}{N} R_c(t) R_w(t) \quad (5.16)$$

appears to be theoretically sound but no analytical means of determining the individual reliabilities $R_c(t)$ and $R_w(t)$ from observed failure data was found without combining them

into the single reliability $R_G(t) = R_c(t) R_w(t)$. Unfortunately, this combination destroys the usefulness of the expression as a tool for analysing the individual chance and wearout failure modes.

Less sound theoretically but perhaps more useful than the combined model is the summation model,

$$R_{ecw}(t) = \frac{N_e}{N} R_e(t) + \frac{N_c}{N} R_c(t) + \frac{N_w}{N} R_w(t) \quad (5.9)$$

It is less sound because its basis is that there are three individual failure subpopulations, which is not quite true. Theoretically, there are only two failure subpopulations, the substandard and the good. The substandard population providing early failures and the good subpopulation providing both chance and wearout failures. This means that wearout is not a separate subpopulation and components must survive the chance period in order to deteriorate and eventually become a wearout failure. If wearout was in fact a separate subpopulation, components belonging to this subpopulation would not be subjected to the chance failure mechanism. However, even with this theoretical limitation, the summation model does correlate well with observed data and it is the only model of the three considered which provides specific information

concerning all three failure modes.

In comparison with present modeling techniques the summation model was shown to be superior in three ways:

1. It is more accurate than methods presently in use.

2. It's greater flexibility permits the modeling of data which is beyond the capabilities of present statistical methods.

3. It yields important information for use by managers as well as theoreticians concerning failure periods and underlying failure causes information which is obscured by present modeling methods.

11.2 Recommendations

It has been shown in this thesis that the proposed summation model, with graphically determined subpopulation sizes and Weibull parameters, may be used very satisfactorily to represent observed failure data at the .05 significance level using the Kolmogorov-Smirnov Test. Further, it has been demonstrated that the proposed model offers significant advantages over present modeling techniques. Therefore, it is recommended that the reliability summation model be adopted for use in those cases in which failure data encompass the three failure periods: early, chance, and wearout. This might include complex systems such as

tanks and mechanical components such as fuel pumps in addition to electronic components.

The adoption of the proposed modeling technique should result in a better analysis of the manufacturer's quality control; it would pinpoint the required burn-in period and the time at which wearout begins; and this knowledge, effectively applied, would reduce the number of sub-standard components accepted by the military services and subsequently placed into the respective supply systems. With fewer unreliable repair parts or components available in supply channels, maintenance required on end items would go down while operational readiness would increase. In the example of magnetrons used by the Army it was shown that approximately one quarter of the type magnetrons considered were unreliable and failed shortly after installation into operational radars. Had the methods proposed in this thesis been employed, an additional burn-in period would have been required of the manufacturer and the unreliable magnetrons would have failed prior to entry into the Army supply system with a resultant savings in money, manpower, storage and transportation requirements, and an increase in end item operational readiness.

APPENDIXES

APPENDIX A

ATTEMPTED EXTENSION OF KAO'S METHOD FOR GRAPHICAL ESTIMATION OF MIXED WEIBULL PARAMETERS (18)

In order to use equation (6.1) to compute component reliability, it is first necessary to find the three subpopulation sizes N_e , N_c , and N_w and the respective Weibull parameters $\delta_e, \beta_e, \eta_e, \delta_c, \beta_c, \eta_c, \delta_w, \beta_w$, and η_w . Kao (18) suggests a method for finding certain of these parameters for the case of two subpopulations. An unsuccessful attempt was made to extend Kao's graphical procedure to the case of three subpopulations. The steps of the attempted extended procedure are given, followed by a discussion of the problems which arise in their use. The human mortality data of Chapter 7 are used to illustrate the procedure. The steps are:

1. Tabulate the median ranks of the mixed population for each class interval (Table 7.2) and plot the data on Weibull probability paper (Fig. A.1).
2. Fit three straight lines to the plotted data by

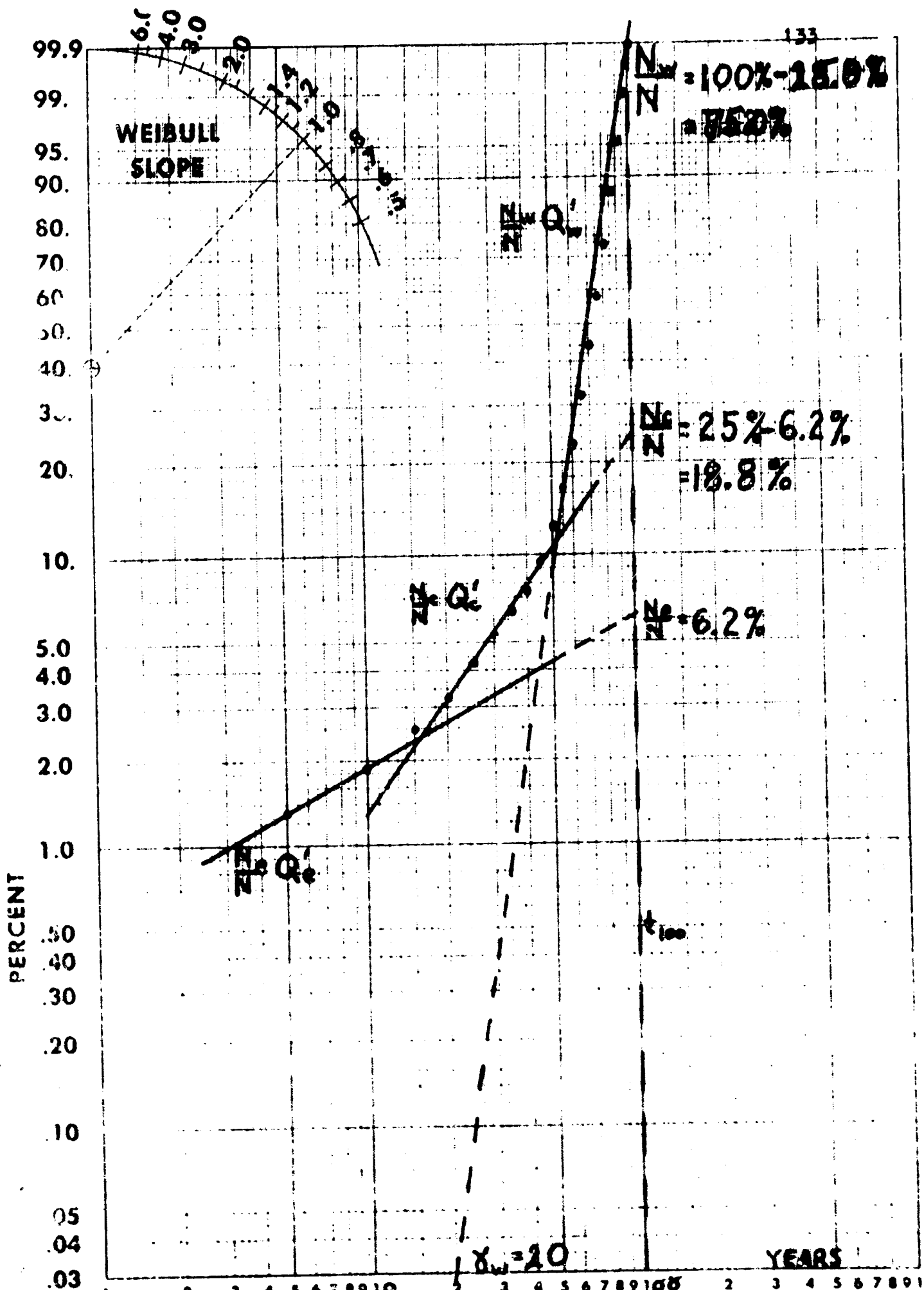


Figure A.1 Weibull Plot of Human Mortality Mixed Population
 1980 (Extended Method) WEIBULL PROBABILITY PAPER

by visual inspection and designate the lines

$$\frac{N_e}{N} Q'_e, \frac{N_c}{N} Q'_c, \text{ and } \frac{N_w}{N} Q'_w \text{ (Fig. A.1).}$$

3. Extend the $\frac{N_w}{N} Q'_w$ line until it intersects the upper border line (99.9% line). From this intersection drop a vertical line, designated t_{100} , representing the estimated time at which 100 percent of the components will have failed (Fig. A.1).

4. Extend the $\frac{N_e}{N} Q'_e$ line upward until it intersects the t_{100} line. The height of this intersection read on the percent failure scale gives the estimate of $\frac{N_e}{N}$ in percent (Fig. A.1).

5. Extend the $\frac{N_c}{N} Q'_c$ line upward until it intersects the t_{100} line. The height of this intersection read on the percent failure scale gives the estimate of $\frac{N_e + N_c}{N}$ in percent (Fig. A.1).

6. Since $\frac{N_e}{N} + \frac{N_c}{N} + \frac{N_w}{N} = 1$ the three subpopulation sizes N_e , N_c , and N_w are readily determined.

7. The location parameter for each subpopulation is determined by extending the lines $\frac{N_e}{N} Q'_e$, $\frac{N_c}{N} Q'_c$ and $\frac{N_w}{N} Q'_w$ downward until they intersect the time axis (abscissa). The individual values are the times read at these intersections. Normally, the $\frac{N_e}{N} Q'_e$ line and the $\frac{N_c}{N} Q'_c$ line will not intersect the positive time axis and in this case

$$Y_e = Y_c = 0 \text{ (Fig. A.1).}$$

8. Categorize the failures by relating them to the particular subpopulation line upon which they fall. If a point falls on or near both lines it may be included in both subpopulations.

9. Sufficient information has now been determined from the observed failure data to separate the mixed population into its three constituent subpopulations. Calculate new median ranks by considering the subpopulations individually (Table A.1). Plot the median ranks versus the individual $t-\gamma$ values with δ as determined in Step 7 (Fig. A.2).

10. Fit three straight lines to the subpopulation plots and designate the lines $\frac{N_e}{N} Q_e$, $\frac{N_c}{N} Q_c$, and $\frac{N_w}{N} Q_w$, respectively (Fig. A.2).

11. Find the individual values of η and β for each subpopulation using the method described in Section 3.3 (Fig. A.2).

The following parameters are now determined:

$$\frac{N_e}{N} = .062, \quad \gamma_e = 0, \quad \beta_e = .65, \quad \eta_e = 49$$

$$\frac{N_c}{N} = .188, \quad \gamma_c = 0, \quad \beta_c = 2.5, \quad \eta_c = 57$$

$$\frac{N_w}{N} = .750, \quad \gamma_w = 20, \quad \beta_w = 5.9, \quad \eta_w = 54$$

Table A.1 Mortality Data Prepared for Subpopulation
Replot (Extended Method)

	Point Number	Age at Class Inter- val End Point	Subpop- ulation Values for	Subpop- ulation Cumula- tive Failures	Subpop- ulation Median Ranks
	#	t	t- δ	$N_f(t)$	M.R.
Early					
Subpopulation	1	5	5	13	20.3
($N_e=62, \gamma_e=0$)	2	10	10	19	30.0
Chance	3	15	15	6	3.0
Subpopulation	4	20	20	14	7.3
($N_c=188, \delta_c=0$)	5	25	25	23	12.0
	6	30	30	33	17.4
	7	35	35	44	23.2
	8	40	40	57	30.1
	9	45	45	76	40.1
Wearout	10	50	30	29	3.8
Subpopulation	11	55	35	72	9.6
($N_w=750, \delta_w=20$)	12	60	40	135	18.0
	13	65	45	225	30.0
	14	70	50	346	44.0
	15	75	55	492	65.5
	16	80	60	642	85.6
	17	85	65	774	
	18	90	70	858	
	19	95	75	895	
	20	100	80	905	

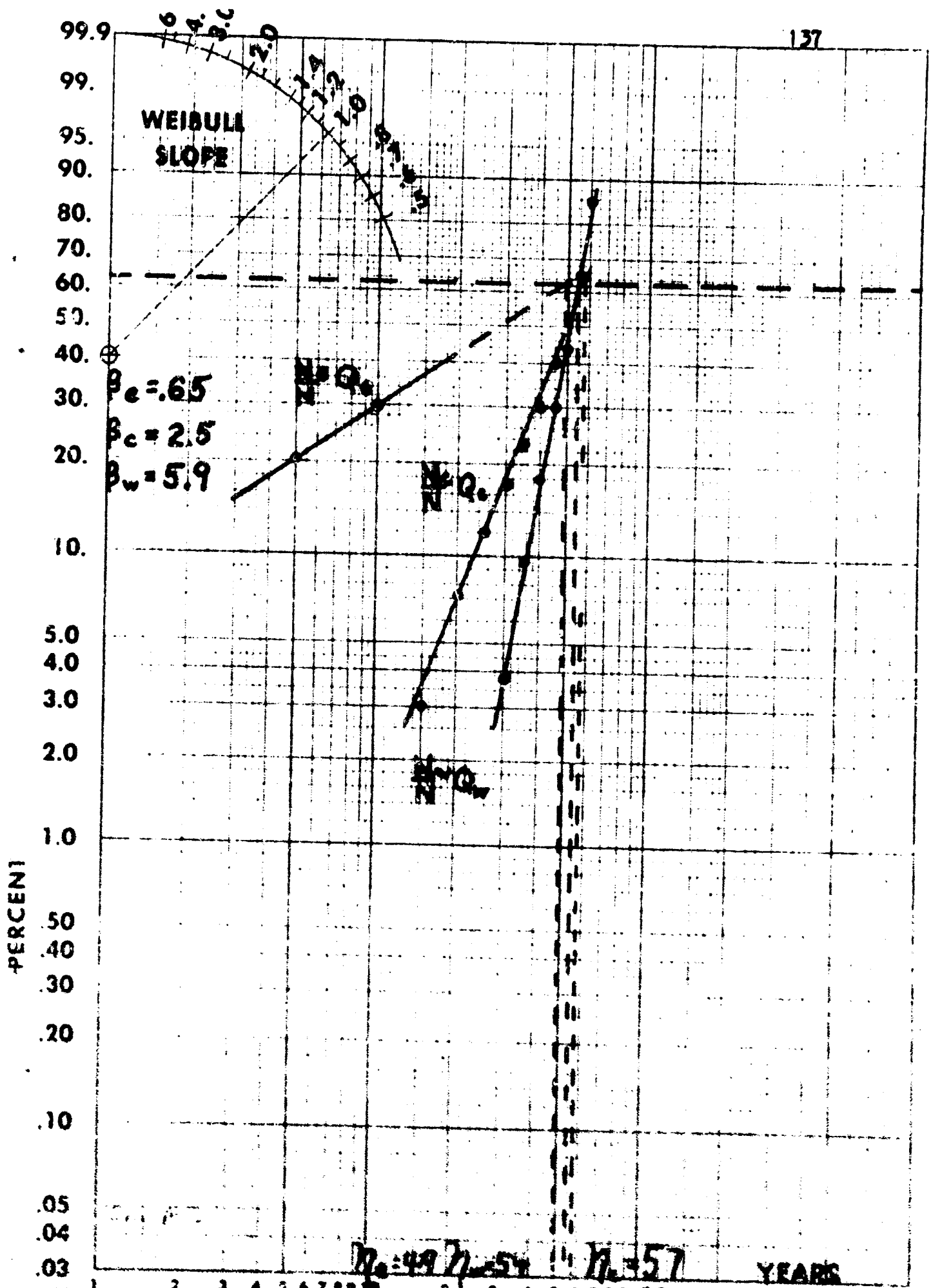


Figure 4.2 Mortality, Early, Chance, and Wearout Subpopulation Replots
 (Extended Method) WEIBULL PROBABILITY PAPER

Table A.2 is a tabulation of the observed Q_{ecw} , the expected Q_{ecw} , and the absolute difference D_1 computed at each class interval end point. The maximum value of D_1 is .124 which is greater than the maximum allowable of .043 at the .05 significance level. It can be concluded, therefore, that the parameters found by the extended method do not describe the observed data at the .05 significance level.

Two problems associated with the extended method have been isolated:

1. There is no apparent justification for using the γ parameter as a delay factor rather than for curvature correction as suggested by most writers in this area. Furthermore, the determination of the γ parameter from the mixed plot rather than from the subpopulation replots unnecessarily limits the flexibility of the Weibull equations. This criticism pertains to both the original and the extended Kao procedures.

2. In the extended procedure the approximation of the subpopulation sizes is quite inaccurate. This results in inaccurate calculation of subpopulation median ranks which leads directly to inaccurate scale and shape parameters. In addition, points which indicated median ranks greater than 100 percent were lost for plotting

Table A.2 Absolute Difference Between Expected and Observed Cumulative Mortality Data (Expected Data Determined by the Extended Method)

Age	Observed	Expected	Absolute Difference
t	$Q_{ecw}(t)$	$Q_{ecw}(t)$	D_i
5	.013	.013	.000
10	.019	.021	.002
15	.025	.029	.004
20	.033	.040	.007
25	.042	.052	.010
30	.052	.066	.014
35	.063	.083	.020
40	.076	.102	.026
45	.095	.126	.031
50	.124	.159	.035
55	.167	.209	.042
60	.230	.287	.057
65	.320	.401	.081
70	.441	.550	.109
75	.587	.711	.124*
80	.737	.849	.112
85	.869	.935	.066
90	.953	.970	.017
95	.990	.981	.009
100	1.000	.984	.016

*Maximum absolute difference

Allowable absolute difference at the .05 significance level is found from Table 3.1 to be:

$$\frac{1.36}{\sqrt{N}} = .043$$

Table A.3 Comparison of Weibull Parameters Determined
By Two Different Methods

Extended Method	Method of Chapter 7
$N_e = 62$	$N_e = 19$
$N_c = 188$	$N_c = 76$
$N_w = 750$	$N_w = 905$
$\delta_e = 0$	$\delta_e = 0$
$\delta_c = 0$	$\delta_c = 0$
$\delta_w = 20$	$\delta_w = 0$
$\pi_e = 49$	$\pi_e = 4.85$
$\pi_c = 57$	$\pi_c = 35.9$
$\pi_w = 54$	$\pi_w = 77.5$
$\beta_e = .65$	$\beta_e = 1.6$
$\beta_c = 2.5$	$\beta_c = 2.81$
$\beta_w = 5.9$	$\beta_w = 7.2$

purposes. Table A.3 provides a comparison of the parameters as determined by the extended method and the method suggested in Chapter 6.

APPENDIX B

BASIC LANGUAGE COMPUTER PROGRAMS FOR APPLYING THE PROPOSED
RELIABILITY SUMMATION MODEL WITH KNOWN THEORIZED, OR GRAPH-
ICALLY ESTIMATED PARAMETERS.

(The programs included in this Appendix are samples of the
programs used to analyze magnetron failures in Chapter 9
and would require modification to be of more general use.)

```
10 READ N,E,B1,N1,C,B2,G2,N2,W,B3,G3,N3
11 LET T=100
15 PRINT N
16 PRINT E,B1,G1,N1
17 PRINT C,B2,G2,N2
18 PRINT W,B3,G3,N3
19 PRINT "38 MAGNETRON FAILURES GROUPED DATA 100 HR CLASS
      INTERVAL"
20 PRINT
22 LET Q1=0
30 LET A1=(T-G1)/N1
35 IF A1>0 THEN 40
36 LET A1=0
40 LET A2=(T-G2)/N2
45 IF A2>0 THEN 50
46 LET A2=0
50 LET A3=(T-G3)/N3
55 IF A3>0 THEN 60
56 LET A3=0
60 LET A4=A1*B1
70 LET A5=A2*B2
80 LET A6=A3*B3
82 LET R8=1-Q1
90 LET R1=EXP(-A4)
100 LET R2=EXP(-A5)
110 LET R3=EXP(-A6)
120 LET R4=(E/N)*R1
130 LET R5=(C/N)*R2
140 LET R6=(W/N)*R3
150 LET R7=R4+R5+R6
160 LET Q1=1-R7
162 LET F1=R8-R7
164 LET L1=F1/R8
169 PRINT
170 PRINT "AGE="T
180 PRINT "R="R8,"PDF="F1,"Q="Q1
181 PRINT "FR="L1
185 PRINT "RE="R1,"RC="R2,"RW="R3
190 LET T=T+100
200 IF T>2500 THEN 900
210 GO TO 30
220 DATA 38,10,.69,0,12.1,25,1.25,0,620,3,20,0,2310
900 END
```

```
10 READ N,E,B1,G1,N1,C,B2,G2,N2,W,B3,G3,N3
15 PRINT N
16 PRINT E,B1,G1,N1
17 PRINT C,B2,G2,N2
18 PRINT W,B3,G3,N3
19 PRINT "38 MAGNETRON FAILURES UNGROUPED DATA"
20 PRINT
21 DIM T(40)
22 FOR I=1 TO 38
23 READ T(I)
30 LET A1=(T(I)-G1)/N1
35 IF A1>0 THEN 40
36 LET A1=0
40 LET A2=(T(I)-G2)/N2
45 IF A2>0 THEN 50
46 LET A2=0
50 LET A3=(T(I)-G3)/N3
55 IF A3>0 THEN 60
56 LET A3=0
60 LET A4=A1*B1
70 LET A5=A2*B2
80 LET A6=A3*B3
82 LET R8=1-Q1
90 LET R1=EXP(-A4)
100 LET R2=EXP(-A5)
110 LET R3=EXP(-A6)
120 LET R4=(E/N)*R1
130 LET R5=(C/N)*R2
140 LET R6=(W/N)*R3
150 LET R7=R4+R5+R6
160 LET Q1=1-R7
162 LET F1=R8-R7
164 LET L1=F1/R8
169 PRINT
170 PRINT "AGE="T(I)
180 PRINT "R="R8,"PDF="F1,"Q="Q1
181 PRINT "FR="L1
185 PRINT "RE="R1,"RC="R2,"RW="R3
190 NEXT I
191 GO TO 23
220 DATA 38,10,.69,0,12.1,25,1.25,0,620,3,20,0,2310
300 DATA 0,1,1.5,1.7,8.3,10,15,15.5,28,36.7,73.6,95
310 DATA 116,120,130,153.5,165,226.4,332.3,363,405.4,409,431
320 DATA 439,525,541.7,577.9,677,739,873,937,1144,1169,1297
330 DATA 1630,2088.9,2340.9,2343
900 END
```

REFERENCES

1. Department of the Army, Washington. Dictionary of United States Army Terms. Army Regulation, AR 310-25, 1 March 1969.
2. Starsman, R. E. "Reliability Life Testing of Mixed Early, Chance, and Wearout Populations" Unpublished report, University of Arizona, 1970.
3. Kececioglu, Dimitri, and R. E. Starsman. "Reliability life Testing with Mixed Early, Chance, and Wearout Sub-Populations," Conference Transactions of the American Society for Quality Control, XXV (1971), 537-546.
4. Myers, R. H., K. L. Wong, and H. M. Gordy. Reliability Engineering for Electronic Systems. New York: John Wiley and Sons, Inc., 1964.
5. Bazovsky, Igor. Reliability Theory and Practice. Englewood Cliffs: Prentice Hall, Inc., 1963.
6. Davis, D. J. "An Analysis of Some Failure Data," Journal of the American Statistical Association, 47 (June, 1952), 113-150.
7. Johnson, Leonard G. Theory and Techniques of Variation Research. London: Elsevier Publishing Co., 1964.
8. King, James R. "Graphical Data Analysis with Probability Papers," TEAM Report, 104 Belrose Avenue, Lowell, Mass.
9. Weibull, W. "A Statistical Distribution Function of Wide Applicability," Journal of Applied Mechanics, 18 (September, 1951), 295-297.
10. Lochner, Robert H. "When and How to Use the Weibull Distribution," Education Department, A. C. Spark Plug Division, General Motors Corporation, October 9, 1963.
11. Massey, F. J., Jr. "The Kolmogorov-Smirnov Test for Goodness-of-Fit," Journal of the American Statistical Association, 46 (1951), 68-78.
12. Earles, D. R., and M. F. Eddins. "Reliability Physics," Avco Corp., Research and Advanced Development Division, March 1962.

13. Mendenhall, W., and R. J. Hader. "Estimation of Parameters of Mixed Exponentially Distributed Failure Time Distributions From Censored Life Test Data," Biometrika, 45 (1958) 504-520.
14. Roberts, Norman H. Mathematical Methods in Reliability Engineering. New York: McGraw-Hill Book Co., 1964.
15. Dietrich, Duane L. "Development and Application of Three Early Failure Math Models." Unpublished report, University of Arizona, 1967.
16. Polovko, A. M. Fundamentals of Reliability Theory. New York: Academic Press, Inc., 1968.
17. Pieruschka, Erich. Principles of Reliability. New Jersey: Prentice Hall, Inc., 1963.
18. Kao, John H. K. "A Graphical Estimation of Mixed Weibull Parameters in Life-Testing of Electron Tubes," Technometrics, 1 (November 1959), 389-407.
19. Commissioners 1958 Standard Ordinary Mortality Table (1958 C S O Table).
20. Doyan, Leonard R., and Martin J. Siegman. "High-Power High Frequency Reliability Techniques," Proceedings 1966 Annual Symposium of Reliability, (1966), 180-197.